



Finite element analysis of sandwich structures with viscoelastic foam cores for mechanical applications

Master Thesis

Khan Muhammad Adeel

Department of Aerospace and Mechanical Engineering

POLITECNICO DI TORINO

Contents

1. Introduction.....	11
1.1 Motivation	11
1.2 Problem Statement	12
1.3 Research Objective.....	12
1.4 Outline of the thesis	12
2. Literature Review.....	14
2.1 Introduction.....	14
2.2 Models for Hyper-elasticity and Viscoelasticity.....	15
2.2.1 Hyper-elasticity	15
2.2.2 Constitutive Models for Linear Viscoelasticity	16
2.3 Elastic, Ideal Viscous and Viscoelastic behavior	17
2.3.1 Elastic Behavior	17
2.3.2 Ideal Viscous Liquid	17
2.3.3 Viscoelastic Material.....	18
2.4 Viscoelasticity	19
2.4.1 Types of Viscoelasticity.....	19
2.4.2 Time-dependent Responses of Viscoelastic Material	20
2.4.3 Dynamic modulus	23
2.4.4 Constitutive models for Linear Viscoelasticity	25
2.4.5 Prony Series	30
2.4.6 Effect of Temperature on Viscoelastic Behavior.....	31
2.4.7 Dynamic mechanical analysis.....	31
2.5 P-alpha EOS.....	32
2.6 Equation of State: Hugoniot Shock wave data	36
3. FE-Based Numerical modelling of Sandwich beam	39
3.1 Explicit Dynamics.....	39
3.2 Problem Statement of Analysis	40
3.2.1 Case A: Simple (One-channel) beam.....	41
3.2.2 Case B: Two-channel beam.....	41
3.3 Analysis Steps	42
3.3.1 Engineering Data.....	43
3.3.2 Geometry	46
3.3.3 Setup.....	51
3.3.4 Loading.....	55
3.3.5 Results	58
4. Results	59
4.1 Simple hollow beam and foam sandwich beam (PU foam 40kg/m ³).....	59
4.1.1 Deformation	60
4.1.2 Reaction Force-time Curve.....	61

4.1.3 Kinetic Energy	63
4.1.4 Velocity (Y-axis).....	64
4.1.5 Acceleration (Y-axis).....	65
4.1.6 Momentum (in direction of collision):.....	66
4.2 Simple hollow beam and foam sandwich beam (PU foam 93kg/m ³).....	68
4.2.1 Deformation.....	69
4.2.2 Force Reaction-time curve.....	71
4.2.3 Kinetic Energy	73
4.2.4 Velocity.....	75
4.2.5 Acceleration.....	77
4.3 Two-Channel Hollow and Sandwich Beam (PU foam 93kg/m ³).....	79
4.3.1 Deformation	80
4.3.2 Reaction Force-time curve.....	82
4.3.3 Velocity (y-axis)	84
4.3.4 Acceleration (y-axis)	85
4.3.5 Acceleration (y-axis)	86
5. Conclusion.....	88

List of Tables

Table 2-1 : Constitutive models for linear viscoelasticity.....	17
Table 2-2 : Maxwell vs Kelvin-Voigt model in Creep and relaxation.....	28
Table 3-1 : Different configurations of hollow beam.....	41
Table 3-2 : Different configurations in two-channel beam.....	41
Table 3-3 : Material properties of Flexible and Rigid PU foam.....	45
Table 3-4: Impactor dimensions and material type.....	47
Table 3-5 : Thickness of different configuration of beam.....	49
Table 4-1 : Types of Polyurethane foam with density.....	59
Table 4-2 : Case 1 - Hollow vs foam sandwich beam.....	59
Table 4-3 : Kinetic energy comparison between hollow and sandwich beam.....	63
Table 4-4 : Hollow vs sandwich beam Polyurethane foam 93 kg/m ³	68
Table 4-5 : Different configuration of beam from Case 3 to Case 6.....	68
Table 4-6 : Two-channel hollow and foam-sandwich beam.....	80
Table 5-1 : Comparison of Simple hollow beam and the foam sandwich beam (PU foam 40 kg/m ³)	89
Table 5-2 : Comparison of Simple hollow beam and the foam sandwich beam (PU foam 93 kg/m ³)	89
Table 5-3 : Comparison of two channel hollow beam and the foam sandwich beam.....	90

List of Figures

Figure 2.1 : Stress-strain phase diagram of elastic behavior vs ideal viscous liquid [12]	18
Figure 2.2 : Stress-strain phase diagram of Viscoelastic material [12]	18
Figure 2.3 : Relaxation curves for a linear viscoelastic material [13]	20
Figure 2.4 : Creep and Relaxation of Non-linear Viscoelastic material [14]	21
Figure 2.5 : Stress relaxation in polymer A vs polymer B [12]	21
Figure 2.6 : Creep curves for a Linear Viscoelastic material [13].....	22
Figure 2.7 : Applied Stress input [11]	23
Figure 2.8 : Induced strain output in Viscoelastic material [11]	23
Figure 2.9 : Maxwell model - Series connection of spring and damper [11].....	26
Figure 2.10 : Kelvin-Voigt model: Parallel combination of spring and damper [11]	27
Figure 2.11 : Zener model or Standard linear model [11]	28
Figure 2.12 Burgers Model [11].....	28
Figure 2.13 : Generalized Maxwell model [11]	29
Figure 2.14 : Relaxation elements [12].....	29
Figure 2.15 : Relaxation curve with different relaxation time [12].....	30
Figure 2.16 : Dynamic mechanical analysis testing machine [15].....	32
Figure 2.17 : Bulk wave velocity vs density [16]	33
Figure 2.18 : Hydrostatic Pressure (P_e) vs density [16]	35
Figure 2.19 : P-alpha parameters of Rigid PU foam 450kg/m ³ [16].....	36
Figure 2.20 Shocked material and Pusher [17]	37
Figure 3.1 : Rectangular curved beam with impactor as rigid body	40
Figure 3.2 : Ansys 19.1 Project schematic and analysis systems	42
Figure 3.3 : Engineering data for Non-linear Structural steel	43
Figure 3.4 : Viscoelasticity and P-alpha parameters for PU foam 40kg/m ³	44
Figure 3.5 : Viscoelasticity and P-alpha parameters for foam 93 kg/m ³	45
Figure 3.6 : Shock data parameters and P-alpha parameters for Rigid PU 93 kg/m ³	46
Figure 3.7 : Isometric view of impactor (rigid body)	47
Figure 3.8 : Front view of impactor (rigid body)	47
Figure 3.9 : Isometric view of hollow beam	48
Figure 3.10 : Front view of hollow beam.....	48
Figure 3.11 : Isometric view of two-channel hollow beam	49
Figure 3.12 : Isometric view of foam filled beam	50
Figure 3.13 : Isometric view of two-channel filled beam	50
Figure 3.14 : Bonded surfaces of foam and beam.....	51
Figure 3.15 : Details of contact region.....	52
Figure 3.16 : Mesh quality distribution of elements	53
Figure 3.17 : Mesh of beam and rigid body	53
Figure 3.18 : Details of Mesh	54
Figure 3.19 : Mesh of foam sandwich beam.....	54
Figure 3.20 : Faces of foam sandwich beam where fixed boundary conditions are applied	55
Figure 3.21 : Faces of hollow beam where fixed conditions are applied	56
Figure 3.22 : End time setting	56
Figure 3.23 : Details of Output control.....	56
Figure 3.24 : Explicit dynamics erosion controls explanation (Ansys help document) [21]	57
Figure 3.25 : Geometric strain limit setting in Erosion controls	58
Figure 4.1 : Maximum deformation of 96 mm (Case 1)	60
Figure 4.2 : Energy graph of hollow beam (Case 1)	60
Figure 4.3 : Energy graph of foam-sandwich beam (Case 2)	61
Figure 4.4 : Reaction force-time graph of hollow beam (Case 1).....	62

Figure 4.5 : Reaction-force graph of foam-sandwich beam (Case 2).....	62
Figure 4.6 : Kinetic energy-time graph of hollow beam (Case 1).....	63
Figure 4.7 : Kinetic energy-time graph of foam-sandwich beam (Case 2).....	64
Figure 4.8 : Velocity-time graph of hollow beam (Case 1).....	65
Figure 4.9 : Velocity-time graph of foam sandwich beam (Case 2).....	65
Figure 4.10 : Acceleration -time graph of hollow beam (Case 1).....	66
Figure 4.11 : : Acceleration -time graph of foam-sandwich beam (Case 2).....	66
Figure 4.12 : Momentum in y-direction of hollow beam (Case 1).....	67
Figure 4.13 : Momentum in y-direction of foam sandwich beam (Case 2).....	67
Figure 4.14 : Energy graph of hollow beam (Case 3).....	69
Figure 4.15 : Energy graph of foam sandwich beam - bonded (Case 4).....	70
Figure 4.16 : Energy graph of foam sandwich beam – non-bonded (Case 5).....	70
Figure 4.17 : Energy graph of foam sandwich beam - rigid and bonded (Case 6).....	71
Figure 4.18 : Reaction force-time graph of hollow beam (Case 3).....	72
Figure 4.19 : : Reaction force-time graph of foam sandwich beam - bonded (Case 5).....	72
Figure 4.20 : : Reaction force-time graph of foam sandwich beam – non-bonded (Case 5).....	73
Figure 4.21 : Reaction force - time graph of foam sandwich beam - rigid and bonded (Case 6).....	73
Figure 4.22 : Kinetic energy-time graph of hollow beam (Case 3).....	74
Figure 4.23 : Kinetic energy-time graph of foam sandwich beam – bonded (Case 4).....	74
Figure 4.24 : Kinetic energy-time graph of foam sandwich beam – non-bonded (Case 4).....	75
Figure 4.25 : Velocity-time graph of hollow beam (Case 3).....	75
Figure 4.26 : Velocity-time graph of foam sandwich beam-bonded (Case 4).....	76
Figure 4.27 : Velocity-time graph of foam sandwich beam – non bonded (Case 5).....	76
Figure 4.28 : Velocity-time graph of foam sandwich beam-rigid and non-bonded (Case 6).....	77
Figure 4.29 : Acceleration-time graph of hollow beam (Case 3).....	78
Figure 4.30 : Acceleration-time graph of foam sandwich beam - bonded (Case 4).....	78
Figure 4.31 : Acceleration-time graph of foam sandwich beam - non-bonded (Case 5).....	79
Figure 4.32 : Acceleration-time graph of foam sandwich beam- rigid and bonded (Case 6).....	79
Figure 4.33 : Maximum deformation of two-channel hollow beam (Case 7).....	80
Figure 4.34 : Maximum deformation of two-channel foam sandwich beam (Case 8).....	81
Figure 4.35 : Energy graph of two channel beam (Case 7).....	82
Figure 4.36 : Energy graph of two channel foam sandwich beam (Case 8).....	82
Figure 4.37 : Reaction force-time graph of two channel hollow beam (Case 7).....	83
Figure 4.38 : Reaction force-time graph of two channel foam sandwich beam (Case 8).....	83
Figure 4.39 : Velocity-time graph of two channel hollow beam (Case 7).....	84
Figure 4.40 : Velocity-time graph of two channel foam sandwich beam (Case 8).....	84
Figure 4.41 : Acceleration-time graph of two channel hollow beam (Case 7).....	85
Figure 4.42 : Velocity-time graph of two channel foam sandwich beam (Case 8).....	85
Figure 4.43 : Kinetic energy graph of two channel hollow beam (Case 7).....	86
Figure 4.44 : Velocity-time graph of two channel foam sandwich beam (Case 8).....	87

List of Symbols

σ	-----	Stress (N/m ²)
ϵ	-----	Strain
γ	-----	Shear strain
$\dot{\epsilon}$	-----	Strain rate (mm/sec)
E	-----	Elastic modulus (N/m ²)
G	-----	Shear modulus (Pa)
G ₀	-----	Shear modulus at t = 0
G [∞]	-----	Long term Shear modulus (at t = ∞)
δ	-----	phase lag
τ	-----	Shear stress (N/m ²)
λ	-----	Relaxation time (sec)
η	-----	Viscosity (m ² /s)
G _i	-----	Relaxation strength
α	-----	Porosity
V _s	-----	Specific volume of material at solid state (m ³)
V	-----	Specific volume of material at porous state (m ³)
ν	-----	Poisson's ratio
C ₀	-----	Bulk wave speed (m/sec)
C _s	-----	Wave speed in solid (m/sec)
P _e	-----	Maximum elastic pressure (N/m ²)
P _s	-----	Hydrostatic pressure (N/m ²)
ρ_0	-----	Porous density Polyurethane foam (kg/m ³)
ρ_s	-----	Solid density of Polyurethane foam (kg/m ³)
σ_h	-----	Yield strength (N/m ²)
G	-----	Grueisen coefficient
s	-----	Grueisen constant
PU	-----	Polyurethane

Abstract

Polyurethane foams are used nowadays for vibration attenuation and energy absorption during impact applications. They are widely used in aerospace and automotive field due to its light weight and good energy absorption capabilities. Therefore, it is interesting to analyze these materials from the point of view of vibration attenuation and impact absorption properties.

Polyurethane foam consists of two types, i.e., flexible polyurethane foam and rigid polyurethane foam. Each type is further divided into two types which are based on type of cells. These cells can be open type or closed. The mechanical properties of Polyurethane foam can be found through empirical formulas in the book "Cellular Solids: Structure and Properties" written by Gibson and Ashby. The mechanical properties of foam materials depend on the initial density as these materials are porous. Therefore, mechanical behavior of these foams depends on the amount of porosity. Moreover, these materials are compressible and exhibits the property of viscoelasticity. The viscoelasticity property is represented by the Prony series, which shows the linear viscoelasticity. The Prony series parameters are determined from different models and can be represented in time domain or frequency domain. At high strain-rates the linear viscoelasticity assumption doesn't hold good and is, therefore, required to use non-linear viscoelasticity approach. The compressible behavior of the foams is captured by using other models such as Blatz-Ko, Ogden foam etc. Among all the models the Ogden foam is popular and have been used widely in the literature.

In this thesis, the impact analysis of different configuration of beams are simulated in the Ansys software V19.1 student license. The beam configuration can be found in different mechanical applications such as turbine blades, wing of an aero-plane, industrial robotic arms and front bumper beam of cars. In this analysis the beam dimensions and loading is simulated by keeping in view the front bumper beam of vehicles and the objective is to minimize the deformations, accelerations of the body and the reaction forces at the support which ultimately causes the reduction in the acceleration experienced by the passengers during impact. The Ansys student license has the limitation in terms of number of elements in meshing, number of bodies and number of faces. In the analysis, the hollow beam and rigid body are modelled in Ansys Design modeler. The rigid body is considered to collide (impact) the beam with a velocity of 15 m/s (54 km/h). The effect of the collision on beam such as deformations, reaction forces, velocity and accelerations with respect to time are studied. The hollow beam is then replaced by the foam sandwich beam in which Polyurethane foam is considered as a core material. Both the contact type in which the foam is bonded and non-bonded with a coefficient of friction is analyzed and the differences in

the behavior of the beam are studied. In this analysis, two types of geometry are considered for beams. One is simple hollow beam and the other is two-channel hollow beam. Similarly, two types of foam-sandwich beams are considered. The one is simple foam sandwich beam while the other is two-channel foam sandwich beam. Furthermore, two different densities, i.e., 40kg/m^3 and 93kg/m^3 of the flexible polyurethane foam are analyzed in order to see the differences and dependence of results on foam density. Moreover, a rigid polyurethane foam of density 93kg/m^3 is also analyzed and compared with the flexible polyurethane foam of the same density.

The beam is considered fixed at both the ends and the initial velocity of 15 m/s is given to a rigid body, which strikes the beam structure. The solver used for this analysis is Autodyn. The output points are increased from 30 to 150 and sweep type mesh is considered. The number of elements are increased in order to obtain good results.

The viscoelasticity of polyurethane foam 40kg/m^3 is modelled in the FEM through 8 - term Prony series parameters, which includes 8 pair of relaxation modulus and relaxation time. These parameters are found in the previous research paper which is conducted on the 40kg/m^3 flexible polyurethane foam and the Prony-parameters are determined. In the literature, different scholars have shown the P-alpha model captures the response of the material to a high degree of accuracy, therefore, in the analysis this model will be used which is also supported in Ansys. The rigid polyurethane foam is modelled through P-alpha model and Hugoniot shock data. The data is obtained from the book "**LASL SHOCK HUGONIOT DATA**" by Stanley P. Marsh.

Different results after impact such as maximum deformations, reaction force-time history, and the acceleration attenuation of the beams are evaluated. The comparison is made between the hollow beams and the foam sandwich beams. The results show that the maximum deformation, reaction force-time history and acceleration levels are less in the foam-sandwich beams as compared to the hollow beam of same weight.

Acknowledgements

I would first like to say thanks and express my sincere gratitude towards my advisor Prof. Marco Gherlone for his guidance, continuous support, motivation, and immense knowledge. His guidance helped me throughout my thesis period, in all the time of research and writing of this thesis. During this period, I could not imagine having a better mentor and advisor for my Master thesis.

1. Introduction

1.1 Motivation

Damping is a material attribute and can be defined as loss of energy. It refers to the extraction of mechanical energy from the vibratory system and its conversion to heat energy by dissipation. It is effective in the applications where it is needed to control the amplitudes of vibration, i.e., dissipation of vibration of the body by internal damping. Numerous applications have been developed in various industries to control the vibrations. One of the special class are sandwich structures.

The sandwich structures are composite systems having low weight and high stiffness in static applications while having high damping in dynamic application. It consists of two stiff skins and a core material, which is usually light. Damping in sandwich structures depends on the core material. There are numerous materials that can be used as core like wood, honeycomb, polymer foams etc. The selection of core material depends on the application and service of the structure. One of the important class of core materials are polymer foams which exhibits both hyper elasticity as well as viscoelasticity and are considered as soft-core materials. The consideration of soft-core materials requires high energy to deform due to internal damping and is known as sandwich treatment. It reduces the amplitude of the oscillation depending on the mechanical properties and volume of core layer in the structure.

Foam materials have a good capability of storing energy when they are deformed in compression. These types of materials exhibit characteristic of both elastic solid and viscous fluid. Such type of behavior is due to the large molecular order and tangled molecules in polymer. In these materials, the mechanical energy is released through cyclic shear and normal deformation. Mostly all polymers ranging from natural rubber to thermoset materials show viscoelastic behavior.

The sandwich structures with viscoelastic core are widely used in applications such as satellites, construction, marine, railroads, automobiles, and sport industry. Due to the use of viscoelastic core, the sandwich structures exhibit time-dependent behavior. Therefore, the response of the viscoelastic materials is not only determined by the current state of load but also by the load-time history.

Polyurethane foam is widely used in automotive industry, packaging and sport industry due to its ability to absorb strain energy and compressibility. Due to excellent behavior in compression and ability to absorb energy, these materials need to be explored in impact applications.

1.2 Problem Statement

In this research, the polyurethane foam is selected as a core material and Structural steel as skin of the sandwich structure. The dimensions of the beam are kept constant and are discussed in the third Chapter. The objective of this work is to simulate the impact response of polyurethane foam sandwich structure in Ansys by using the parameters of viscoelastic and hyper-elastic material parameters of polyurethane foam while keeping the focus on absorbed energy, velocity and acceleration-time histories.

1.3 Research Objective

The objective of this thesis is to determine the response of foam sandwich structures during impact loading by using Finite element simulation software. The objective of this thesis is to learn about

- i. The mechanics of foam materials, their properties and dependence on important parameters.
- ii. To model the foam material in Finite element analysis software, i.e., different models used to describe the foam behavior.
- iii. Learn the FEA steps necessary to perform transient structural and explicit dynamics analysis
- iv. Analyze and compare the deformations, velocities, accelerations and draw necessary conclusions.

1.4 Outline of the thesis

Chapter 2 is review of literature, which gives all the research backgrounds and useful information about this thesis. In this chapter, the concepts of hyper-elasticity and Viscoelasticity is explained. There are different models to capture the hyper-elasticity and viscoelasticity of polymer materials (including foams) and all the models are discussed here. The previous research work related to the mechanical behavior of such type of materials and the necessary constitutive equations are also discussed in the chapter.

In chapter 3, different configuration of the beam is simulated and analyzed by using Ansys software. In this chapter the dimensions of different configuration of the beam and important dimensions are discussed. Explicit Dynamic Analysis (EDA) applied in the FE model. Some vital parameters are discussed which are used to get simulations results. The engineering data parameters and the simulation steps necessary for the simulation are discussed.

In Chapter 4 and Chapter 5, results and conclusions are discussed. The results of different configuration of beams are compared to each other. The comparison is based on some important output variables such as internal energy and kinetic energy dissipation, velocity and acceleration dissipation with respect to time, reaction forces-time curves. The main objective here is to compare the hollow and foam sandwich beams and to find the better alternative.

2. Literature Review

2.1 Introduction

The mechanical behavior of polymer materials under large strain levels and different strain-rate is more complicated. The stress-strain response of such material shows hyper-elastic behavior as well as viscoelastic behavior. The accurate modeling of hyper-viscoelastic materials is a key issue due to their non-linear stress-strain relationship. This is because they are amorphous and comprised of long molecular chains. These chains are highly twisted and randomly oriented in undeformed state. During loading, these chains become untwisted and straightened; when load is removed the chains revert to their original configuration. Mostly the starting point for modeling of hyper-viscoelastic materials is strain energy function and through constitutive equations, their properties are defined. The constitutive equations are the mathematical relation between the stress and strain. In such materials the stress is dependent on other factors rather than the strain, like temperature, strain rate, frequency in case of cyclic loading. Therefore, in literature there are different types of constitutive models developed to model the behavior of such type of materials.

The first model was developed by Kuhn in (1936) [1]; he derived the relation between molecular weight of the chains and the elastic modulus. Mooney [2] investigated the large elastic deformation and is considered as earliest work in this subject. It was later developed by Rivlin [3] and is called Mooney-Rivlin model.

Later, Rivlin and Sanuders [4], introduced an important development in which they adopted the procedure of choosing the conjugate values of λ_1 and λ_2 in the biaxial strain experiment. The experiment was done in such a way that one of the two strain invariants were varied while keeping the other one constant.

In uniaxial compression, polyurethane foam shows the hysteretic response during unloading after prior loading in uniaxial compression. The stress during unloading is less than the loading with the same strain rate. Because of the viscoelastic behavior, the polyurethane foam cannot recover immediately when the load is released. To capture the viscoelastic phenomena, Yang et al [5] developed a visco-hyperelastic model.

2.2 Models for Hyper-elasticity and Viscoelasticity

There are different models used to describe the behavior of hyper-elasticity and viscoelasticity in polymer materials. These models developed with the passage of time to capture the behavior of these materials accurately even at large strain-rates. Each model has some limitations and advantages over the other and it completely depends upon the applications and type of material class. For example, the Neo-hookean model is a hyper-elastic material model and one of the earliest models used to predict the response of hyper-elasticity [6]. It is based on statistical thermodynamics approach and the model is first order material model. The advantage of this model is that it is easy to use and only a single experiment is needed to use this model which makes it a low-cost material model. The disadvantage is that it does not accurately predicts the material response at high strain rates and is not recommended for the application in which the strain-rate is high, i.e., for more than 30% strain-rate, it can't be used. In contrast to this, the Ogden model accurately predicts the response of the material at high strain rates, i.e., at 700% [7] but is highly costly to use it due to the need of mechanical test data of at-least four different experimental tests. Similarly, some of the models are best for predicting the response of foam materials such as Blatz-Ko and Ogden foam etc.

2.2.1 Hyper-elasticity

The hyperelastic material is also called green elastic material. In the constitutive model for hyper-elastic material, the stress-strain relationship can be derived from strain energy density function. The hyperelastic material is a special case of a Cauchy elastic material. It is important to mention that linear elastic models don't work in capturing the behavior of the hyper elastic materials, e.g., rubber behavior can be defined as isotropic, incompressible, non-linear elastic and independent of strain-rate. An unfilled, vulcanized elastomer is an example of closely hyperelastic ideal. Melvin Mooney and Ronald Rivlin were the pioneers in developing the hyperelastic models, i.e., Neo-Hookean and Mooney-Rivlin solids. Other widely used hyperelastic models are Arruda-Boyce model and Ogden model. [8]

2.2.1.1 Constitutive Models for Hyper-elasticity

There are many hyperelastic models in the literature such as 2 term Mooney-Rivlin, 3-term Mooney-Rivlin, 5 term Mooney-Rivlin, Neo Hookean, 3 -term Ogden Model. They are represented by the strain energy function. For example, The strain energy density function for an incompressible neo-Hookean material in a three-dimensional description is Neo-Hookean [9]

$$W = \frac{\mu}{2}(I_1 - 3)$$

where μ = material constant

I_1 is the first invariant (trace), of the right Cauchy-Green deformation tensor

Similarly, Mooney-Rivlin model is also used frequently. The strain energy function of the two-term Mooney-Rivlin model can be expressed as:

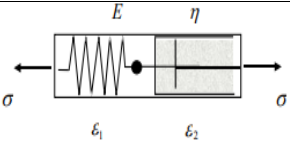
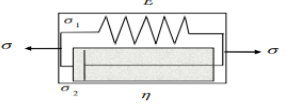
$$W = C_{10}(I_1 - 3) + C_{01}(I_2 - 3)$$

Where C_{10} and C_{01} are empirically determined material constants, and I_1 and I_2 are the first and the second invariant.[10]

The other models used widely are Ogden Model, Yeoh model, Arruda-Boyce and Gent model

2.2.2 Constitutive Models for Linear Viscoelasticity

There are different rheological models of linear viscoelasticity:

S/No	Models	Representation [11]	Uses [11]
1	Maxwell Model		Good with modeling relaxation in materials but not good in modeling creep in materials
2	Kelvin-Voigt model		Good with modeling creep in materials but not good in modeling relaxation in materials

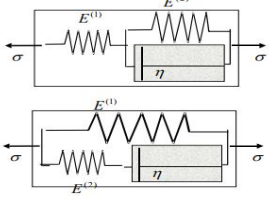
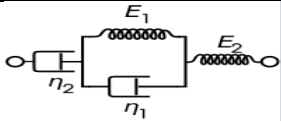
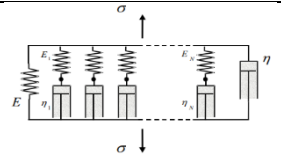
3	Standard Linear solid model or Zener Model		Good in modeling relaxation as well as creep in materials but gives inaccurate results for strain under specific loading conditions.
4	Burgers Model		Used for creep behavior of materials
5	Generalized Maxwell model		Most general form of the linear model for viscoelasticity used mainly for relaxation behavior of materials

Table 2-1 : Constitutive models for linear viscoelasticity

2.3 Elastic, Ideal Viscous and Viscoelastic behavior

2.3.1 Elastic Behavior

An ideal elastic solid follows the Hook's law in which stress is proportional to strain. In this case stress and strain are in phase to each other, i.e., if an elastic solid is subjected to sinusoidal strain, the result will be the sinusoidal stress which will be in phase to the strain.

2.3.2 Ideal Viscous Liquid

Liquid like behavior can be described by a Newtonian model, i.e., representing by using dashpot as shown in the figure. A Newtonian fluid is a fluid in which the shear stresses are linearly proportional to shear strain rate. The constant of proportionality is called viscosity. In ideal viscous liquid the stress is 90° out of phase with the strain. The reason is that viscous liquid is incapable of storing input energy.

The diagram of the pure elastic (stress in-phase) and ideal viscous (stress out-phase) is shown as:

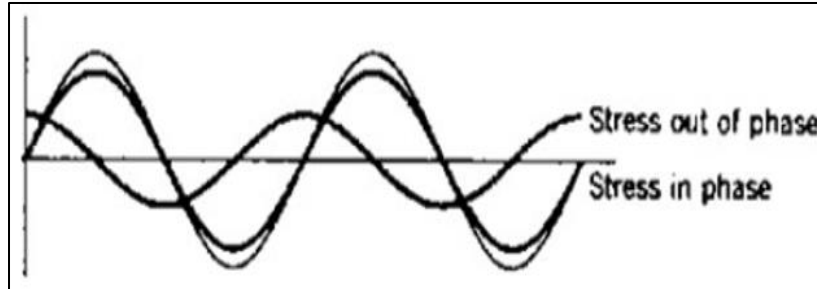


Figure 2.1 : Stress-strain phase diagram of elastic behavior vs ideal viscous liquid [12]

2.3.3 Viscoelastic Material

The viscoelastic materials have the dynamic behavior in between the pure elastic and pure viscous. Therefore, we can easily resolve the response of the material that is 90° out of phase (ideal viscous) and into the component in which the response is in phase with the applied strain (pure elastic). The diagram of the viscoelastic, pure elastic and ideal viscous is shown as:

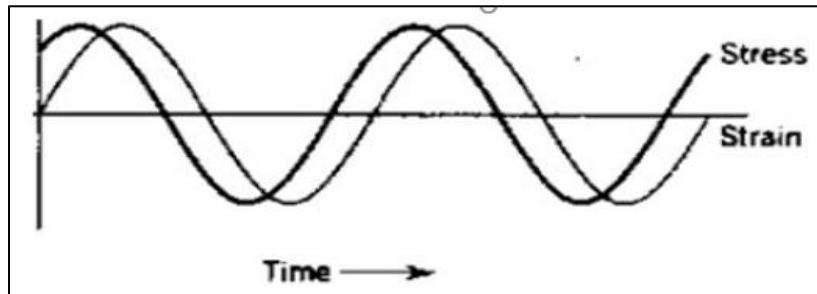


Figure 2.2 : Stress-strain phase diagram of Viscoelastic material [12]

2.3.3.1 Elastic Vs Viscoelastic Behavior

A viscoelastic material has two components, **Elastic component** and **Viscoelastic component**. Purely elastic materials don't dissipate energy when they are loaded and then removed while viscoelastic materials dissipate the energy when the load is applied and then removed, which is called **Hysteresis**. Hence a viscous material will lose energy through a loading cycle.

Viscoelasticity is the molecular arrangement. When the load is applied on the polymer, some parts of polymer chain changes positions. This movement of the polymer chains or rearrangement is called creep. When these chains are rearranging the polymer remains a solid. To accompany the

applied stress, these rearrangement of polymer chains creates a back stress in the material. When this back-stress is equal to the applied stress in magnitude, the material no longer creeps. When the material is unloaded, i.e., stress is taken away the accumulated stress caused the polymer to return to its original shape and fully recovers. So, this is the reason that such type of material is called viscoelastic material because they possess both creep and elasticity.

2.4 Viscoelasticity

Viscoelasticity is the property of the material that exhibits both elastic as well as viscous characteristics while undergoing deformation. The elastic material when stretched; returns to its original position when the force is removed. The viscous material such as water, oil etc., resists the shear stress linearly with time when the stress is applied.

Viscoelastic materials exhibit time-dependent strain. Viscoelasticity is the behavior of the material that exhibits time-dependent or strain-rate dependent response to applied stress. This property can be often found in polymers, e.g. Elastomers, Polyurethane foam etc. Viscoelastic materials exhibit stress relaxation, creep and hysteresis.

2.4.1 Types of Viscoelasticity

There are two types of viscoelasticity:

2.4.1.1 Linear Viscoelasticity

The creep and relaxation function are only time-dependent. In a linear viscoelastic material, the relaxation is proportional to the applied strain. Linear viscoelasticity is applicable for small deformations such that polymers are slightly disturbed from equilibrium configuration. Under these conditions stress is linearly proportional to strain as shown:

$$\sigma(t) = G(t) \gamma_0 \quad 2.1$$

Dynamic measurements are used to examine Linear viscoelasticity in polymers by examining the dynamic elasticity as a function of time and temperature. Mostly, we impose a small sinusoidal shear strain and measure the stress or vice-versa.

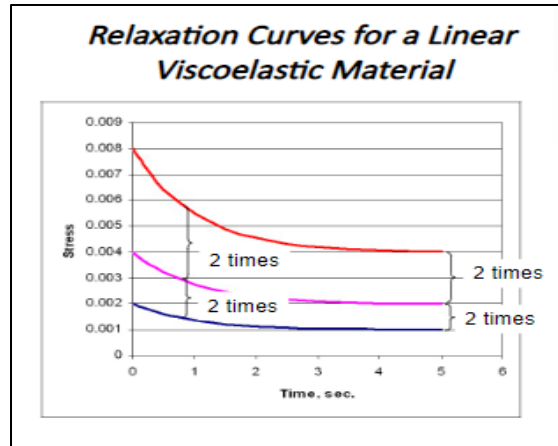


Figure 2.3 : Relaxation curves for a linear viscoelastic material [13]

2.4.1.2 Non-linear Viscoelasticity

The creep and relaxation function are time dependent as well as stress or strain dependent. When the deformations are large, the material properties change and thus assumption of linear viscoelasticity cannot be used in such case.

2.4.2 Time-dependent Responses of Viscoelastic Material

Polymers respond different to different type of time-dependent loading:

- i. Instantaneous elasticity
- ii. Relaxation (constant strain)
- iii. Creep (constant stress)

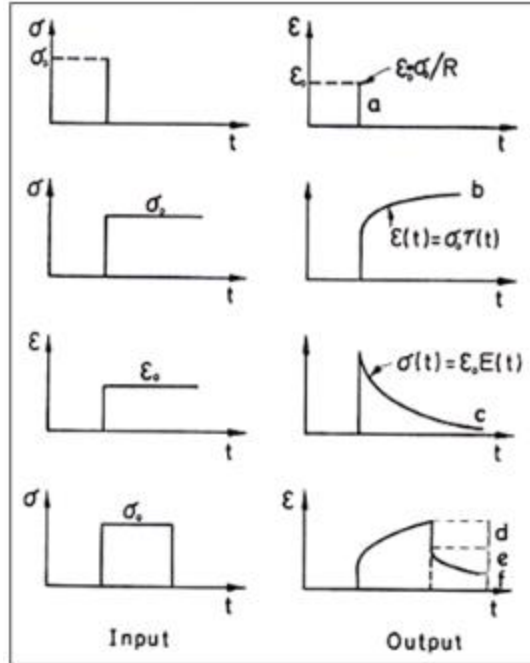


Figure 2.4 : Creep and Relaxation of Non-linear Viscoelastic material [14]

2.4.2.1 Stress Relaxation

When the viscoelastic material is subjected to constant strain, the stresses in the material will relax with the passage of time and at the last, it will attain a steady state value as shown in the diagram:

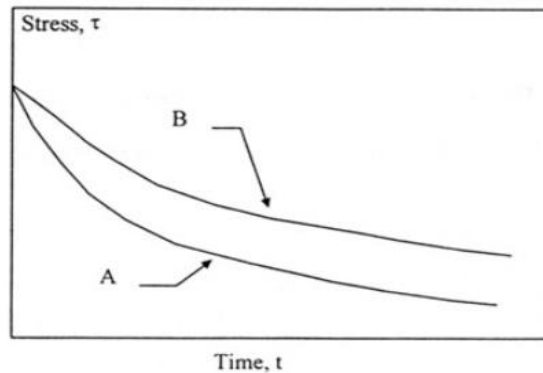


Figure 2.5 : Stress relaxation in polymer A vs polymer B [12]

In the above figure, polymer B relaxes slower as compared to polymer A, as a result of greater elasticity.

The relaxation modulus can be defined as:

$$\text{Tension: } \frac{\sigma}{\varepsilon_0} = E \quad 2.2$$

$$\text{Shear: } \frac{\tau}{\gamma} = G \quad 2.3$$

2.4.2.2 Creep Compliance

Viscoelastic materials experience a time dependent increase in strain when subjected to a step constant stress. This phenomenon is also known as viscoelastic creep. The viscoelastic material creep when subjected to a constant stress, i.e., strain will continue to increase to a steady state value. In linear viscoelastic material, the creep response is proportional to the applied stress as shown in the figure.

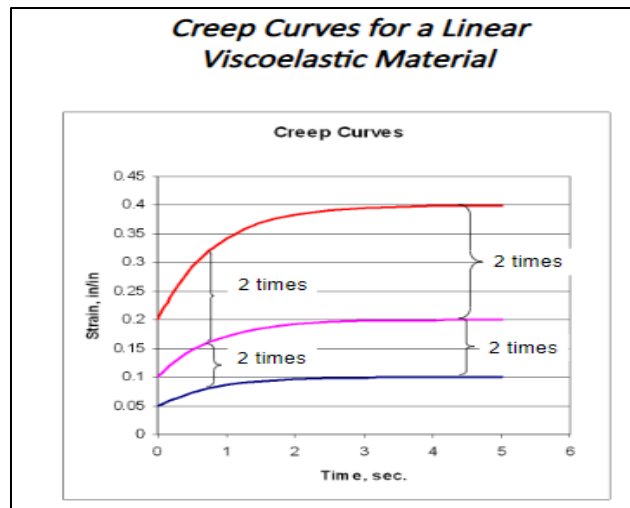


Figure 2.6 : Creep curves for a Linear Viscoelastic material [13]

The creep compliance can be defined as:

$$\frac{\sigma}{\varepsilon} = J \quad 2.4$$

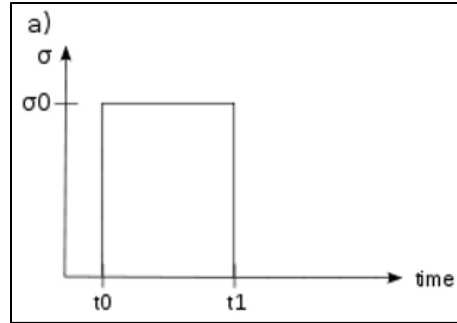


Figure 2.7 : Applied Stress input [11]

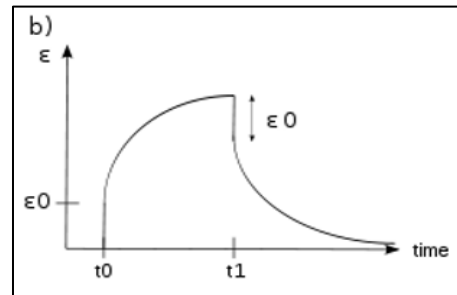


Figure 2.8 : Induced strain output in Viscoelastic material [11]

In the above figure, we can see that if the material is stressed at $t = t_0$ and the stress is maintained for a long time period. If it is for the viscoelastic liquid, the material will strain when the stress is applied that increases until the material fails. When the stress is maintained for a shorter period, the material undergoes initial strain at $t = t_1$. After t_1 , the strain immediately decreases and then gradually decreases when $t > t_1$ to a residual strain.

2.4.3 Dynamic modulus

Dynamic modulus is the property of viscoelastic material and can be defined as “Ratio of stress to strain under vibratory condition”. Dynamic modulus is calculated from the free or forced vibration test data under elongation, compression or shear. In viscoelastic material, the stress and strain can be represented as following equations:

$$\text{Strain: } \epsilon = \epsilon_0 \sin(\omega t) \quad 2.5$$

$$\text{Stress: } \sigma = \sigma_0 \sin(\omega t + \delta) \quad 2.6$$

where

$$\omega = 2\pi f \quad 2.7$$

f is frequency of strain oscillation

t is time

δ is phase lag between stress and strain

In this way the static Young modulus is replaced by the complex dynamic modulus and can be written as sum of in-phase modulus (also called storage modulus) and out of phase modulus (also called loss modulus)

$$G^* = G' + iG'' \quad 2.8$$

The in-phase modulus represented by G' reflects the elastic component of viscoelastic material's response to the applied strain (stored energy). The out-of-phase modulus represented by G'' reflects the viscous component (dissipated as heat) of material response to the applied strain.

The storage and loss modulus can be written either in form of tensile storage (or loss) or shear storage as shown by following equations:

$$\textbf{Tensile: } E^* = E' + iE'' \quad 2.9$$

$$\text{i. Storage: } E' = \frac{\sigma_0}{\varepsilon_0} \cos \delta \quad 2.10$$

$$\text{ii. Loss: } E'' = \frac{\sigma_0}{\varepsilon_0} \sin \delta \quad 2.11$$

$$\textbf{Shear: } G^* = G' + iG'' \quad 2.12$$

$$\text{i. Storage: } E' = \frac{\sigma_0}{\varepsilon_0} \cos \delta \quad 2.13$$

$$\text{ii. Loss: } E'' = \frac{\sigma_0}{\varepsilon_0} \sin \delta \quad 2.14$$

where σ_0 and ε_0 are the amplitudes of stress and strain respectively and δ is the phase shift between them.

2.4.3.1 Loss Tangent

In viscoelastic material, the ratio between a storage and loss moduli is defined as $\tan \delta$, which represents the damping in the material. For example, a material with greater $\tan \delta$, than the other will have more damping. The reason that $\tan \delta$ greater than 1 shows more damping because the loss modulus is greater than the storage modulus. It means that the material is dissipating energy more than it is storing.

2.4.4 Constitutive models for Linear Viscoelasticity

Most of the polymers shows the viscoelastic behavior such as amorphous polymers, biopolymers, semi-crystalline polymers and even the living tissue and cells. Viscoelastic materials can be modeled to determine the force and displacements or stress and strains. The models used for viscoelastic behavior are Maxwell model, Kelvin-Voight model, Burgers Model and Standard linear solid model. These models predict the material response to different loading conditions. The viscoelastic behavior can be divided into elastic behavior and viscous behavior and these behaviors are represented by connections of spring and dashpots. In each model discussed the arrangement of these elements are different and all these viscoelastic models can be modeled as electrical circuits.

The elastic component can be modeled as spring while the viscous component can be modeled as dashpot, given the formula

i. Spring $\sigma = E\epsilon$ 2.15

ii. Dashpot $\sigma = \eta \frac{d\epsilon}{dt}$ 2.16

The stress-strain relationship for a specific stress rates can be simplified. For example, if the stress state is high or the time period is very short, the time derivative components of the stress–strain relationship dominate. A dashpot resists changes in length, and in a high stress state it can be approximated as a rigid rod. Since a rigid rod cannot be stretched past its original length, no strain is added to the system.

In opposite to this, for low stress states/longer time periods, the time derivative components are negligible, and the damper can be effectively removed from the system. As a result, only the spring connected in parallel to the dashpot will contribute to the total strain in the system.

2.4.4.1 Maxwell Model

The Maxwell model can be represented by series connection of purely elastic spring and purely viscous damper as shown in the diagram.

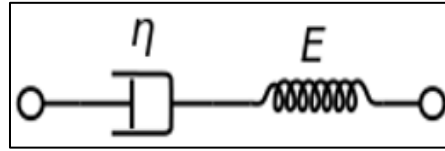


Figure 2.9 : Maxwell model - Series connection of spring and damper [11]

The deformation rate in the Maxwell model is equal to the sum of the deformation rate of spring and dashpot. Mathematically

Total shear strain = Shear strain (dashpot) + Shear strain (spring)

$$\dot{\gamma} = \frac{\tau}{\eta} + \frac{\dot{\tau}}{G} \quad 2.17$$

$$\eta\dot{\gamma} = \tau + \frac{\dot{\tau}\eta}{G} \quad 2.18$$

$$\tau + \dot{\tau}\lambda = \eta\dot{\gamma} \quad 2.19$$

Where $\lambda = \frac{\eta}{G}$ is called the **relaxation time**, η is **viscosity** $\dot{\gamma}$ is **shear strain rate**, and G is **shear modulus**.

If the mechanical model is suddenly extended to a position and held there ($\dot{\gamma} = 0$), then the final equation becomes as

$$\tau = \tau_0 e^{\frac{-t}{\lambda}} \quad 2.20$$

where λ is the “relaxation time” and τ_0 is shear stress at time 0.

The Maxwell model can be represented by the following equation

$$\sigma + \frac{\eta}{E}\dot{\sigma} = \eta\dot{\epsilon} \quad 2.21$$

Under this model, if the material is put under the constant strain, the stresses relax gradually. If the material is put under constant stress, the strain has two components. The spring which

represents the elastic component stretches instantaneously and relaxes immediately if the load is removed. In contrast to the spring, the damper which represents the viscous component gradually grows with the time if the stress is applied.

The Maxwell model predicts that stresses decay exponentially with time, which is accurate for most polymers. The limitation of this model is that it does not predicts the creep accurately. Because the model predicts that the response of the material under constant stress will increase with the time. However, experimental results of most of the polymers shows that strain rate decrease with the time.

2.4.4.2 Kelvin–Voigt model

It is also known as Voigt model and this model consists of Hookean elastic spring and Newtonian damper in parallel connection as shown in the figure. The schematic representation of kelvin-Voigt model is shown in the figure

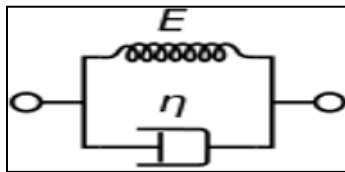


Figure 2.10 : Kelvin-Voigt model: Parallel combination of spring and damper [11]

The kelvin-Voigt model can be represented by the following equation:

$$\sigma = E\varepsilon + \eta\dot{\varepsilon} \quad 2.22$$

where σ = stress, η = viscosity, ε =strain

Upon application of a constant stress, the material deforms at a decreasing rate, asymptotically approaching the steady-state strain.

This model also has some limitations as this model is extremely good in predicting the material response under constant stress, i.e., creep but doesn't predict accurately the behavior of the material under constant strain.

The applications of this model are: rubber, organic polymers, wood etc.

Response	Maxwell	Kelvin-Voigt
Creep	Bad	Good
Relaxation	Good	Bad

Table 2-2 : Maxwell vs Kelvin-Voigt model in Creep and relaxation

2.4.4.3 Standard Linear Solid Model

It is also known as Zener model and it consists of two springs and one dashpot. It is the simplest model that predicts the stress relaxation and creep behaviors of the viscoelastic materials. For this model, the governing constitutive relations are:

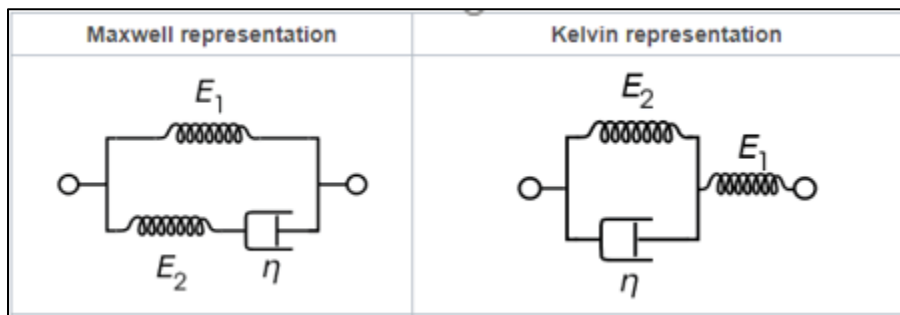


Figure 2.11 : Zener model or Standard linear model [11]

It can be seen from the model that under constant stress, the modeled material will deform to some strain which is the instantaneous strain part. After that it will continue to deform and approach the steady-state strain. This model predicts the material response more accurately than the Maxwell model and Kelvin-Voigt model but for a certain specific loading conditions, it returns inaccurate results for strains.

2.4.4.4 Burgers Model

This model is the combination of Maxwell and Kelvin-Voigt model in series as shown in the figure

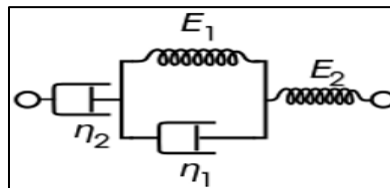


Figure 2.12 Burgers Model [11]

2.4.4.5 Generalized Maxwell model

The Maxwell model is conceptually reasonable, but it does not fit the data very well. This is the reason, we use generalized Maxwell model. It is the most used form of linear model for the viscoelasticity and also known as Maxwell-Weichert model. In this model, the series connection of several spring and dashpot which are normally called Maxwell elements are assembled in parallel. The reason for this is that in a viscoelastic material the relaxation doesn't at a single time, but in a set of time. This varying time contribution is due to the presence of different lengths of molecular segments in the material. These different lengths contribute different and hence there is varying time distribution. The schematic representation of the generalized Maxwell model is shown in the figure

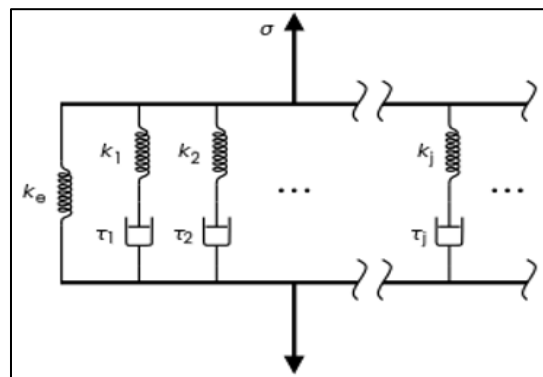


Figure 2.13 : Generalized Maxwell model [11]

The relaxation of every element is:

$$\tau_i = (G_i \gamma_0) e^{-\frac{t}{\tau_i}} \quad 2.23$$

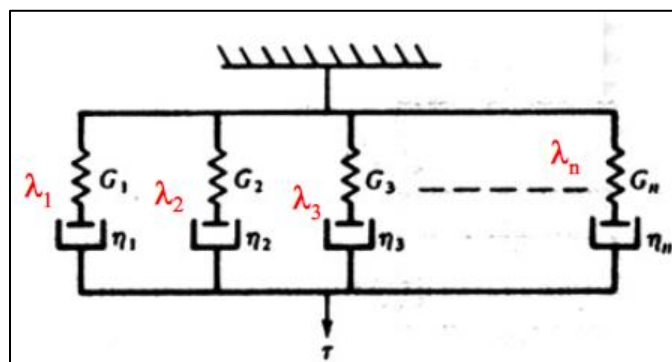


Figure 2.14 : Relaxation elements [12]

The relaxation of the generalized model is:

$$\tau = \sum_{i=1}^n \tau_i = \gamma \sum_{i=1}^n G_i \cdot e^{-\frac{t}{\lambda_i}} \quad 2.24$$

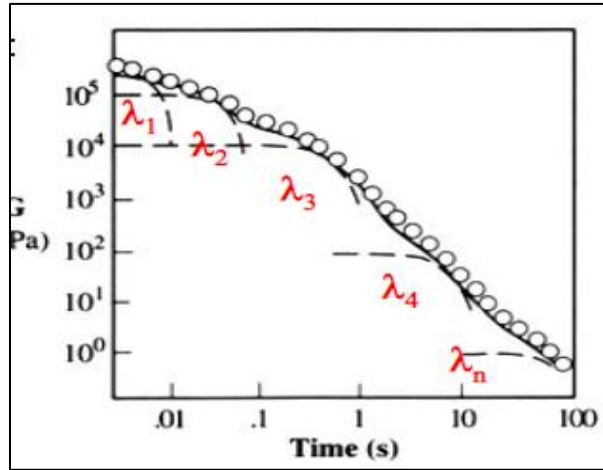


Figure 2.15 : Relaxation curve with different relaxation time [12]

$$G = \frac{\tau}{\gamma_0} = \sum_{i=1}^n G_i e^{-\frac{t}{\lambda_i}} \quad 2.25$$

Where $G(i)$ is a weighting constant or also called “relaxation strength” and λ the “relaxation time”.

2.4.5 Prony Series

In 1d relaxation test, a material is subjected to constant strain and this strain is kept constant over time., while the stress is measured over time. The initial stress is due to elastic response of the material, while after some time the stress relaxes due to viscous effects in material. The strain type can be tensile, compression, shear, or bulk compression. The resulting stress vs time history plot can be fitted with several equations, called models. In the equation, only the notation changes with different type of strains applied, e.g., E is used in tensile-compression relaxation. G is used for shear strain, K is used for bulk. The Prony series for the shear relaxation can be expressed as:

$$G = G_{\infty} + \sum_{i=1}^n G_i e^{-\frac{t}{\tau_i}} \quad 2.26$$

where G_{∞} = long term modulus when the material is relaxed totally

T_i = relaxation time

The higher the value of the relaxation time, i.e., T_i , the longer it will take the time for the stress to relax. The minimization algorithm is used during fitting the data to the equation that adjust the parameters G_∞ , G_i , T_i to minimize the error between actual data and predicted curve-fitting.

Sometimes an alternative form is used in which elastic modulus, i.e., modulus at $t = 0$ is related to long term modulus such as:

$$G(t = 0) = G_0 = G_\infty + \sum_{i=1}^n G_i \quad 2.27$$

Therefore,

$$G(t) = G_0 - \sum_{i=1}^n G_i \left(1 - e^{-\frac{t}{T_i}}\right) \quad 2.28$$

where G_0 = elastic shear modulus

The above equation is useful when the G_0 is obtained independently from relaxation test data and when desired to specify elastic properties separately from viscous properties.

Usually creep experiment is easier than the relaxation one but there is no closed form of for creep in terms of coefficient of the Prony series. So, it's not easy to get Prony coefficients for creep (compliance) data as compared to the relaxation test data.

2.4.6 Effect of Temperature on Viscoelastic Behavior

The viscoelastic properties of the viscoelastic material changes with increasing or decreasing temperature. The reason for this is that due to thermal motion, the secondary bonds constantly breaks and reforms. In most cases the creep modulus (applied stress/time-dependent strain) decreases with increasing temperature or, at higher temperature it takes less time to stretch a viscoelastic material at an equal distance at higher temperature as compared to lower temperature.

Extreme cold temperature can cause the material to behave as brittle because the viscoelastic materials change to glass phase at lower temperature.

2.4.7 Dynamic mechanical analysis

Dynamic mechanical analysis (also abbreviated as DMA) is used to study the Viscoelasticity. In such analysis, a small oscillatory stress is applied, and the resulting strain is measured. This allows to determine the complex modulus. The dynamic mechanical analysis machine is shown in the figure

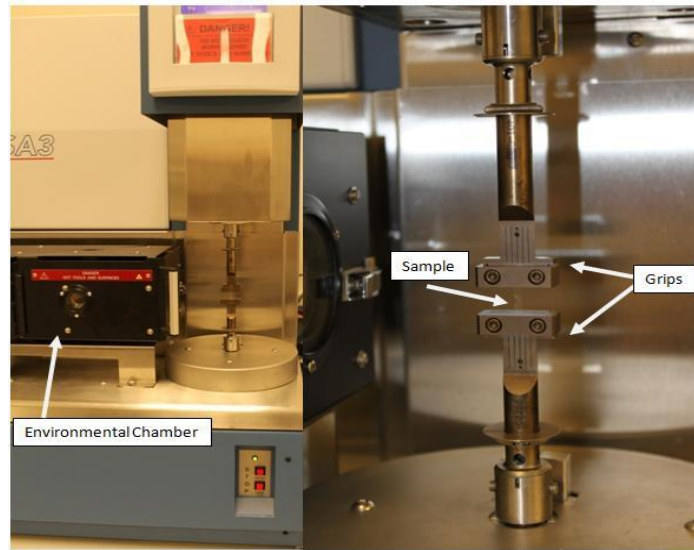


Figure 2.16 : Dynamic mechanical analysis testing machine [15]

2.5 P-alpha EOS

An equation of state is a thermodynamic equation, which provides a mathematical relationship between two or more state functions associated with the matter, such as its temperature, pressure, volume, or internal energy.

There are many other compaction models for modeling the behavior and distribution of stresses in porous materials such as foams, powders etc. Although these compaction models predict the behavior and give good results for low stress levels and low α materials but for large stress levels, it does not give good results. Therefore, it is desirable to obtain a formulation which can give good results at high stress levels and for large variety of porous materials.

The p-alpha EOS model was developed by Hermann. The Hermann model describes reasonable accurate behavior at high stress levels and as well as at low stress levels. The assumption in this model is that specific internal energy is same for material at solid density and for porous material at identical condition of temperature and pressure. According to this model the porosity can be defined as:

$$\alpha = \frac{v}{v_s} \quad 2.29$$

Where V_s is the specific volume of the material in solid state and V is the specific volume of the material at porous state. When the material is fully compressed, then $\alpha = 1$.

Next step is to define the bulk sound speed and how it depends on the initial density ρ_0 of the foams. According to Gibson and Ashby, the Young's modulus for open cell foams vary with the square of the density, while Poisson's ratio remains constant. In the literature the bulk wave speed equation can be written as:

$$c_0 = \sqrt{\frac{k}{\rho_s}} \quad 2.30$$

Where c_0 = bulk wave speed, k = bulk modulus, ρ_s = Solid density

The bulk wave speed increases with the increase in initial density as shown in the graph

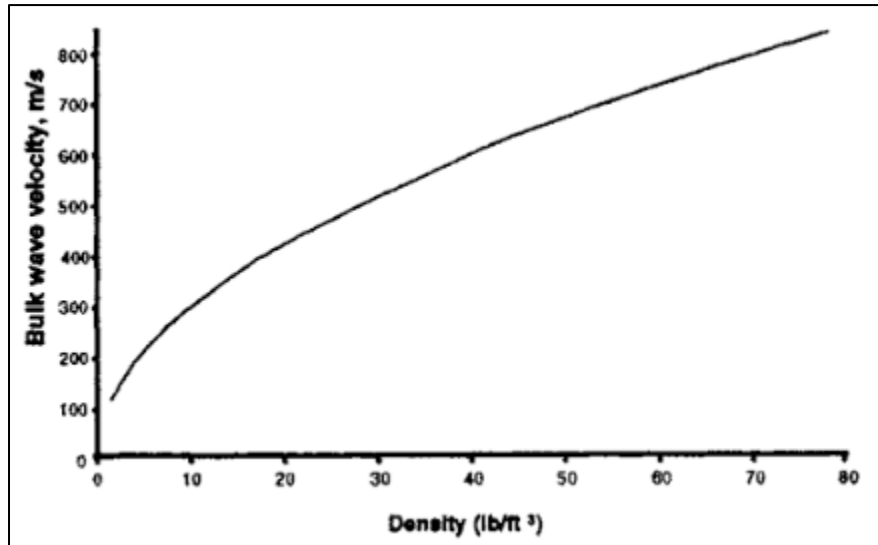


Figure 2.17 : Bulk wave velocity vs density [16]

and as we know that for isotropic material k can be defined as:

$$k = \frac{E}{3(1-2\nu)} \quad 2.31$$

As we discussed earlier that E is proportional to the square of density. And K is directly proportional to E , hence, E is proportional to the square of density. Finally, we find that bulk wave velocity varies with the square of density and can be written as:

$$C_e = \sqrt{\frac{E_s \rho_0}{3(1-2\nu)}} \quad 2.32$$

The subscript “s” denotes the properties of dense solid of state of the material.

The next task is to determine the maximum elastic pressure “P_e”. This is the pressure at which irreversible compaction begins.

According to Ashby and Gibson [19], for an open cell foam, the collapse occurs when the moment on the cell wall exceeds the moment required to deform the walls plastically creating plastic hinges. The yield strength increases as three-halves power of the initial density as shown by the following expression [19]

$$\sigma_h \propto \left(\frac{\rho_0}{\rho_s}\right)^{3/2} \quad 2.33$$

The above equation is a reasonable model; however, a refined model does exist which shows the relationship of yield strength and density. [19]

$$\sigma_h = C_y \left(\frac{\rho_0}{\rho_s}\right)^{3/2} \left(1 + \left(\frac{\rho_0}{\rho_s}\right)^{1/2}\right) \quad 2.34$$

The constant C_y = 15 MPa for flexible Polyurethane foams while C_y = 35 MPa for rigid Polyurethane foams. [19]

The above relations are valid up to a certain range of densities where the assumption is valid to model the cell walls as beams that deform plastically. At higher densities, i.e., $\rho_0 = 0.3\rho_s$, the cell wall become very thick as compared to its length and the previous assumption of considering it a slender beam doesn't hold true. Instead the walls yield under axial loading before they bend under a moment. In such case, the dense foams can be considered as solid with holes rather than a foam. In case of rigid polymer, the elastic collapse precedes the plastic collapse.

We can determine “P_e” from yield strength “σ_h”. The yield strength measured under the uniaxial stress can be found from the yield strength measured under uniaxial strength by following relation: [19]

$$\sigma_y = \frac{1-2\nu}{1-\nu} \sigma_h \quad 2.35$$

The mean hydrostatic pressure “ P_e ” at which yield initiates is then calculated from, [19]

$$P_e = \frac{1+\nu}{3(1-\nu)} \sigma_h \quad 2.36$$

In this analysis, we have considered the poisson’s ratio to be 0. The basis for this assumption can be found in the previous research papers, where during compression the poisson’s ratio is close to 0 and hence this assumption is valid.

From the above equation we can relate the P_e to initial density as shown in the figure:

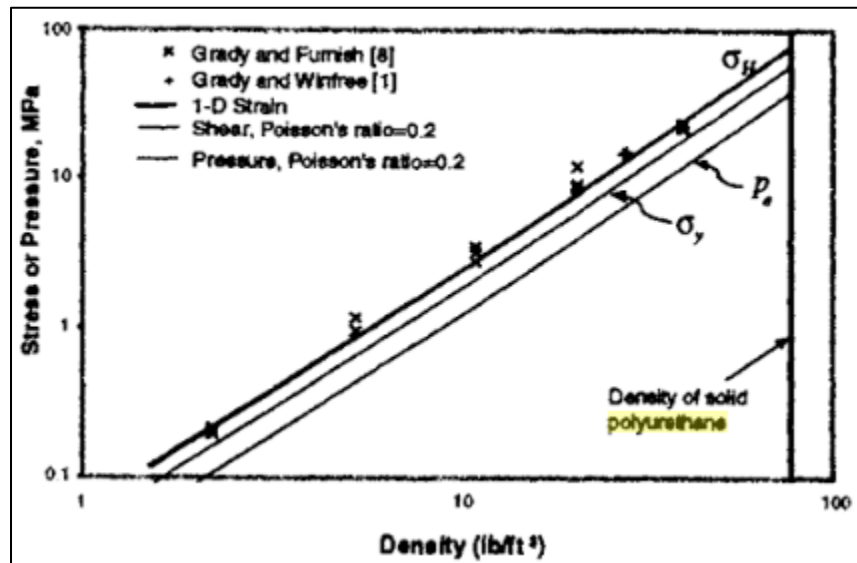


Figure 2.18 : Hydrostatic Pressure (P_e) vs density [16]

Finally, the compaction pressure denoted by “ P_s ” can be found by putting $\rho_y = \rho_s$ in the above equation σ_y .

Where “ ρ_s ” is the density of solid polyurethane in its free configuration.

The compaction exponent denoted by “ n ” can also be found by the relation found in literature and it mainly depends on the initial density. The relation is

$$n = 0.5 + 5.6 \frac{\rho_0}{\rho_s} \quad 2.37$$

By using all the equations above, the P- α properties for Morton Thiokol rigid 28lb/ft³, Polyurethane foam found in the book “Fundamental issues and Applications of Shock-Wave and High-Strain-rate phenomena by K.P. Staudhammer, L.E. Murr, M.A. Meyers are listed just as an example:

Density	ρ_o	450 kg/m ³
Bulk Elastic Sound Speed	c_e	830 m/s
Crush Strength	p_e	8 MPa
Crush Completion	p_s	38 MPa

Figure 2.19 : P-alpha parameters of Rigid PU foam 450kg/m³ [16]

2.6 Equation of State: Hugoniot Shock wave data

The shock wave experiments are used to determine equation of state at high temperature and pressure. These experiments are well established and applied on wide range of materials such as water, aluminum, iron. In this experiment and external pressure is applied on the pusher which drives it with the velocity U_p into a material at initial conditions (P_o , T_o , ρ_o). This impact generates a shock wave, which travels at a velocity U_s as shown in the figure. From this the final equation of state at conditions (P , T , ρ) can be determined.

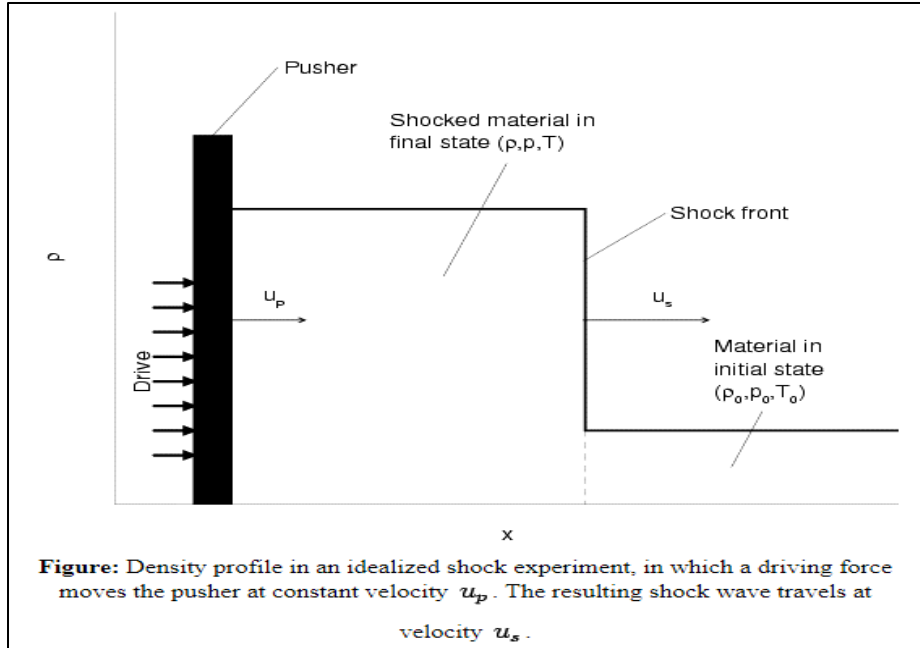


Figure 2.20 Shocked material and Pusher [17]

Shock EOS is a Mie-Gruneisen form of EOS and it uses the shock Hugoniot as reference curve. In many dynamic experiments, it has been found after measuring U_s and U_p that for most solid and liquids over a wide range of pressure the relationship between them is linear and is represented by following equation

$$U_s = C_1 + S_1 U_p \quad 2.38$$

U_p = pusher constant velocity
 U_s = Shock wave velocity

whereas Gruneisen coefficient "G" is often approximated as

$$G = 2s_1 - 1 \quad 2.39$$

The accurate modeling of hyper-viscoelastic materials is a key issue due to their non-linear stress-strain relationship. This is because they are amorphous and comprised of long molecular chains. These chains are highly twisted and randomly oriented in undeformed state. During loading, these chains become untwisted and straightened; when load is removed the chains revert to their original configuration. Mostly the starting point for modeling of hyper-viscoelastic materials is strain energy function and through constitutive equations, their properties are defined. The constitutive equations are the mathematical relation between the stress and strain. In such

materials the stress is dependent on other factors rather than the strain, like temperature, strain rate, frequency in case of cyclic loading. Therefore, in literature there are different types of constitutive models developed to model the behavior of such type of materials.

3. FE-Based Numerical modelling of Sandwich beam

In this chapter, numerical simulation of foam sandwich beam is performed. The numerical simulation is performed in Ansys 19.1 student version. Ansys is a FEM software used widely in academics and professional institutions. Ansys 19.1 offers different type of analysis in which a few are listed as below:

- i. Structural analysis
- ii. Modal analysis
- iii. Transient structural
- iv. Explicit dynamics
- v. Rigid dynamics
- vi. Harmonic response
- vii. Topology Optimization

3.1 Explicit Dynamics

In this analysis, explicit dynamics simulation is done. Explicit dynamics is preferred when simulation time is less, i.e., in milli-seconds and consumes less computational time as compared to implicit analysis as it handles large number of small increments in a very efficient manner. Explicit dynamics is a transient dynamic and an application of Workbench which can perform various engineering simulation involving all type of non-linearities such as geometrical non-linearity, contact non-linearities or material non-linearities. This tool is used for simulation of impacts or short duration pressure loadings and the time of study is usually small, i.e., in milliseconds. Following type of analysis can be performed in explicit dynamics:

- i. Drop test
- ii. Explosive loading
- iii. Explosive formation
- iv. Material failure
- v. High speed and hyper velocity impacts
- vi. Penetration mechanics
- vii. Blast-structure interactions

To ensure stability and accuracy of the solution, the size of the time step used in Explicit time integration is limited by the CFL (Courant-Friedrichs-Levy) condition. This condition implies that the time step be limited such that a disturbance (stress wave) cannot travel further than the smallest characteristic element dimension in the mesh, in a single time step. The time steps used for explicit time integration will generally be much smaller than those used for implicit time integration.

For example, for a mesh with a characteristic dimension of 1 mm and a material sound speed of 5000 m/s. The resulting stability time step would be 0.18 μ -seconds. To solve this simulation to a termination time of 0.1 seconds will require 555,556 cycles.

3.2 Problem Statement of Analysis

In this analysis, the curved beam having a rectangular cross-section is modeled in Ansys v 19.1.

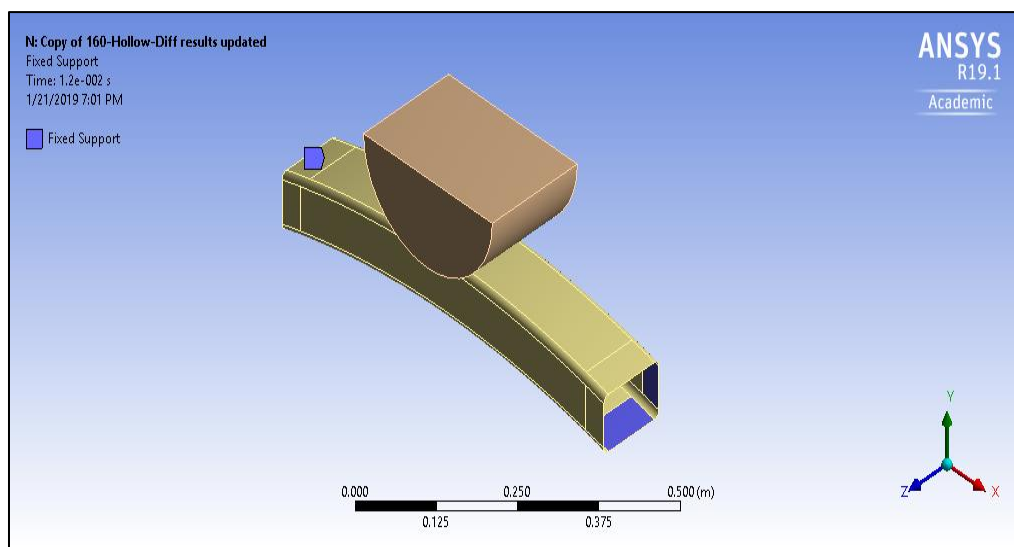


Figure 3.1 : Rectangular curved beam with impactor as rigid body

The system is composed of two bodies. In real world-applications this beam represents like a front bumper beam of car fixed at both ends and the impactor represents an external body striking the beam with a certain velocity. The analysis type is explicit dynamics and one body is called impactor which strikes/collides the beam with an initial velocity of 15m/sec in the y-axis. The ends of the beam are fixed supported in all the cases. The impact time is kept 12ms. The reason for not keeping the time not more than 12ms is because the analysis takes much computational time. The interaction is considered a frictionless again to save computational time. Further, the impactor is considered as rigid body because we are not interested in the study of impactor body after

collision. The analysis is highly non-linear, i.e., geometric non-linearity, contact non-linearity as well as material non-linearity; therefore, the structural steel non-linear properties are entered before the analysis, i.e., the linear elastic properties will give the wrong results and can't be used.

Different configuration of the beams is considered, and two different densities of polyurethane foam are considered as the core material. The effect of impact is studied on the hollow beam and then compared it with the beam having two different flexible Polyurethane foam as the core material and the conclusions are drawn. Following table shows the detail of different configuration of beam.

3.2.1 Case A: Simple (One-channel) beam

This further consists of 6 sub-cases. The detail of the cases is mentioned in the table below:

Type	Nomenclature	Remarks
Case 1	Simple hollow beam (equal weight to Case 3)	Weight adjusted equal to case 3 by increasing thickness
Case 2	Simple hollow beam (equal weight to Case 4)	Weight adjusted equal to case 4 by increasing thickness
Case 3	Foam-sandwich beam (Flexible PU Foam 40 kg/m ³ -bonded)	
Case 4	Foam-sandwich-beam (Flexible PU Foam 93kg/m ³ -bonded)	
Case 5	Foam-sandwich-beam (Flexible PU Foam 93kg/m ³ -non-bonded)	
Case 6	Foam-sandwich-beam (Rigid Polyurethane Foam 93kg/m ³ -bonded)	

Table 3-1 : Different configurations of hollow beam

3.2.2 Case B: Two-channel beam

Case 7	Simple two-channel beam (equal weight to Case 6)	Weight adjusted equal to case 6 by increasing thickness
Case 8	Foam-sandwich-two-channel beam (Polyurethane foam 93 kg/m ³ -bonded)	

Table 3-2 : Different configurations in two-channel beam

3.3 Analysis Steps

In Ansys and in almost all other FEM software's such as ABAQUS, NASTRAN the simulation can be completed by following the steps explained below in a hierarchal order.

- i. Engineering Data
- ii. Geometry
- iii. Model
- iv. Setup
- v. Solution
- vi. Results

As already stated above, an explicit dynamics analysis is chosen for our simulation. To perform analysis in Explicit Dynamics, first the explicit dynamics analysis system is dragged from Toolbox to Project schematic area by holding the left-click of the mouse button as shown in the image below:

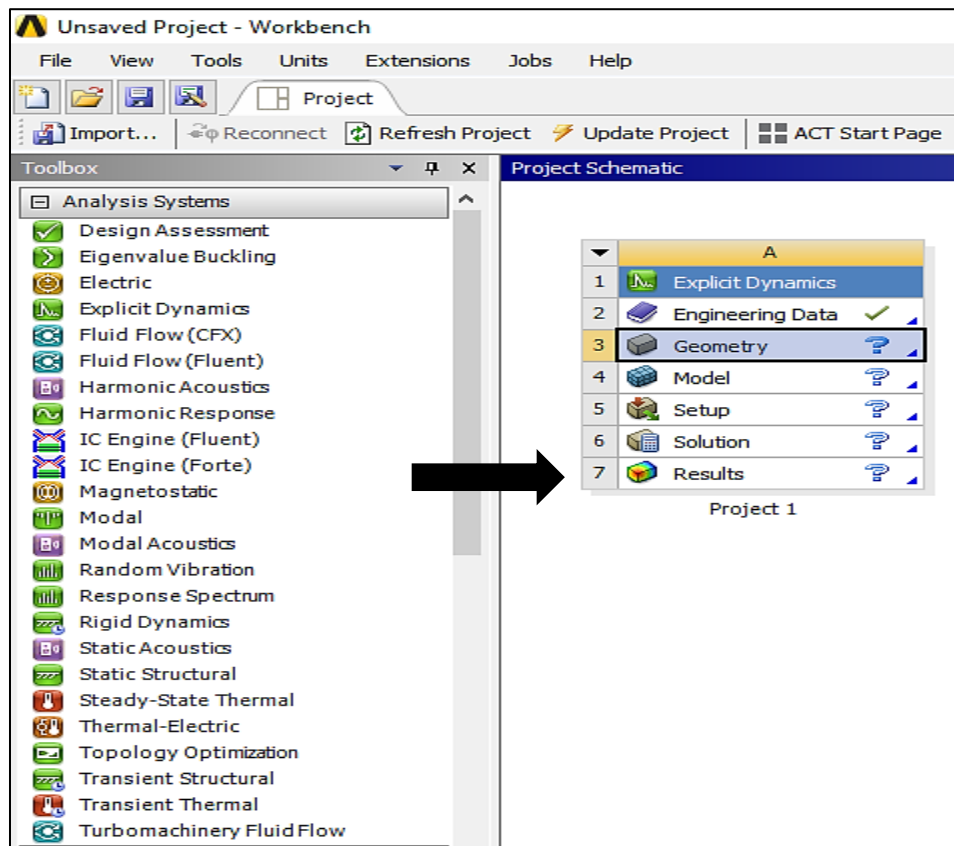


Figure 3.2 : Ansys 19.1 Project schematic and analysis systems

3.3.1 Engineering Data

All the engineering parameters of the materials are entered which is necessary to perform the analysis. Ansys have a material library in which many of the materials along with the parameters can be found easily. This also include non-linear materials, hyper elastic materials, polymers, epoxies etc. Moreover, a user can create his own custom material.

In this analysis, the hollow structure is assigned as non-linear structural steel and the necessary parameters, i.e., related to plasticity are entered. It is because during collision, the structure will deform so the parameters related to plasticity is necessary to be entered, otherwise the software will give the wrong results. There are different plasticity models in which bilinear isotropic hardening is used mostly for isotropic linear elastic materials. The parameters of the non-linear structural steel necessary for this simulation are entered as shown in the figure:

Properties of Outline Row 8: Structural Steel NL			
	A	B	C
1	Property	Value	Unit
2	Material Field Variables	Table	
3	Density	7850	kg m ⁻³
4	Isotropic Elasticity		
5	Derive from	Young's Modulu...	
6	Young's Modulus	2E+11	Pa
7	Poisson's Ratio	0.3	
8	Bulk Modulus	1.6667E+11	Pa
9	Shear Modulus	7.6923E+10	Pa
10	Bilinear Isotropic Hardening		
11	Yield Strength	2.5E+08	Pa
12	Tangent Modulus	1.45E+09	Pa
13	Specific Heat, C _p	434	J kg ⁻¹ C ⁻¹

Figure 3.3 : Engineering data for Non-linear Structural steel

Similarly, for polyurethane foam which is an isotropic and non-linear elastic material, the parameters such as density and viscoelasticity parameters are entered. For viscoelasticity, instantaneous shear modulus and decay constant are entered. These values are taken from the reference paper [20]. As flexible polyurethane foam is porous, therefore in all FEM software's,

there are some models which are used to analyze the porous materials. The models for porous materials available in Ansys are:

- i. Crushable Foam
- ii. Compaction EOS linear
- iii. Compaction EOS non-linear
- iv. P- α EOS

In Ansys help document, it is found that P- α EOS is more appropriate to be used in terms of accuracy of results and correct prediction of the behavior of porous material. Therefore, in this analysis, the P- α model is used for polyurethane foam under impact loading. In P - α model the following parameters are found by using the formulas explained in section 2.5.

	A	B	C
1	Property	Value	Unit
2	Material Field Variables	Table	
3	Density	40	kg m ⁻³
4	Viscoelastic		
5	Instantaneous Shear Modulus (High Rate) G0	18750	Pa
6	Viscoelastic Decay Constant	6.15E-05	s ⁻¹
7	Bulk Modulus	1.6667E+05	Pa
8	Shear Modulus	18750	Pa
9	P-alpha EOS		
10	Solid Density	1200	kg m ⁻³
11	Porous Soundspeed	20	m s ⁻¹
12	Initial Compaction Pressure Pe	36000	Pa
13	Solid Compaction Pressure Ps	1E+07	Pa
14	Compaction Exponent n	0.69	

Figure 3.4 : Viscoelasticity and P-alpha parameters for PU foam 40kg/m³

Similarly, for foam of density of 93 kg/m³, the viscoelasticity data is assumed the same as that of previous one, which means that the relaxation of a polyurethane foam of density 93 kg/m³ is same as that of 40 kg/m³. This assumption is due to unavailability of data and on the fact that by slightly changing the viscoelasticity have no effect in impact problems and for problems where time duration study is kept small. Although in the previous researches, it is found that by increasing the crosslink density, the viscoelasticity increases. The p-alpha EOS variables are calculated in the same fashion as explained in the section 2.5.

Properties of Outline Row 9: visco-hyper				
	A	B	C	D E
1	Property	Value	Unit	<input type="checkbox"/> <input type="checkbox"/>
2	Material Field Variables	Table		
3	Density	93	kg m ⁻³	<input type="checkbox"/> <input type="checkbox"/>
4	Viscoelastic			<input type="checkbox"/>
5	Instantaneous Shear Modulus (High Rate) G0	1.0136E+05	Pa	<input type="checkbox"/>
6	Viscoelastic Decay Constant	6.15E-05	s ⁻¹	<input type="checkbox"/>
7	Bulk Modulus	3.875E+05	Pa	<input type="checkbox"/> <input type="checkbox"/>
8	Shear Modulus	1.0136E+05	Pa	<input type="checkbox"/> <input type="checkbox"/>
9	P-alpha EOS			<input type="checkbox"/>
10	Solid Density	1200	kg m ⁻³	<input type="checkbox"/>
11	Porous Soundspeed	31	m s ⁻¹	<input type="checkbox"/>
12	Initial Compaction Pressure Pe	1.3667E+05	Pa	<input type="checkbox"/>
13	Solid Compaction Pressure Ps	1E+07	Pa	<input type="checkbox"/>
14	Compaction Exponent n	0.934		<input type="checkbox"/>

Figure 3.5 : Viscoelasticity and P-alpha parameters for foam 93 kg/m³

The bulk modulus parameter must be entered with this model as shown in the above figures and is found by using the formula explained in section 2.5.

PU Rigid Body Hugoniot data

The Hugoniot data for rigid polyurethane foam of density 93kg/m³ is taken from the book “LASL Handbook”. These parameters along with P- α model parameters are entered to describe the behavior of the rigid PU foam. It is important to mention that the P- α parameters of rigid PU foam of density 93 kg/m³ is different from the flexible PU foam of density 93 kg/m³ due to difference in the elastic modulus of both types of PU foam while the density is same. The solid elastic modulus and solid density of both type of Polyurethane foam is shown in table.

Type of Foam	Elastic modulus (E _s , MPa)	Solid Density (ρ_s , kg/m ³)
Flexible Polyurethane foam	1600	1200
Rigid Polyurethane foam	45	1200

Table 3-3 : Material properties of Flexible and Rigid PU foam

The Shock Hugoniot data found in the “LASL handbook” and the P- α model parameters are calculated by using the formulas described in section 2.5 and 2.6.

Properties of Outline Row 7: PU93				
	A	B	C	D E
1	Property	Value	Unit	<input checked="" type="checkbox"/> <input checked="" type="checkbox"/>
2	Material Field Variables	Table		
3	Density	93	kg m ⁻³	<input type="checkbox"/> <input type="checkbox"/>
4	<input checked="" type="checkbox"/> Isotropic Elasticity			<input checked="" type="checkbox"/>
10	<input checked="" type="checkbox"/> Viscoelastic			<input checked="" type="checkbox"/>
13	Bulk Modulus	1.378E+07	Pa	<input checked="" type="checkbox"/>
14	Shear Modulus	3.6E+06	Pa	<input type="checkbox"/> <input type="checkbox"/>
15	<input checked="" type="checkbox"/> Shock EOS Linear			<input checked="" type="checkbox"/>
16	Gruneisen Coefficient	0.5		<input type="checkbox"/>
17	Parameter C1	1110	m s ⁻¹	<input type="checkbox"/>
18	Parameter S1	0.75		<input type="checkbox"/>
19	Parameter Quadratic S2	0	s m ⁻¹	<input type="checkbox"/>
20	<input checked="" type="checkbox"/> P-alpha EOS			<input type="checkbox"/>
21	Solid Density	1200	kg m ⁻³	<input type="checkbox"/>
22	Porous Soundspeed	207	m s ⁻¹	<input type="checkbox"/>
23	Initial Compaction Pressure Pe	5.5E+05	Pa	<input type="checkbox"/>
24	Solid Compaction Pressure Ps	3.2E+07	Pa	<input type="checkbox"/>
25	Compaction Exponent n	0.94		<input type="checkbox"/>

Figure 3.6 : Shock data parameters and P-alpha parameters for Rigid PU 93 kg/m3

3.3.2 Geometry

This section is used to create a geometry or import a geometry from another CAD file. Ansys offers its own modeling tool such as Design Modeler or Spaceclaim. The design modeler can be used as geometry editor of existing CAD models or 2d sketches/parts/assemblies can be created from the scratch. It is a parametric feature based solid modeling software. Design modeler or Spaceclaim provides all the tools necessary to setup the problem for analysis.

In this analysis the beam and the rigid body is modeled using design modeler. As discussed early, our system is composed of the impactor and the beam. Moreover, our beam geometry is considered of two different types, i.e., single and two-channel beam. The modeling is carried out in Ansys Design modeler. Further details and dimensions of each part are explained in detail.

3.3.2.1 Impactor

The impactor is a hemi-spherical body and is used in this simulation to collide the beam with an initial velocity. During impact, we are not interested in the stress distribution and deformations on

this body. Therefore, this body is considered as a rigid body. This rigid body assumption also saves a computational time as ANSYS only considers the contact surface of the rigid body while ignoring the rest of the surfaces which ultimately leads to reduction in computational time. The part drawing is shown in the figure 3.7 and 3.8.

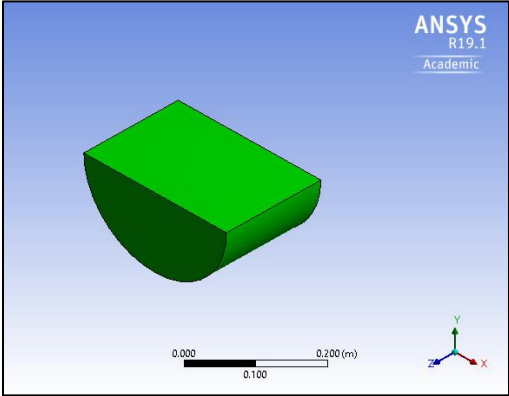


Figure 3.7 : Isometric view of impactor (rigid body)

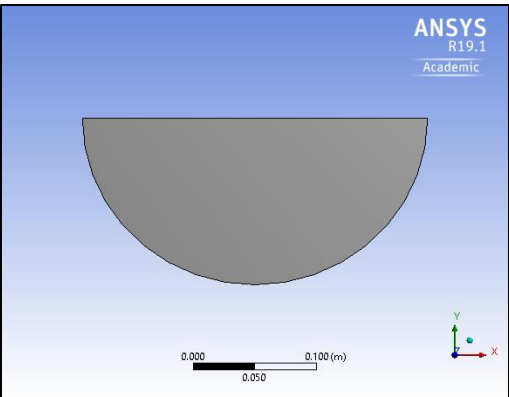


Figure 3.8 : Front view of impactor (rigid body)

The material, dimensions, properties and the initial velocity of the impactor are given in the following table:

Parameters	Values
Material	Structural Steel
Type	Rigid
Mass	51kg
Initial Velocity	15 m/s
Diameter	280 mm
Extrude Length	92.5 mm

Table 3-4: Impactor dimensions and material type

3.3.2.2 Beam Body (Skin)

The beam structure has a rectangular cross-section and curved having a certain radius of curvature. The beam material is considered as non-linear structural steel. The beam is hollow and is modelled through sweep command. The isometric view of the hollow beam is given in the figure 3.9 and 3.10.

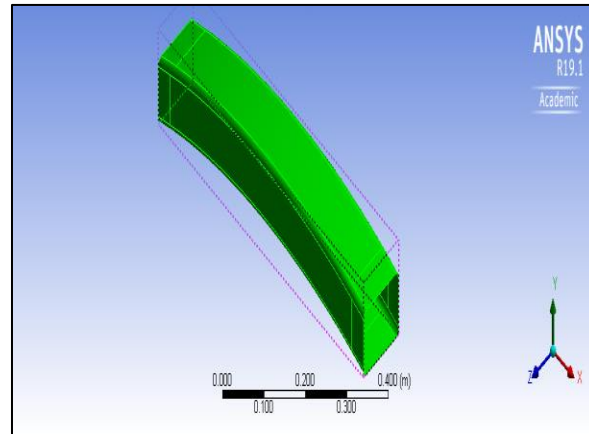


Figure 3.9 : Isometric view of hollow beam

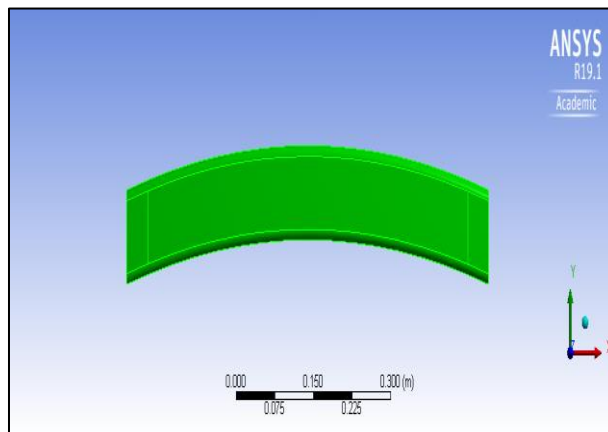


Figure 3.10 : Front view of hollow beam

Similarly, a two-channel beam is also drawn through sweep command and is shown in the figure below:

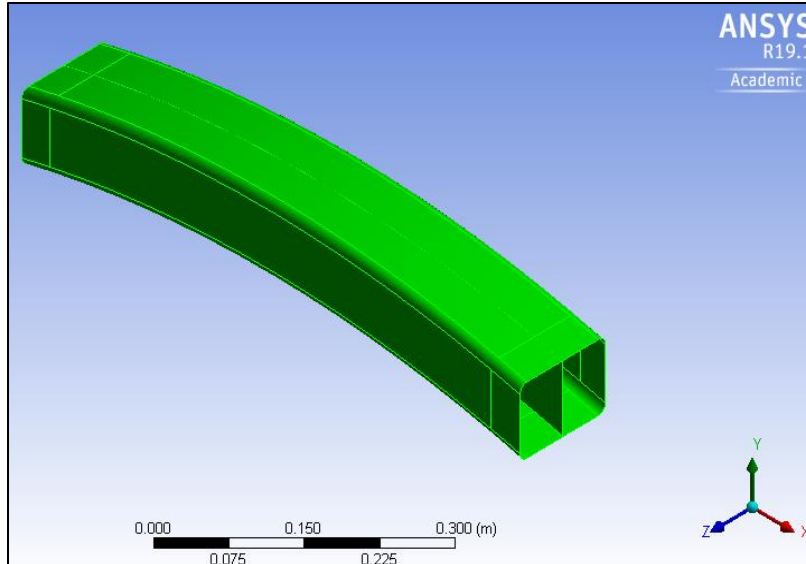


Figure 3.11 : Isometric view of two-channel hollow beam

As already discussed in the beginning of this chapter that we have considered 8 different configuration which has same (fixed) outer dimensions, but the thicknesses are varied to in order to make same weight. The dimensions of the 8 different configurations of beams are given in the following table:

Parameters	Values
Material	Non-linear Structural Steel
Type	Flexible
Dimensions	
Width of X-sec (outer)	121 mm
Height of X-sec (outer)	91 mm
Radius	1480 mm
Thickness	
Case 1	2.13 mm
Case 2	2.3 mm
Case 3	2 mm
Case 4	2 mm
Case 5	2 mm
Case 6	2 mm
Case 7	2.24 mm
Case 8	2 mm

Table 3-5 : Thickness of different configuration of beam

3.3.2.2 Foam

The hollow space is filled with foam material through sweep command, therefore, the geometry is rectangular as the skin material. The dimensions of the foam vary with the configuration as the thickness changes. The foam is considered to fill all the empty space of the hollow beam. The foam material is polyurethane foam (flexible and rigid). The mass of the polyurethane foam in each configuration depends on its density as in this analysis two types of densities are considered, i.e., 40kg/m^3 and 93 kg/m^3 . Following figure shows the polyurethane foam filled beam.

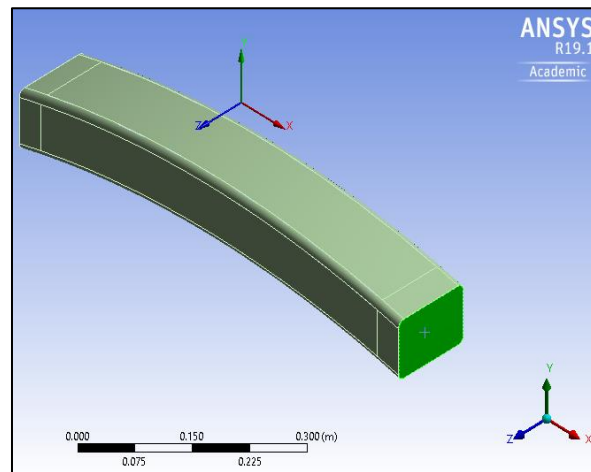


Figure 3.12 : Isometric view of foam filled beam

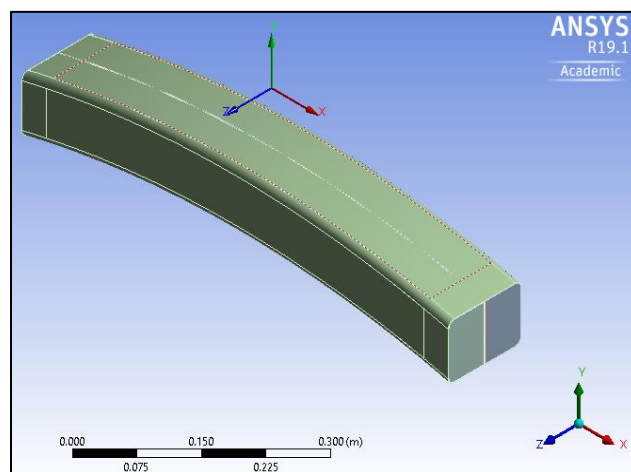


Figure 3.13 : Isometric view of two-channel filled beam

3.3.3 Setup

The setup category allows the user to setup all the necessary initial conditions, boundary conditions, mesh, type of loading and the required results for the analysis. This is the most critical step as the solution time and the accuracy of the results is mainly dependent on this step. Any mistake done in this step leads to inaccurate results or adding more constraints or refining mesh than necessary will increase the computational time.

In this analysis, first the bonded and non-bonded (frictional) connection is defined as connection between the inner surface of the beam and polyurethane foam. The bonded connection means that both the bodies are glued perfectly to each other and there is no relative motion between the parts after impact. The non-bonded connection means that the foam moves relative to the inner surface of the beam. Ansys also provides other types of connection and it depends on the function of the part and the user. Other connection includes frictionless, no separation etc. Ansys has provided a detail description in the help on each type of connection. The connection of single-channel hollow beam with the core PU foam is shown in the figure.

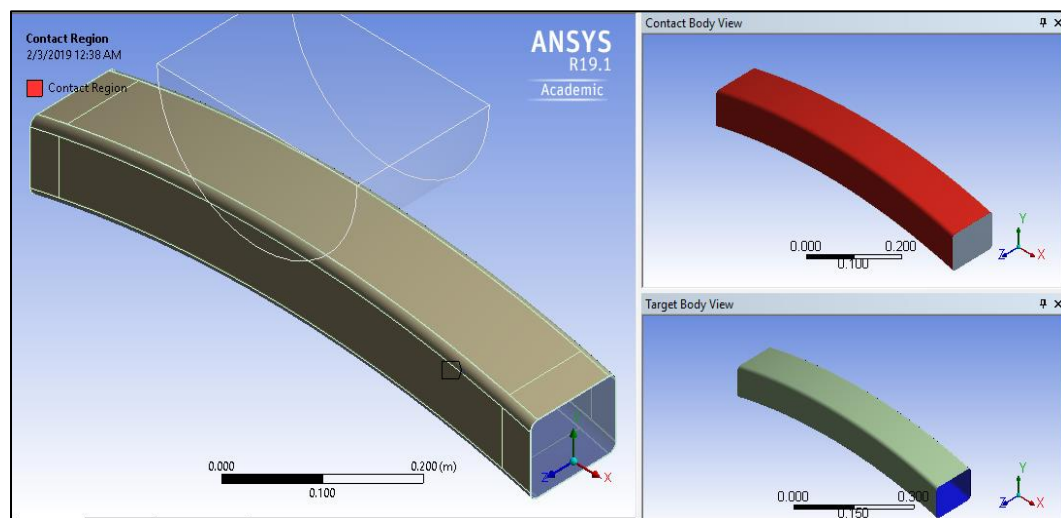


Figure 3.14 : Bonded surfaces of foam and beam

The details of the contact region in which the type bonded is selected. The contact bodies and target bodies also do appear in the details as shown

Details of "Contact Region"	
[-] Scope	
Scoping Method	Geometry Selection
Contact	8 Faces
Target	16 Faces
Contact Bodies	Solid
Target Bodies	Skin
Target Shell Face	Program Controlled
Shell Thickness Effect	No
Protected	No
[-] Definition	
Type	Bonded
Scope Mode	Automatic
Behavior	Program Controlled
Trim Contact	Program Controlled
Trim Tolerance	1.9353e-003 m
Maximum Offset	1.2e-003 m
Breakable	No
Suppressed	No

Figure 3.15 : Details of contact region

The second step is to set the mesh. This is the most critical step in almost all kind of engineering analysis simulation. The finer the mesh the better the accuracy of the results but it will increase the simulation time and specially in explicit dynamics the computational time increases too much because the minimum time step depends on the mesh size as discussed above in the CFL condition. Secondly it also depends on the type of mesh elements such as triangular, hexa, quadrilateral etc. Each type of elements has its own limitations and advantages and are preferred/not preferred in some specific type loading conditions and type of geometries. For example, for complex geometries the tetrahedral elements are recommended while in bending the same are not recommended because they give stiffer results. Similarly, for simpler geometries sweep mesh is best and time efficient. Moreover, after meshing Ansys does provide some mesh statistics so that the user can evaluate the quality of mesh.

It is worthy to mention that in this analysis Ansys 19.1 student edition is used which has some limitations in terms of number of elements/nodes during meshing. In student edition, the elements/nodes are not allowed to be more than 32000. The number of faces should not be more than 300 and the number of bodies should not be more than 50. In this analysis we have two bodies and the number of faces is also below 10. The mesh in this analysis is refined such that it fulfills the limitation of 32000 elements and the mesh type is selected sweep mesh as the geometry is simple. Explicit dynamics require a refined mesh due to all type of non-linearities, i.e.,

contact non-linearity, material non-linearity, and geometrical non-linearity. The average quality of the mesh obtained in this analysis is 93% which is pretty good, and the maximum elements are hexahedral elements. The distribution of different quality of elements in a mesh are shown in the figure. From this distribution, the average quality of mesh is obtained.

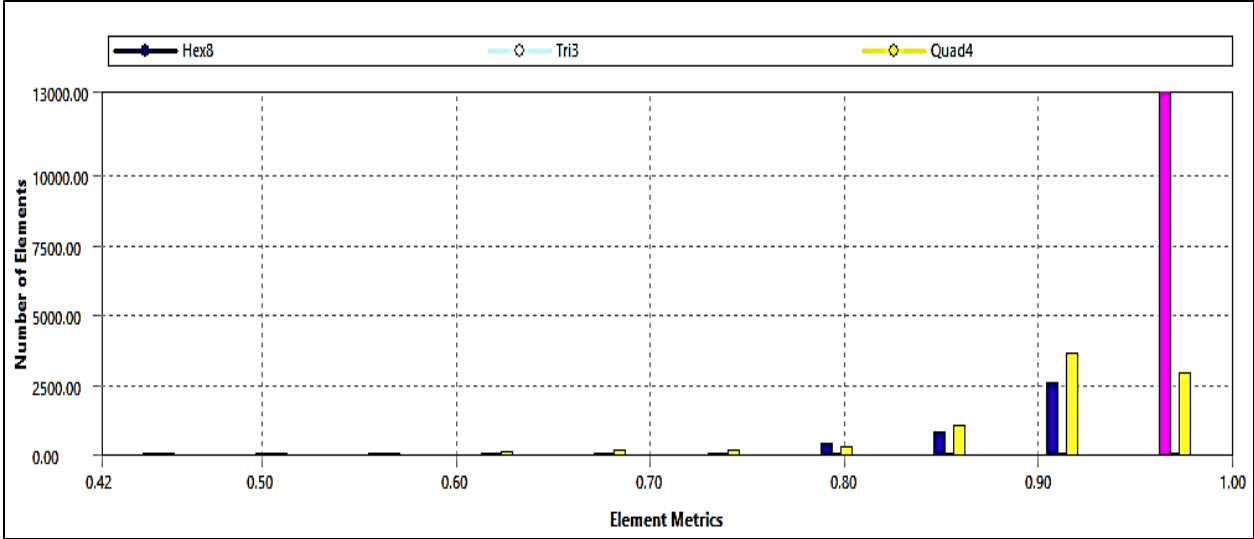


Figure 3.16 : Mesh quality distribution of elements

The mesh of hollow beam as well as sandwich beam (polyurethane foam core) is shown

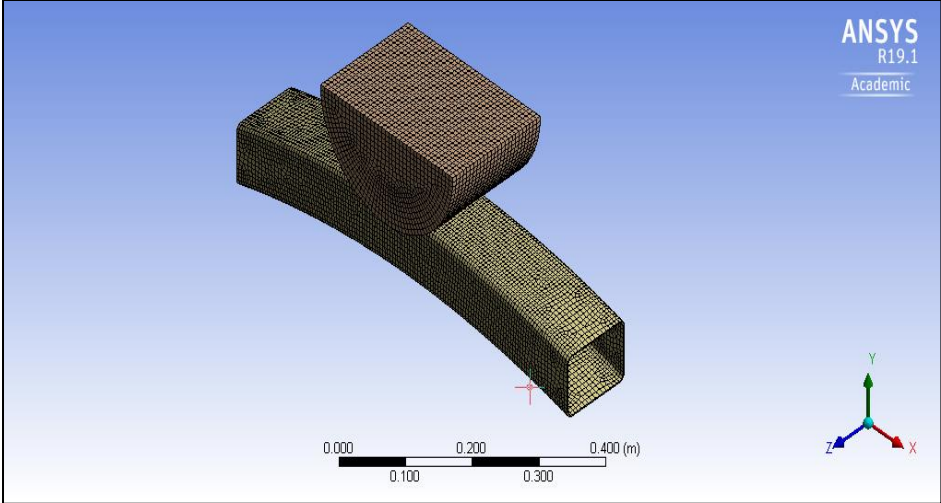


Figure 3.17 : Mesh of beam and rigid body

Details of "Mesh"	
<input type="checkbox"/> Quality	
Check Mesh Qua...	Yes, Errors
<input type="checkbox"/> Target Quality	Default (0.050000)
Smoothing	Medium
Mesh Metric	Element Quality
<input type="checkbox"/> Min	0.43134
<input type="checkbox"/> Max	0.99977
<input type="checkbox"/> Average	0.94783
<input type="checkbox"/> Standard Devi...	5.648e-002
<input type="checkbox"/> Inflation	
<input type="checkbox"/> Advanced	
<input type="checkbox"/> Statistics	
<input type="checkbox"/> Nodes	26573
<input type="checkbox"/> Elements	24591

Figure 3.18 : Details of Mesh

The foam-sandwich beam mesh is shown in the figure:

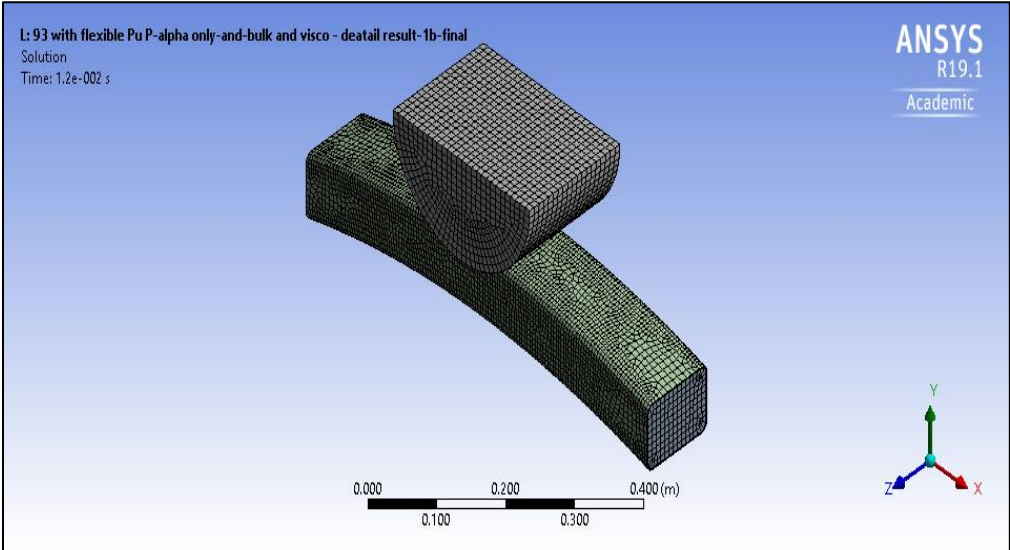


Figure 3.19 : Mesh of foam sandwich beam

3.3.4 Loading

After mesh, the initial and boundary conditions are defined. In initial condition the rigid body is selected, and the magnitude of the velocity is entered 15m/s. The ends of the beam are considered fixed. The fixed condition is applied to both ends and to small surface area of dimensions 50mm x 100mm on all four sides of beam. The area is shown on two visible faces of the beam in the figure with the help of black arrows

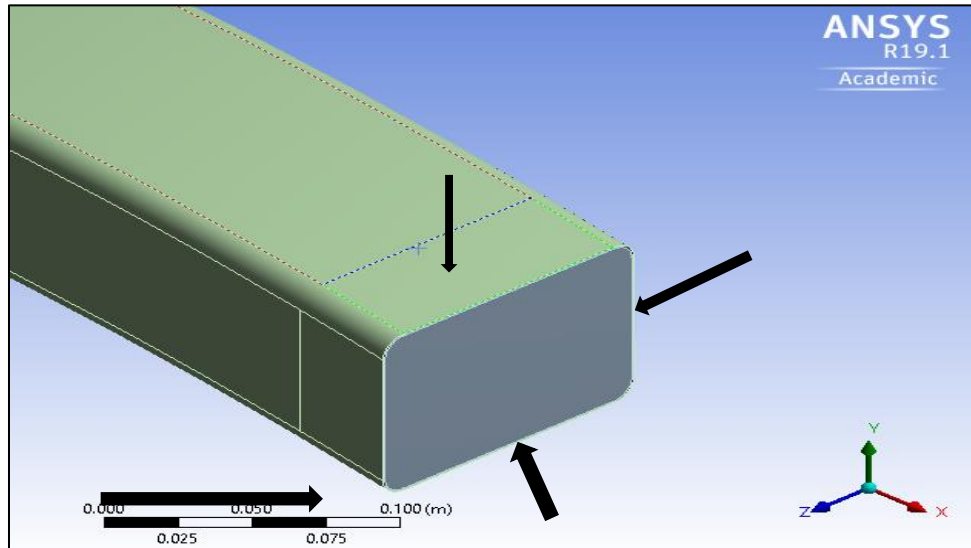


Figure 3.20 : Faces of foam sandwich beam where fixed boundary conditions are applied

The fixed support condition is applied in all the configurations, i.e., hollow and foam-sandwich beams. In the figure, the fixed conditions applied to the ends of the beams are shown

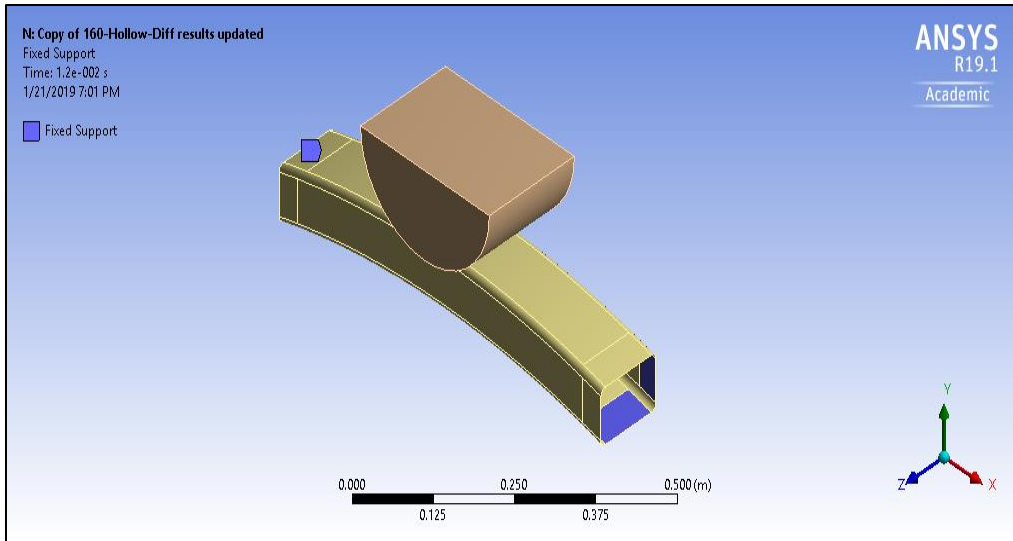


Figure 3.21 : Faces of hollow beam where fixed conditions are applied

In the analysis settings, the end time of 12 milli-second is selected, and the output result points are increased from 20 to 100. The solver type Autodyn is selected. The results such as reaction forces, kinetic energy, deformations are added. The settings are shown in the figure

Details of "Analysis Settings"	
[-] Analysis Settings Preference	
Type	Custom
[-] Step Controls	
Number Of Steps	1
Current Step Number	1
End Time	1.2e-002
Resume From Cycle	0

Figure 3.22 : End time setting

Details of "Analysis Settings"	
Retain Inertia of Eroded Material	Yes
[-] Output Controls	
Save Results on	Equally Spaced Points
Result Number Of Points	100
Save Restart Files on	Equally Spaced Points
Restart Number Of Points	5
Save Result Tracker Data on	Cycles

Figure 3.23 : Details of Output control

3.3.4.1 Erosion Controls

The erosion controls setting is also an important step in the explicit dynamics. It is a numerical mechanism in which the very distorted elements are automatically removed during a simulation before the elements become degenerated. This automatic removal helps to ensure the stability timestep at reasonable level and the continuation of solution till the end time. It is also used for the simulation of cutting, penetration and material fracture.

There are several mechanisms available to initiate erosion of elements. The erosion options can be used in any combination. Elements will erode if any of the criteria are met. The following document is taken from Ansys v19.1 help, which explains the erosion controls.

Explicit Dynamics Erosion Controls		
Field	Options	Description
On Geometric Strain Limit		If set to Yes , elements will automatically erode if the geometric strain in the element exceeds the specified limit. This field is not available for Explicit Dynamics (LS-DYNA Export) systems.
Geometric Strain Limit		The geometric strain limit for erosion. Recommended values are in the range from 0.75 to 3.0. The default value is 1.5. This field is not available for Explicit Dynamics (LS-DYNA Export) systems.
On Material Failure		If set to Yes , elements will automatically erode if a material failure property is defined in the material used in the elements, and the failure criteria has been reached. Elements with materials including a damage model will also erode if damage reaches a value of 1.0. This field is not available for Explicit Dynamics (LS-DYNA Export) systems.
On Minimum Element Time Step		If set to Yes , elements will automatically erode if their calculated time step falls below the specified value.
Minimum Element Time Step		The minimum controlling time step that an element can have. If the element time step drops below the specified value, the element will be eroded. This field is not displayed for Explicit Dynamics (LS-DYNA Export) systems when On Minimum Element Time Step is set to No .
Retain Inertia of Eroded Material		If all elements that are connected to a node in the mesh erode, the inertia of the resulting free node can be retained if this option is set to Yes . The mass and momentum of the free node is retained and can be involved in subsequent impact events to transfer momentum in the system. If set to No , all free nodes will be automatically removed from the analysis. This field is not displayed for Explicit Dynamics (LS-DYNA Export) systems when On Minimum Element Time Step is set to No .

Figure 3.24 : Explicit dynamics erosion controls explanation (Ansys help document) [21]

In this Analysis the erosion control is set on geometric strain limit and the value of geometric strain limit is set 1.5. This value is recommended by Ansys for low velocity impacts, i.e., velocities less than 100 m/s.

Details of "Analysis Settings"	
<input type="checkbox"/> Erosion Controls	
On Geometric Strain Limit	Yes
Geometric Strain Limit	1.5
On Material Failure	No
On Minimum Element Time Step	No
Retain Inertia of Eroded Material	Yes

Figure 3.25 : Geometric strain limit setting in Erosion controls

3.3.5 Results

In this category, user can select and see all types of results such as deformations, stresses, strains, energies, reaction forces etc., which will be explained in the next chapter. In this analysis, we are interested in the reaction forces, acceleration and deformations. Further, the animation tool allows the user to observe the simulation of parts during interaction with other objects. In addition to this, Ansys does also offer user-defined results in which many other variables such as kinetic energy, internal energy, bond status etc. can be selected from the worksheet. To view this, it must be first selected before the start of the simulation. The results along with the comparison will be explained in the next chapter.

4. RESULTS

The impact of the rigid body and different configuration of beams is simulated with dimensions and predefined conditions already discussed in the previous chapter. One is the hollow beam and the other beam is a sandwich beam with polyurethane foam. The type and density of polyurethane foams selected in this analysis are:

Type	Density (kg/m ³)
Flexible Polyurethane Foam	40
Flexible Polyurethane Foam	93
Rigid Polyurethane Foam	93

Table 4-1 : Types of Polyurethane foam with density

4.1 Simple hollow beam and foam sandwich beam (PU foam 40kg/m³)

In the first simulation (Case 1), the hollow beam is considered, and the rigid body is colliding the beam with an initial velocity of 15m/s. In Case 2, the sandwich beam is considered with polyurethane foam of density 40 kg/m³ provided that the outer dimensions of the beam are same in both the cases and the hollow beam thickness is increased so that both the hollow and sandwich beams are of same weight. The weight of the part details for Case 1 and 2 are:

Nomenclature	Material	Hollow	Sandwich
Skin Weight	SS Non-linear	4.45 kg	4.45 kg
Foam Weight	Flexible Polyurethane foam	Nil	0.28
Skin thickness	-	2.13 mm	2 mm
Total Weight	-	4.73 kg	4.73 kg

Table 4-2 : Case 1 - Hollow vs foam sandwich beam

The following conclusions and differences are observed despite of the equal weight:

4.1.1 Deformation

The hollow beam maximum deflection at the end time (12 milli-second) is observed to be 96 mm.as shown in the figure 4.1.

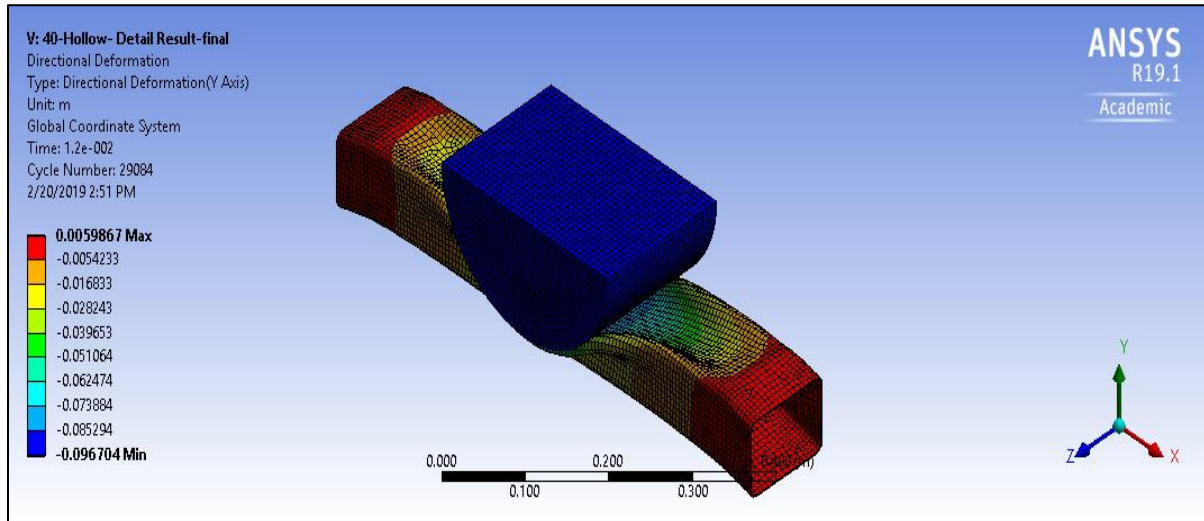


Figure 4.1 : Maximum deformation of 96 mm (Case 1)

The energy graph of hollow beam shows that the structure does stop the kinetic energy of the rigid body between 10 - 11 milli-second as shown in the figure 4.2.

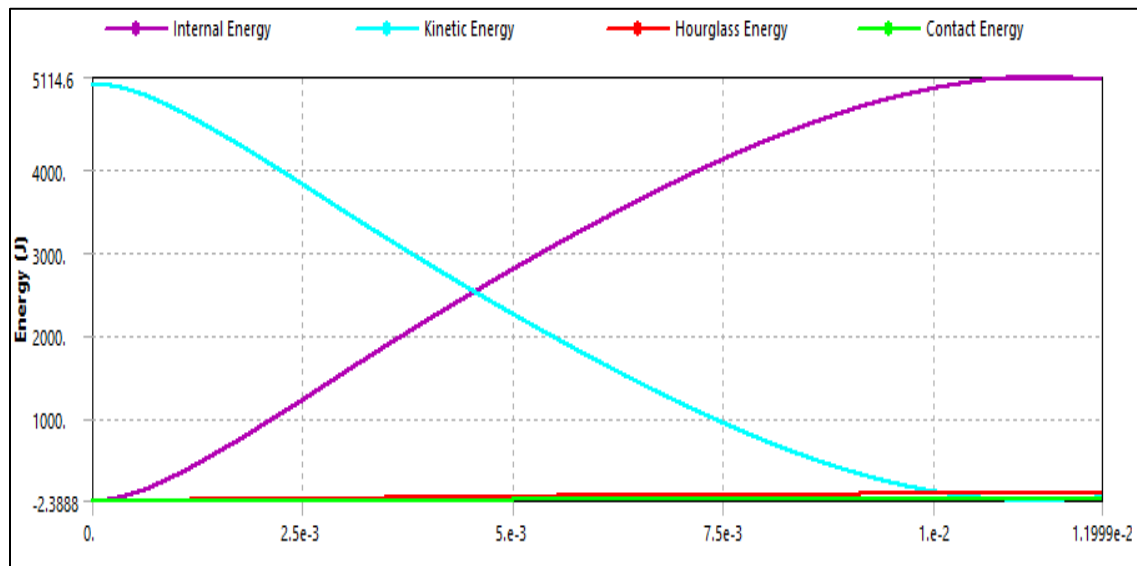


Figure 4.2 : Energy graph of hollow beam (Case 1)

In contrast, the sandwich beam is maximum deformed 71mm by keeping the same initial and simulation conditions. The energy graph of sandwich beam shows that it can stop the rigid body at around 8.7 milli-second. Hence, by having the equal weight the sandwich beam with foam of 40kg/m^3 proved to be a better alternative in terms of stopping the body earlier with less damage; as compared to hollow one. Then energy graph of foam sandwich beam (Case 2) can be seen in the following figure 4.3.

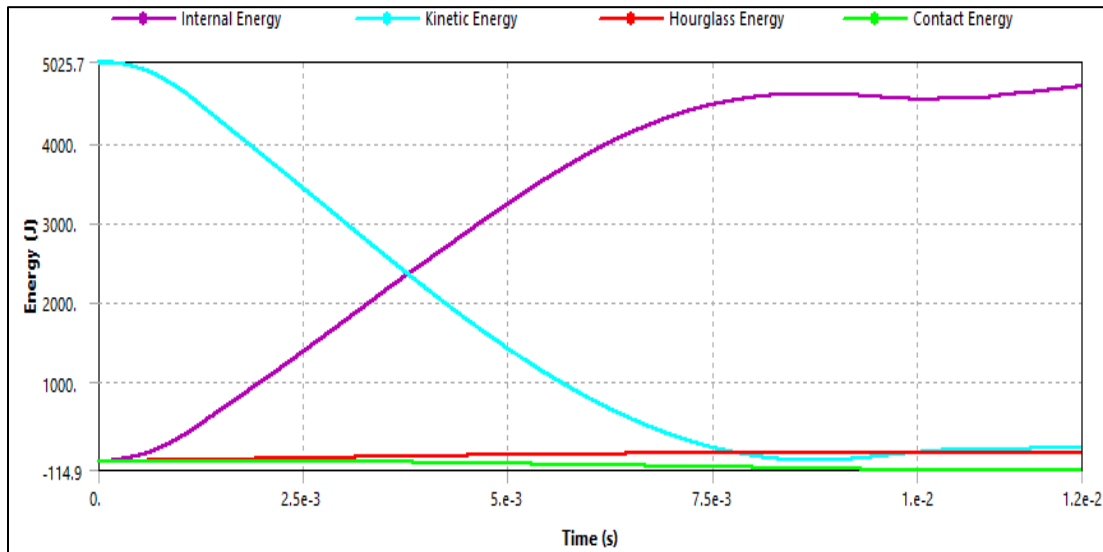


Figure 4.3 : Energy graph of foam-sandwich beam (Case 2)

The hourglass energy as explained in the first chapter is below the 10% of internal energy in both the cases and thus it is a kind of check for correctness of our simulation settings, i.e., mesh size along with elements and connections. Moreover, the average element quality is also 93%, which shows a good mesh is generated.

4.1.2 Reaction Force-time Curve

The peak reaction force of the hollow beam at the supports is 13450 N as shown in the figure, while in the foam sandwich beam the peak reaction force is 13428 N. This doesn't show a significant difference. Hence, it needs to be further explored that whether the reaction force does increase or decrease by increasing the density of foam. Apart from peak magnitude of reaction force which have no significant difference in both the configuration, it can be clearly seen that the reaction force quickly diminishes with respect to time in case of foam sandwich beam. The difference is quite evident at time 10 milli-seconds as shown in the figure 4.4

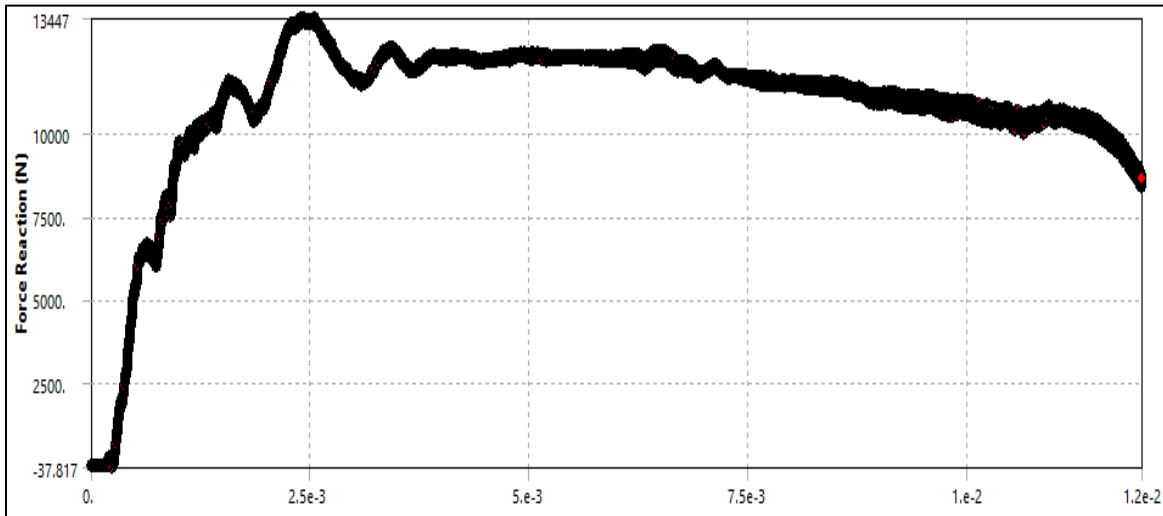


Figure 4.4 : Reaction force-time graph of hollow beam (Case 1)

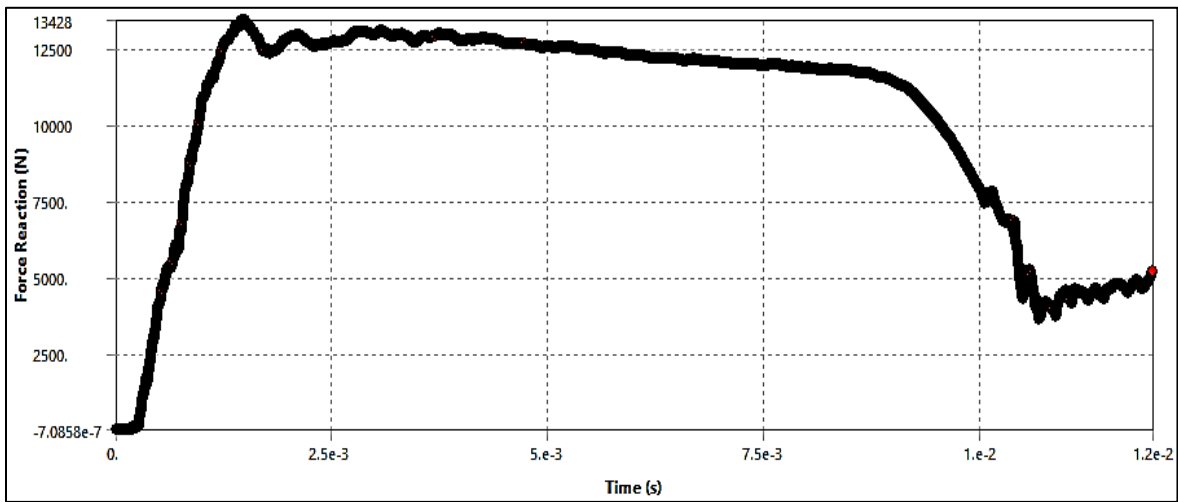


Figure 4.5 : Reaction-force graph of foam-sandwich beam (Case 2)

This shows that the foam density beam can absorb more impact energy (and thus transmit less force to the supports) as compared to the hollow one, which is beneficial specially in vehicles where the front bumper beam is required to transmit the force to crash-box.

4.1.3 Kinetic Energy

The Kinetic Energy of both the structures with respect to time are also important and is evaluated here. Keeping in view that the masses are same in both the cases, the greater kinetic energy shows that the structure will have a high velocity after impact and vice-versa. By comparing the Kinetic energy-time graph of both the configurations, it is observed that the sandwich structure peak Kinetic energy is less than that of hollow structure. Moreover, the sandwich structure can dissipate the energy at higher rate as compared to hollow structure. For example, the following table shows the comparison of Kinetic energy of both the structures at 3.5 milli-seconds and 7.5 milli-seconds.

Time (sec) -Range	Kinetic Energy (J) [Hollow]	Kinetic Energy (J) [Sandwich]
3.3 – 3.7	77	62
7.3 – 7.7	30	5

Table 4-3 : Kinetic energy comparison between hollow and sandwich beam

The same results can also be viewed from the graphs of both configurations shown in Fig 4.6 and 4.7.

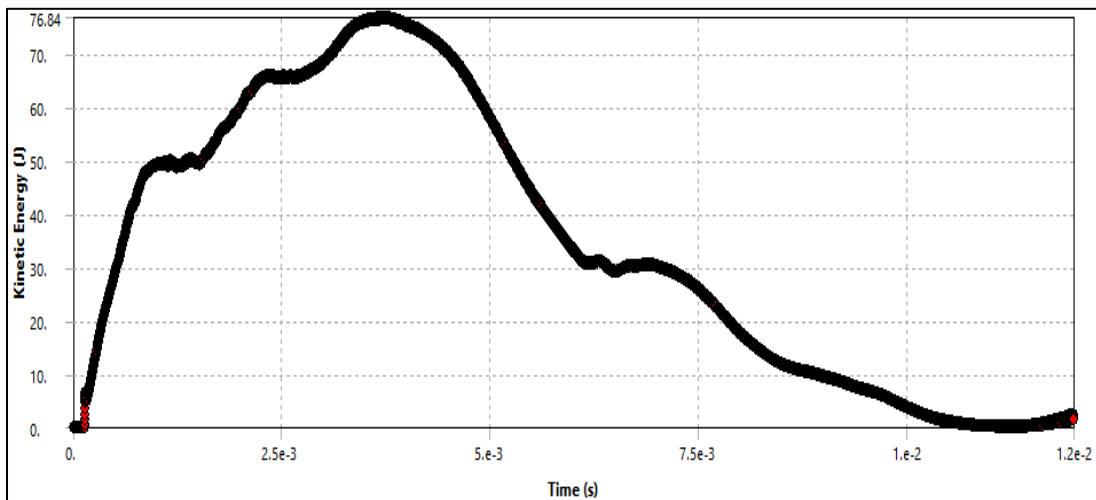


Figure 4.6 : Kinetic energy-time graph of hollow beam (Case 1)

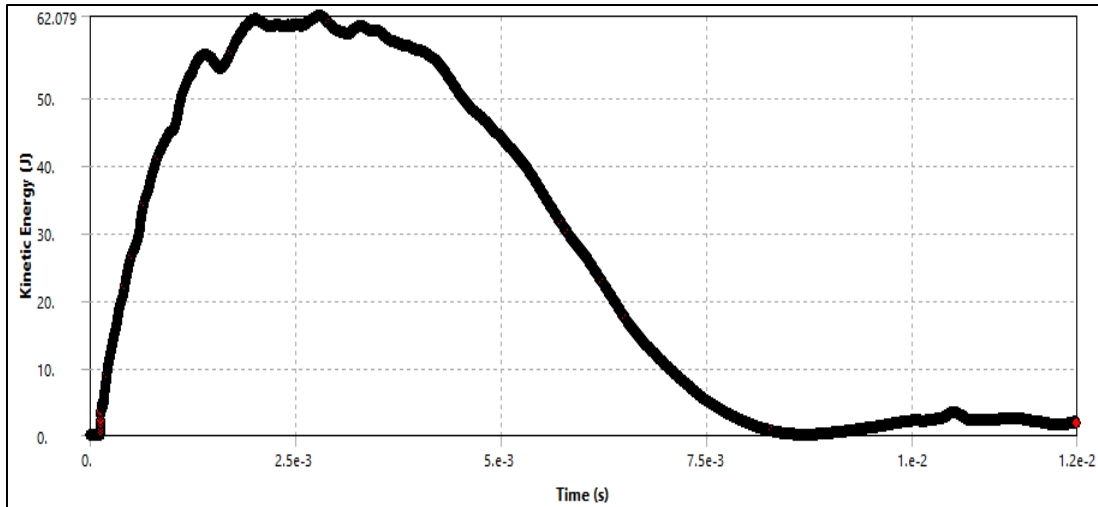


Figure 4.7 : Kinetic energy-time graph of foam-sandwich beam (Case 2)

4.1.4 Velocity (Y-axis)

The Y-axis velocity graph is obtained from Ansys results to compare the peak velocities and velocity diminishing with respect to time to get a clear picture in terms of velocity. It is observed that the sandwich beam proves good in dissipation of energy as compared to hollow. But the foam sandwich beam reaches to maximum velocity quicker than the hollow beam which means high acceleration but after a certain time-interval the dissipation is faster than the hollow beam. For example, at 2.5 milli-second, the hollow body gained the velocity (in direction of collision) of 3 m/s, whereas at the same time the foam-sandwich beam gained the velocity of approx. 3.8 m/s. But, after 5 milli-second the foam-sandwich beam show quicker reduction in velocity as compared to its competitor. Further, the maximum peak velocity of sandwich beam is also less than the hollow beam. The velocity-time graph of both the structures are shown:

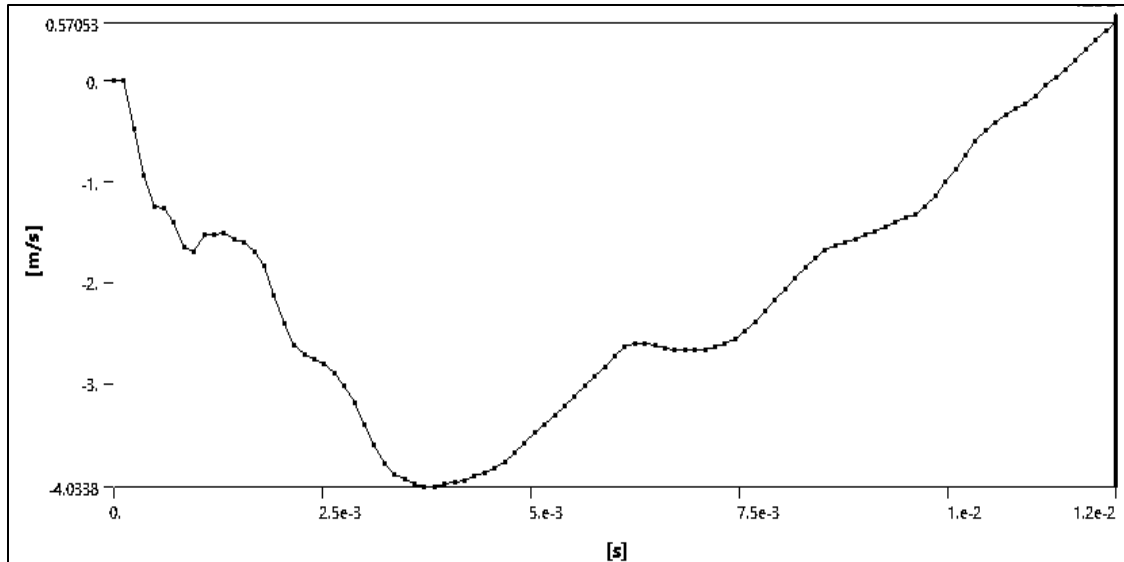


Figure 4.8 : Velocity-time graph of hollow beam (Case 1)

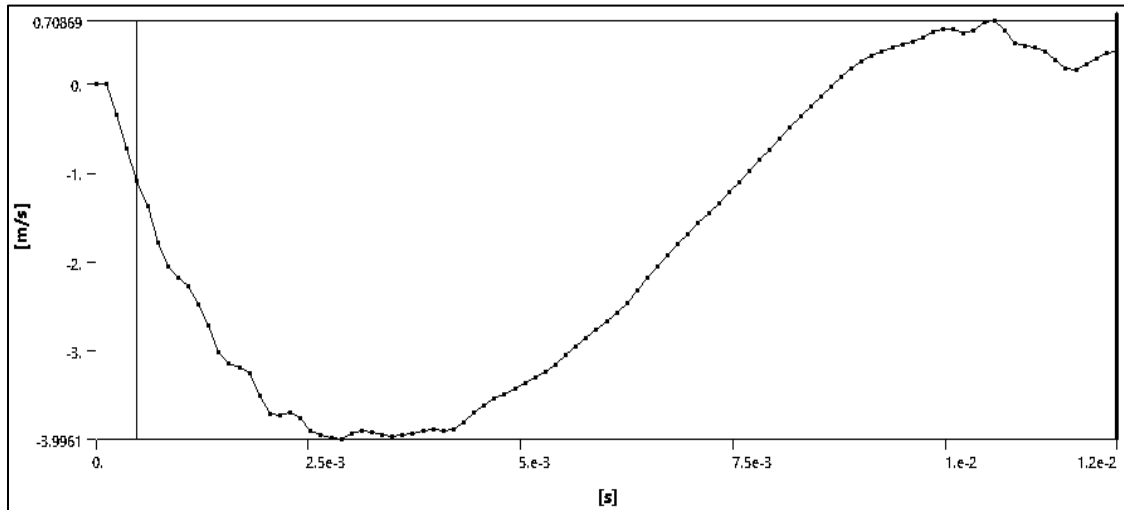


Figure 4.9 : Velocity-time graph of foam sandwich beam (Case 2)

4.1.5 Acceleration (Y-axis)

The acceleration-time histories of both the beams (case 1 and case 2) are compared and found that the sandwich beam shows good damping capability as compared to the hollow beam as well as the peak magnitude of acceleration gained by foam-sandwich beam is lesser. The graphs of both the beams obtained from the Ansys results are given below in Fig 4.10 and 4.11:

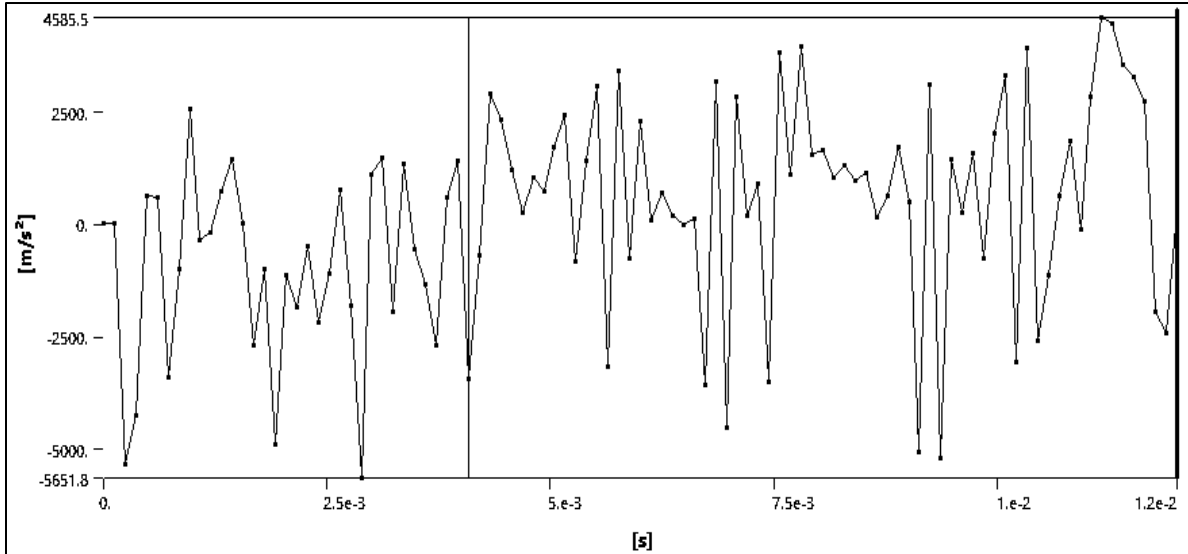


Figure 4.10 : Acceleration -time graph of hollow beam (Case 1)

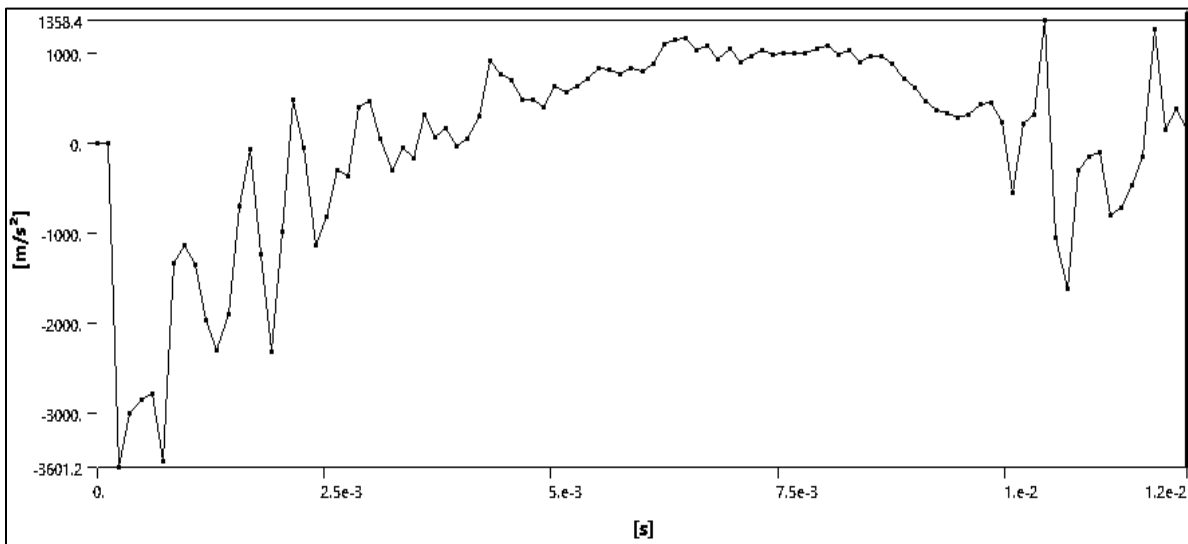


Figure 4.11 : : Acceleration -time graph of foam-sandwich beam (Case 2)

4.1.6 Momentum (in direction of collision):

The momentum gained in the direction of collision of both the beams are compared and the time-history graph is obtained. From the graph, we can see that the peak magnitude of sandwich structure is less when compared to hollow beam despite having the same weight and external dimensions of the beam. Moreover, the structure momentum reduces to zero quickly in foam sandwich configuration while slowly in hollow configuration. For example, at approximately 9 milli-

seconds the momentum reduces to zero in foam sandwich beam while in hollow beam the momentum is approximately 8 N-sec.

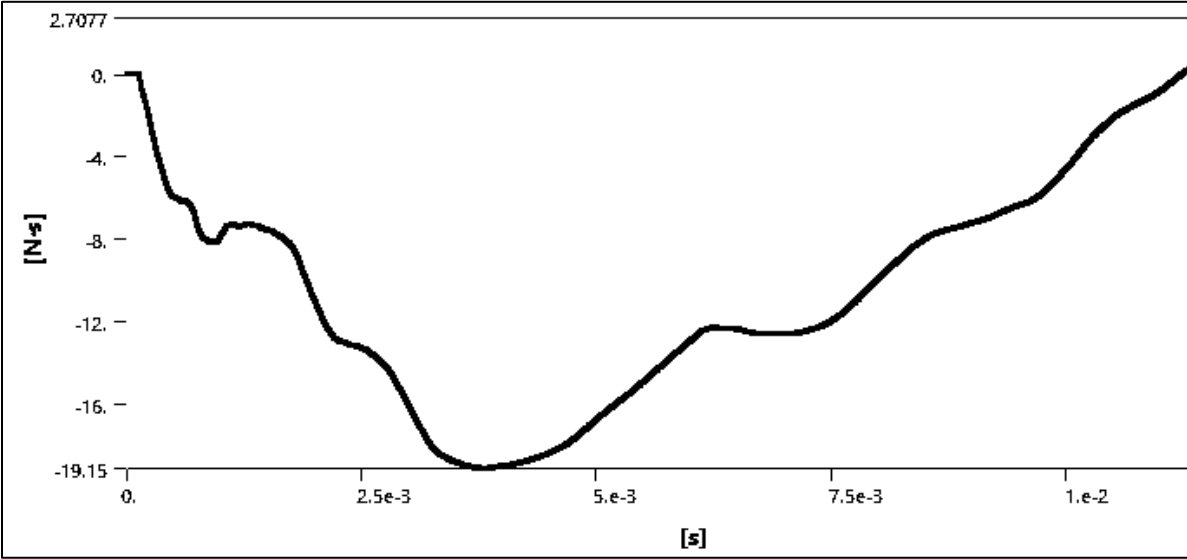


Figure 4.12 : Momentum in y-direction of hollow beam (Case 1)

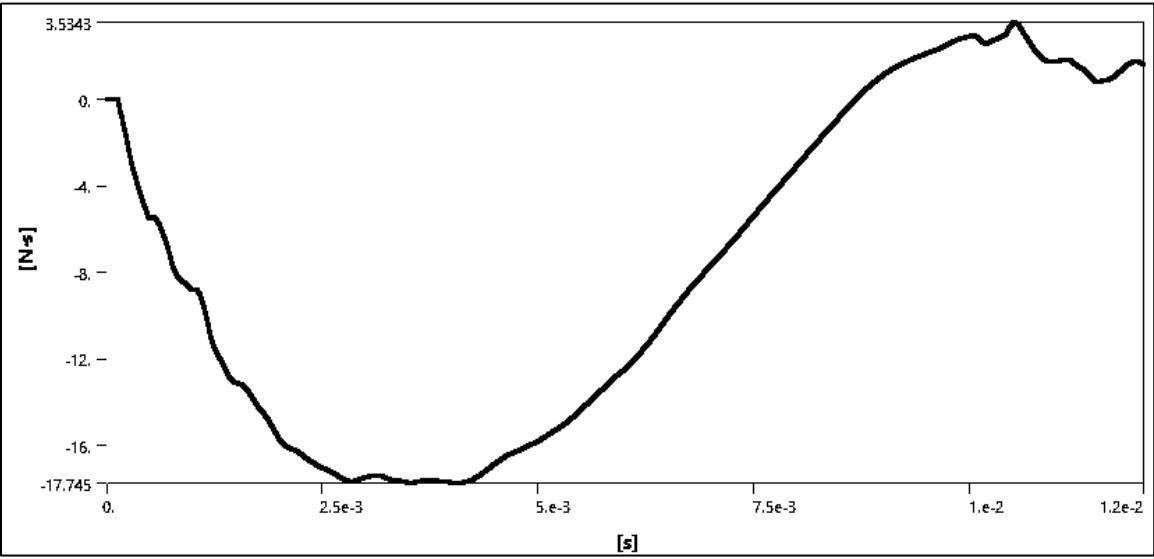


Figure 4.13 : Momentum in y-direction of foam sandwich beam (Case 2)

4.2 Simple hollow beam and foam sandwich beam (PU foam 93kg/m³)

The Polyurethane foam of 40 kg/m³ density proved to be better in most of the selected parameters as mentioned previously, however, the response can change with the number of factors such as very high strain rate, increasing/decreasing the area of contact, other material combinations, increasing foam density etc. Hence, we have selected to make comparison by changing the density and type of polyurethane foam. Again, the weight of all configurations that are compared with each other are kept same. The other conditions such as boundary conditions, area of contact, mass of rigid body, velocity of rigid body is also same. The summary of weight of each component is given in the table 4- 4:

Nomenclature	Material	Hollow	Sandwich (Bonded/Non-bonded)
Skin Weight	SS Non-linear	4.45 kg	4.45 kg
Foam Weight	Flexible/Rigid Polyurethane foam	Nil	0.67 kg
Skin thickness	-	2.3 mm	2.0 mm
Total Weight	-	5.12	5.12 kg

Table 4-4 : Hollow vs sandwich beam Polyurethane foam 93 kg/m³

Previously we have discussed and compared Case 1 and Case 2. Further, now we will take 4 different configurations, i.e., Case 4 to Case 8 by keeping the foam density 93 kg/m³ instead of 40kg/m³ in foam sandwich beam. The difference and all types are summarized in the table 4-5

Configuration Name	Core material	Type
Case 3	Nil	Hollow
Case 4	Flexible PU foam	Bonded
Case 5	Flexible PU foam	Non-bonded (Coefficient of friction = 0.1)
Case 6	Rigid PU foam	Bonded

Table 4-5 : Different configuration of beam from Case 3 to Case 6

In Case 5, the non-bonded means that the foam is not bonded to the inner surface of the steel beam. In this case the coefficient of friction is kept 0.1, which is assumed. In case 6, we used rigid

polyurethane foam instead of flexible polyurethane foam while the connection status is bonded. The material properties of both type of polyurethane foam are already explained in the previous chapter.

The following conclusions and differences are observed during comparison of all the four cases:

4.2.1 Deformation

A rigid mass of 51kg strikes a hollow beam with the velocity 15 m/s. The hollow body deforms 87mm while the foam sandwich beam deforms 66mm. Hence the foam sandwich proves to be stiffer than hollow beam. The energy summary graph also shows that the dissipation is more in foam sandwich beam. For example, in case of hollow beam, the time at which kinetic energy becomes equal to internal energy is above 4 milli-second, while in foam sandwich beam it is below 3.5 milli-second. Similarly, at 7.5 milli-second, the energy summary graph shows 15J of kinetic energy of rigid body in case of hollow beam while in the other case, the kinetic energy is almost 0. This clearly shows that rigid body kinetic energy is reduced to 0.

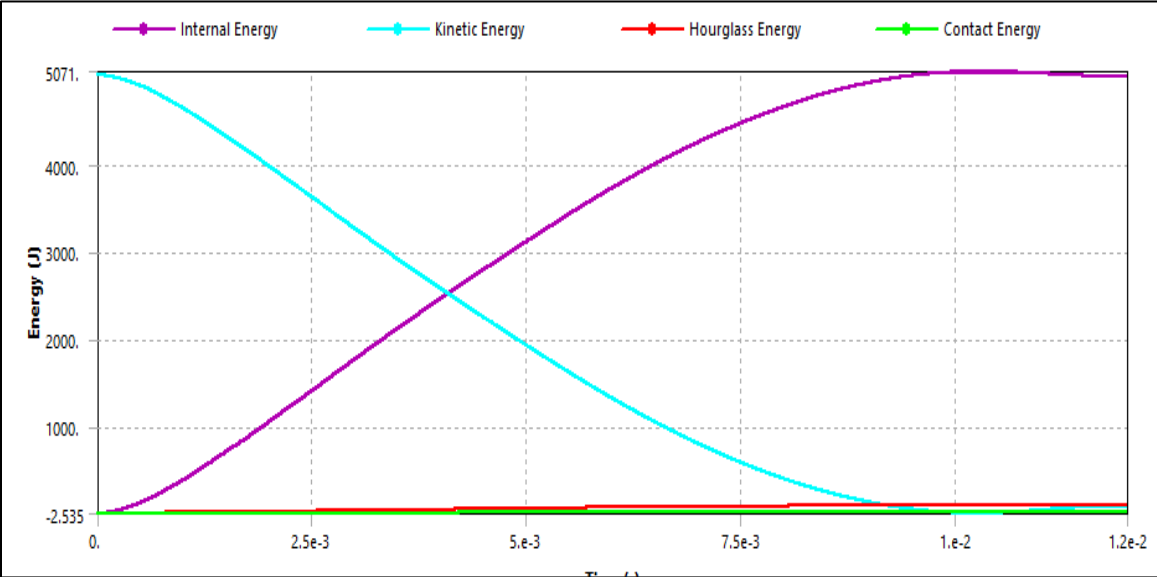


Figure 4.14 : Energy graph of hollow beam (Case 3)

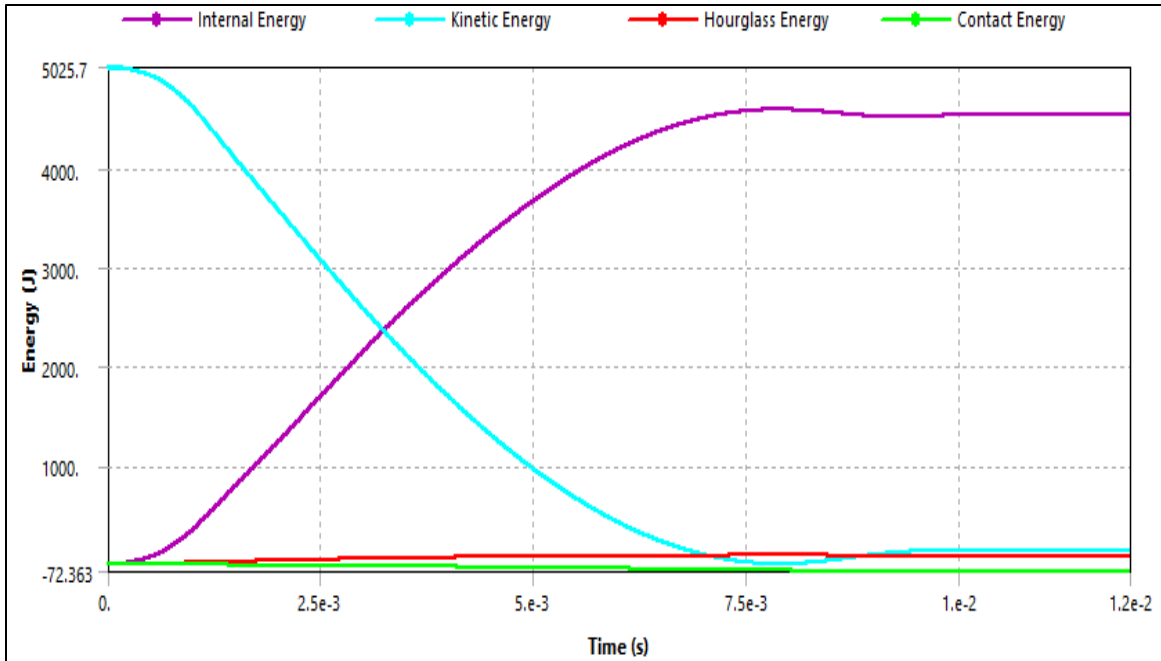


Figure 4.15 : Energy graph of foam sandwich beam - bonded (Case 4)

Similarly, if we analyze the foam-sandwich beam with foam not bonded with a coefficient of friction 0.1, we can see clearly that the maximum deformation of the structure is much more than the previous two. The maximum deformation in this case is 98mm. The energy summary graph shows that the beam is absorbing the energy at a slow rate as shown in the figure by observing the stiffness of the kinetic energy line of the graph given in the Fig 4.16.

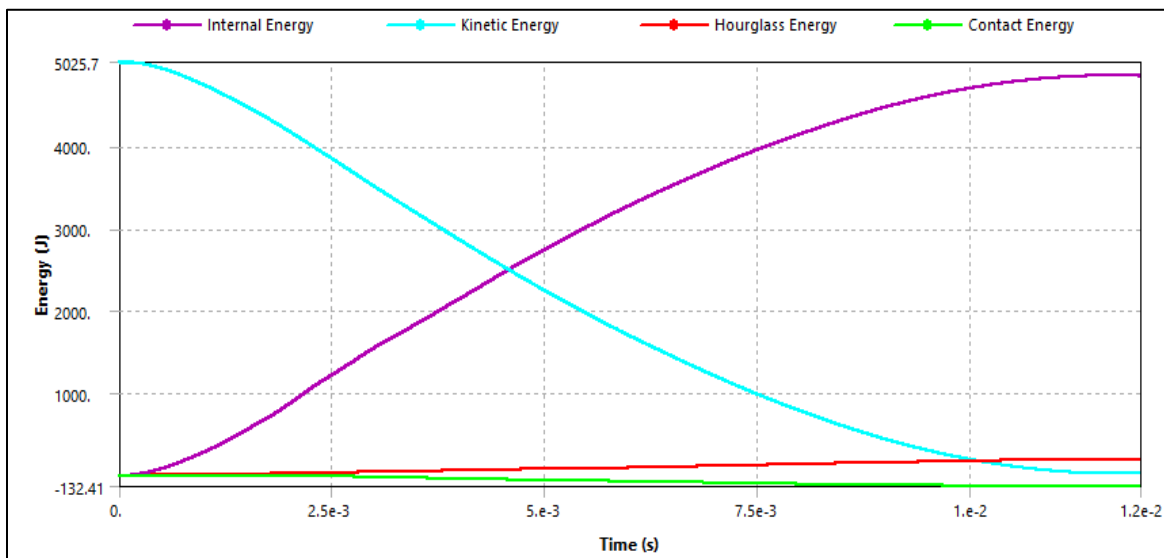


Figure 4.16 : Energy graph of foam sandwich beam – non-bonded (Case 5)

The last alternative is a rigid polyurethane foam which is already explained in the first chapter while the engineering data parameters of the rigid polyurethane foam is explained in the previous chapter. The maximum deformation in this case, while keeping the same boundary conditions and initial conditions is minimum among all the configurations and is 54mm. The energy graph shows that this type of configuration is best among the all-in terms of quick energy absorption.

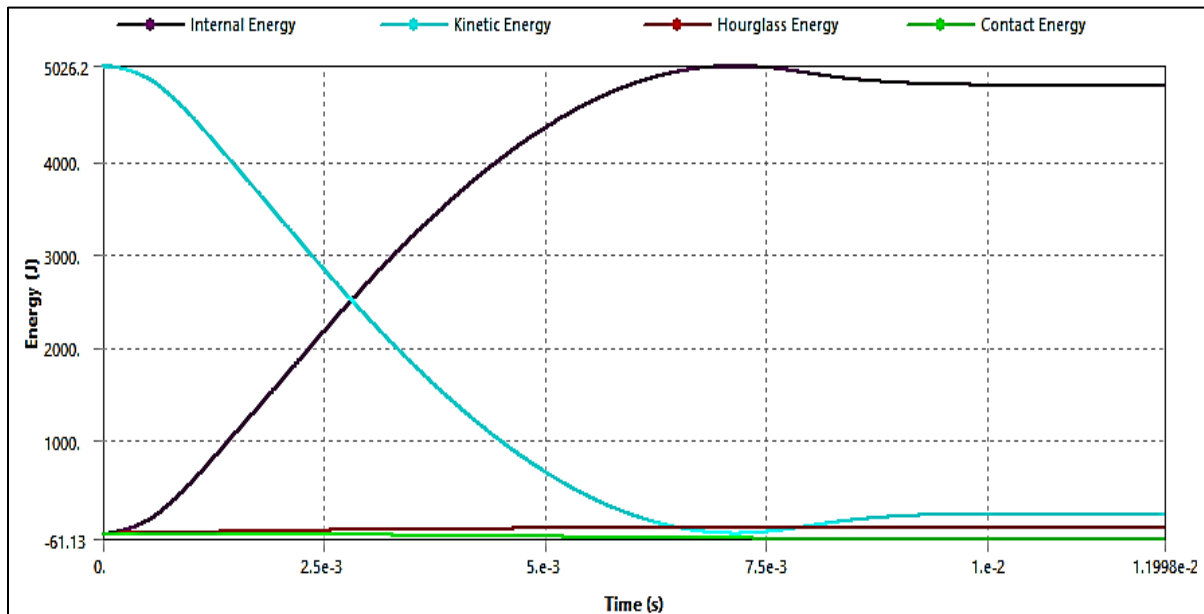


Figure 4.17 : Energy graph of foam sandwich beam - rigid and bonded (Case 6)

4.2.2 Force Reaction-time curve

The force reaction in case of hollow beam is greater in magnitude as well as in time-history as compared to the foam-sandwiched beam. The peak force reaction is 15400 N in case of hollow beam while 14617 N in the other case. Similarly, if we look at both the graphs, around 10 milliseconds, the reaction force is still around 12500N, while in the other case it diminishes to 5000N. For the third configuration in which the foam is not-bonded, the peak reaction force is less among all, i.e., 12546N, but between 5ms to 12ms the magnitude remains constant around 8750N. The fourth configuration is rigid foam bonded and shows the peak reaction force of 14384 N and later after 7.5 ms it reduces to 7500N. So, if we compare all the configurations, the third configuration, i.e., foam with non-bonded and 0.1 coefficient of friction proves to be best in terms of less peak reaction force as well as reduction of reaction force with respect to time.

The reaction force graphs of all the 4 type (Case 3 – Case 6) of beam configuration are shown in the Fig 4.18 – 4.21.

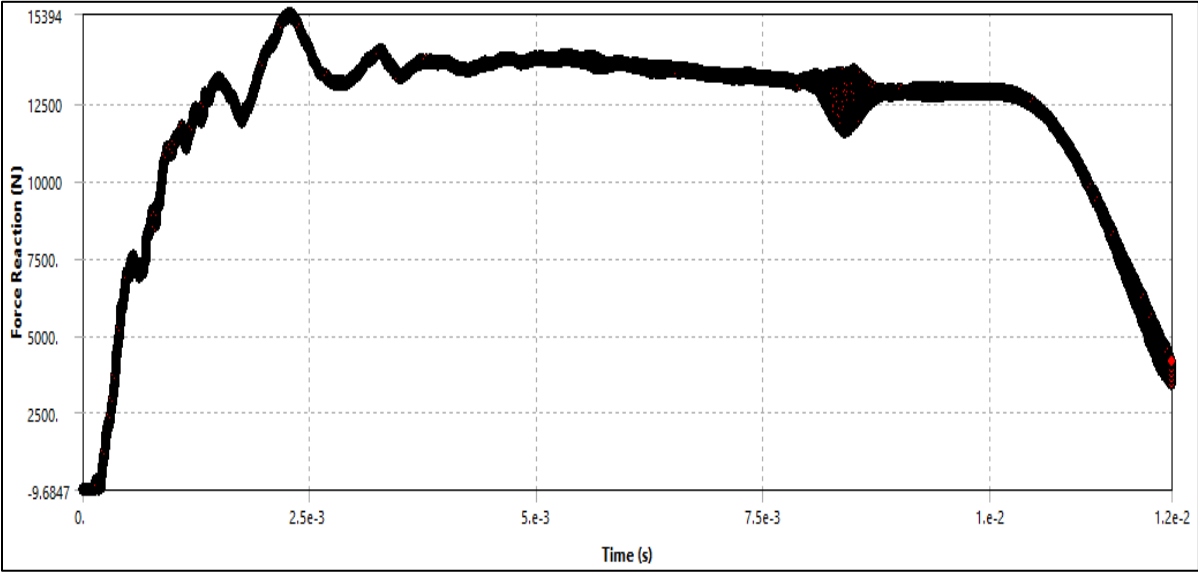


Figure 4.18 : Reaction force-time graph of hollow beam (Case 3)

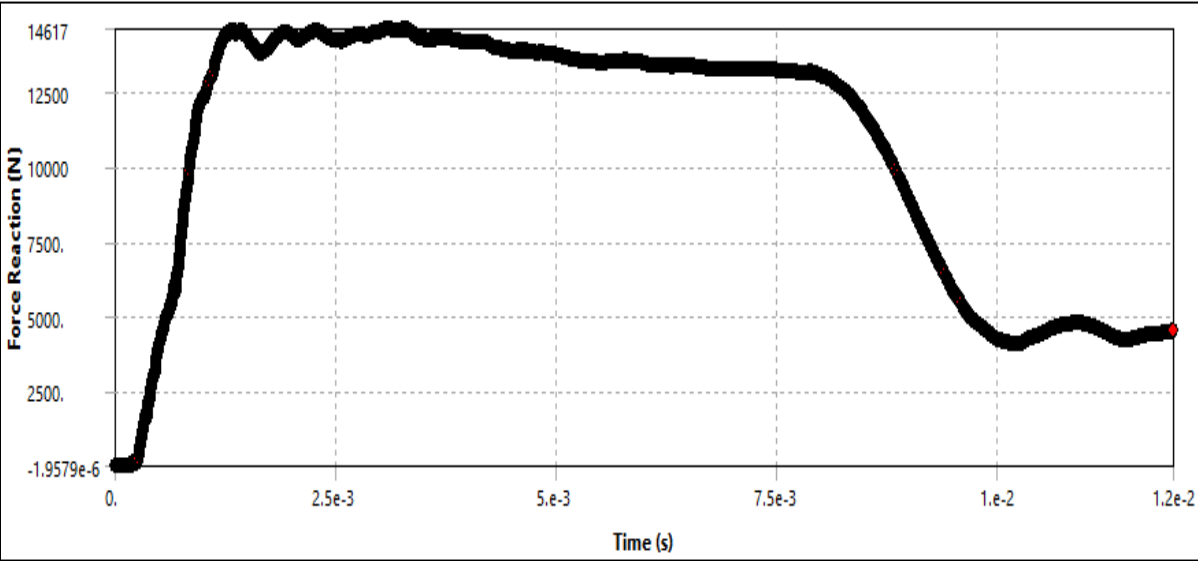


Figure 4.19 : : Reaction force-time graph of foam sandwich beam - bonded (Case 5)

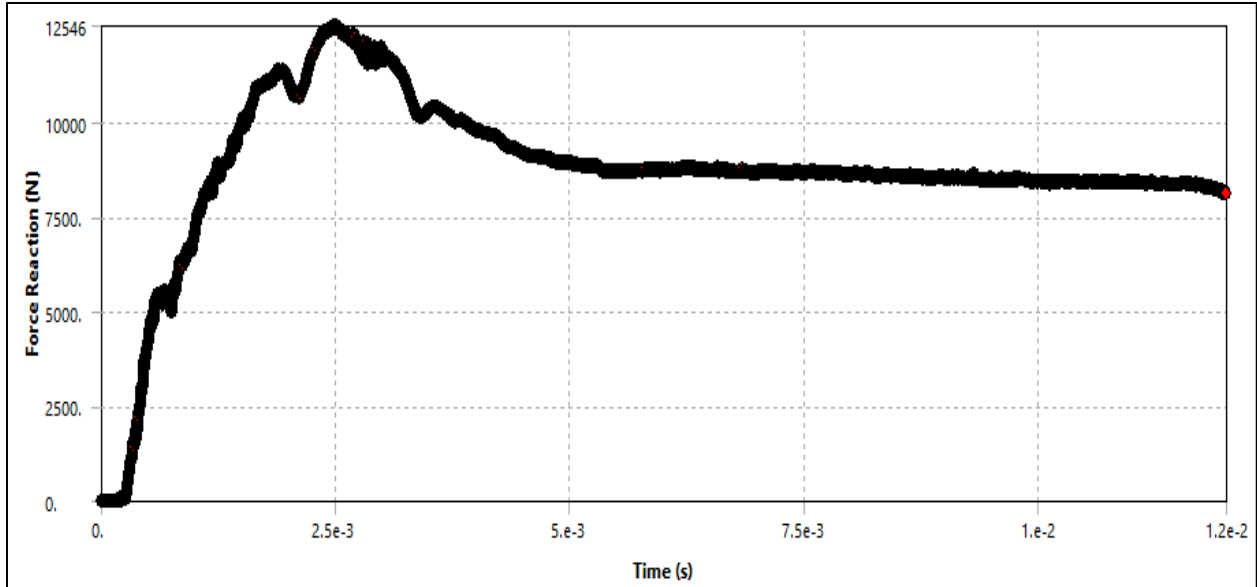


Figure 4.20 : : Reaction force-time graph of foam sandwich beam – non-bonded (Case 5)

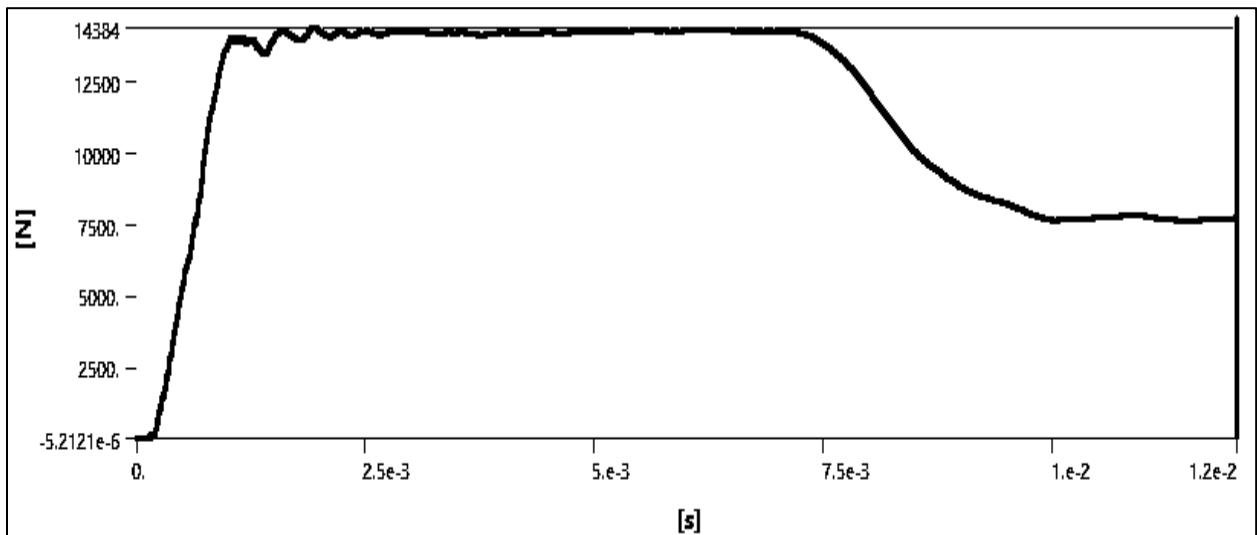


Figure 4.21 : Reaction force - time graph of foam sandwich beam - rigid and bonded (Case 6)

4.2.3 Kinetic Energy

The peak kinetic energy is less in hollow beam as compared to its competitor, but the kinetic energy quickly diminishes in foam sandwich structures. At 7.5 milli-second it is completely reduced to 0 while in case of hollow structure, the Kinetic energy at 7.5 milli-seconds is 15 J. This shows that the stability after impact in the foam-sandwich structure is more as compared to its competitor. Also, by increasing the density of the foam, the stability increases after impact if we compare it with the foam-sandwich beam of 40 kg/m³ density. The kinetic energy graph of non-

bonded foam sandwich and rigid polyurethane foam are also shown in the figure 4.22 – 4.24. Although the peak energy in non-bonded is best but not good in dissipation.

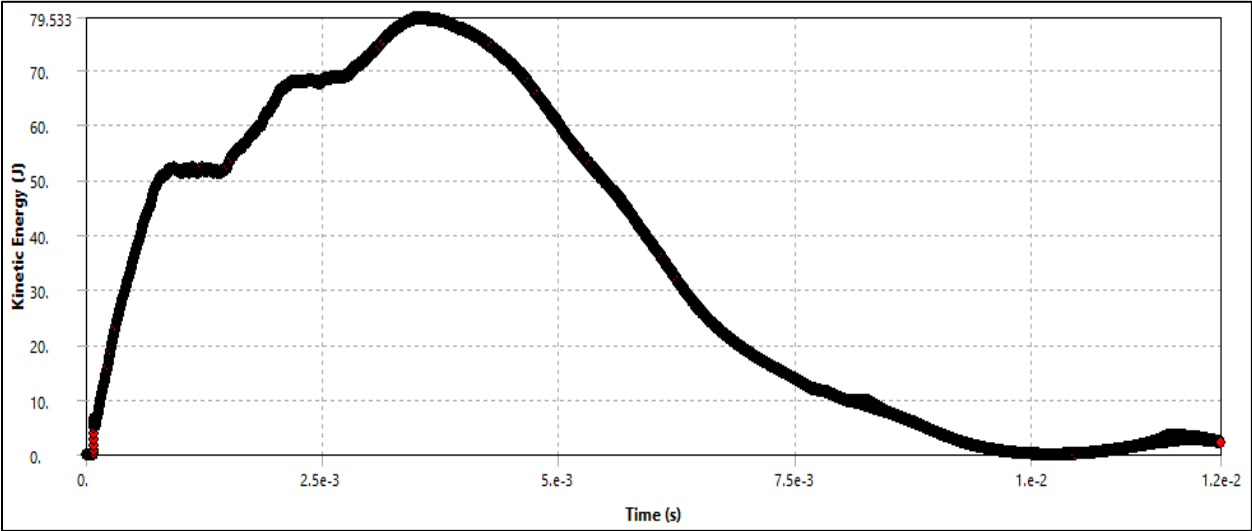


Figure 4.22 : Kinetic energy-time graph of hollow beam (Case 3)

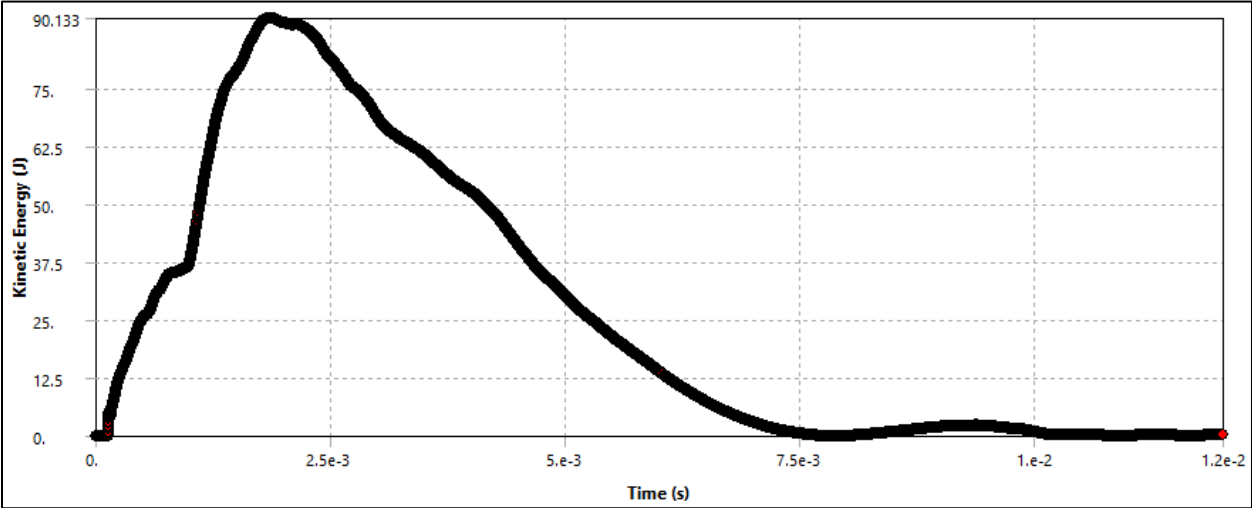


Figure 4.23 : Kinetic energy-time graph of foam sandwich beam – bonded (Case 4)

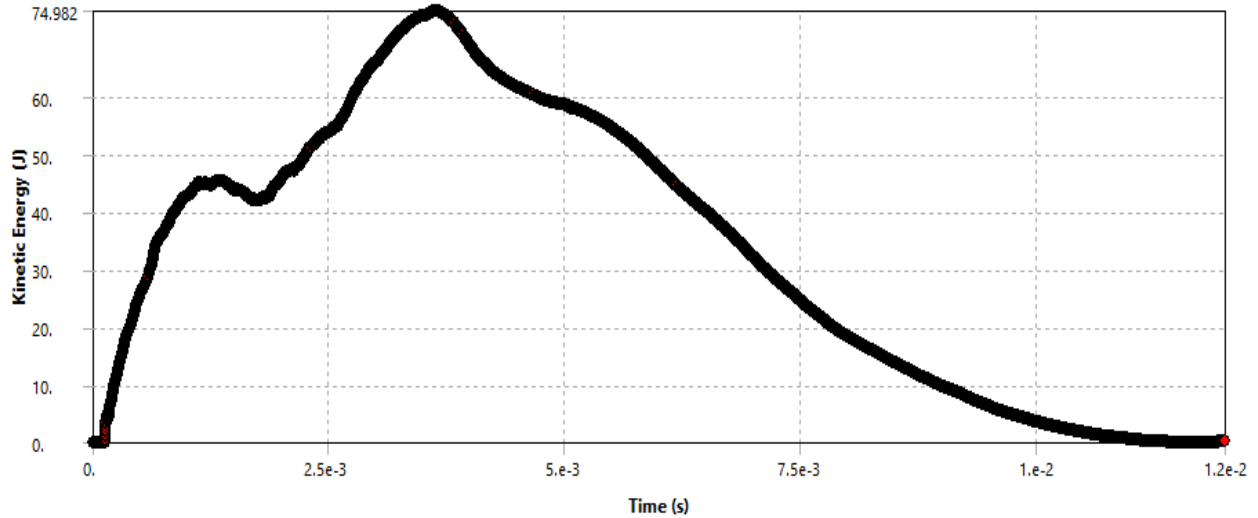


Figure 4.24 : Kinetic energy-time graph of foam sandwich beam – non-bonded (Case 4)

4.2.4 Velocity

The velocity of all the 4 types of configuration in the direction of collision is compared. By comparing the case 3 (hollow) and case 4 (foam-sandwich) velocity-time history graph, initially the hollow beam gains less velocity as compared to foam-sandwich beam but later the foam-sandwich turns to rest quickly than the hollow beam. This shows that the dissipation of kinetic energy in the foam-sandwich beam is more, while the peak velocity of hollow beam is less than the other.

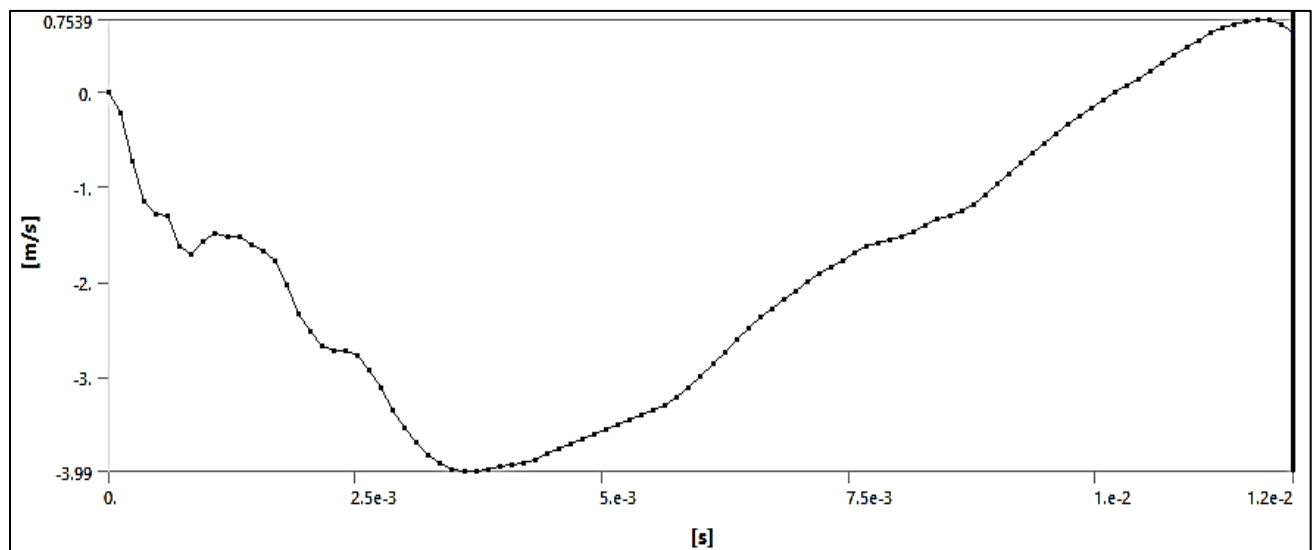


Figure 4.25 : Velocity-time graph of hollow beam (Case 3)

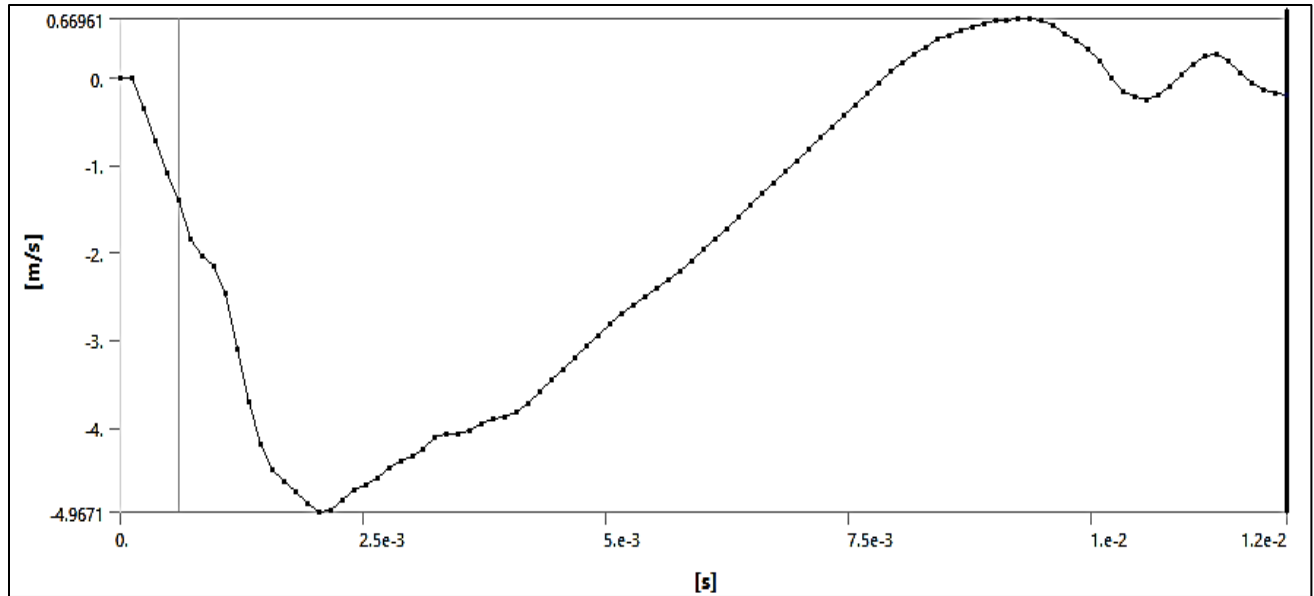


Figure 4.26 : Velocity-time graph of foam sandwich beam-bonded (Case 4)

The velocity profile of the non-bonded foam-sandwich beam and rigid body is given, and the velocity is found to diminish quickly in rigid polyurethane foam.

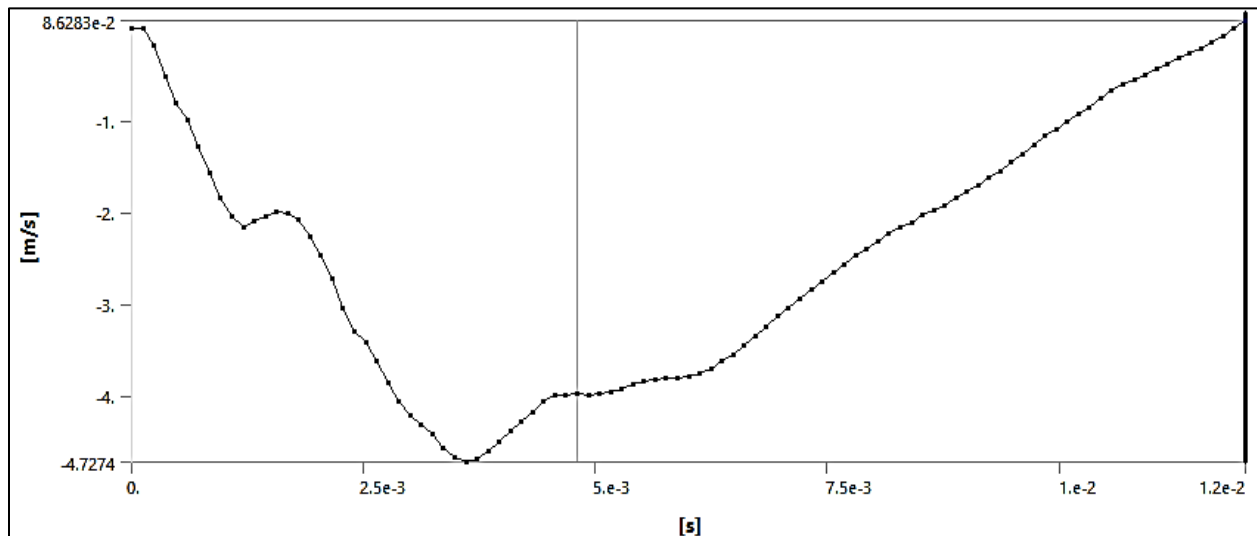


Figure 4.27 : Velocity-time graph of foam sandwich beam – non bonded (Case 5)

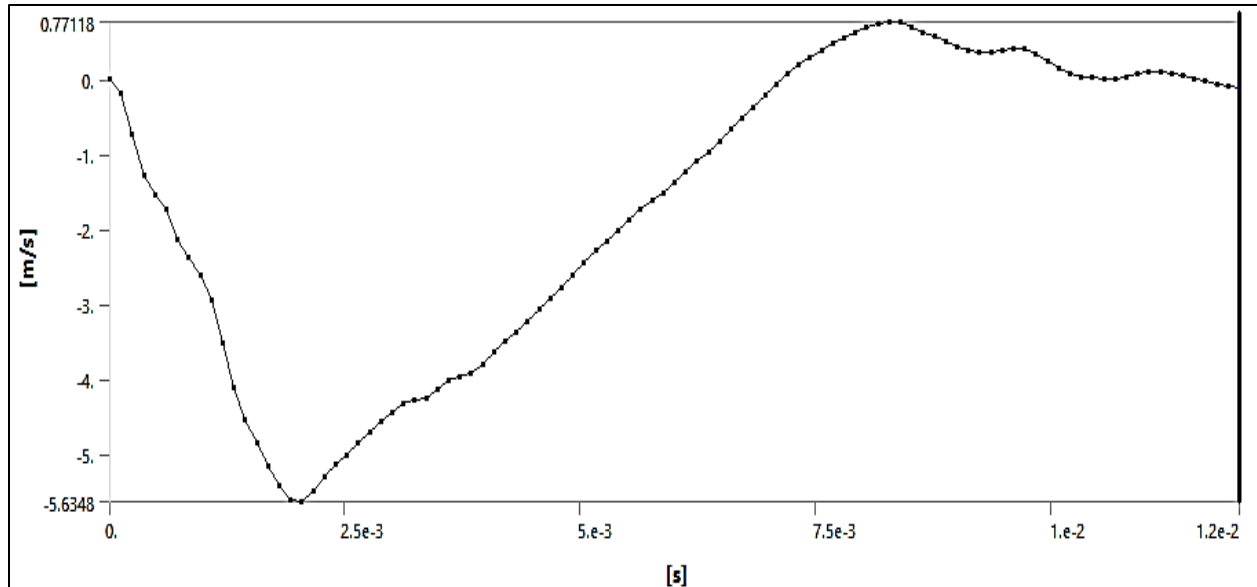


Figure 4.28 : Velocity-time graph of foam sandwich beam-rigid and non-bonded (Case 6)

4.2.5 Acceleration

The same case is shown in the acceleration-time plot history in all the configurations

The hollow beam shows random acceleration during entire time-history while in bonded configuration the structure shows good damping and after approximately 2.5 milli-second the acceleration of the structure is reduced considerably but the peak magnitude of acceleration shifts earlier than the hollow structure and is greater in magnitude. If we look to the graph of non-bonded foam-beam, it shows much low acceleration level in terms of peak magnitude as well as over the rest of time as compared to previous configurations. At last, the rigid polyurethane foam achieves maximum acceleration among all. Hence, in terms of damping and controlled acceleration level of the structure the non-bonded configuration is the best.

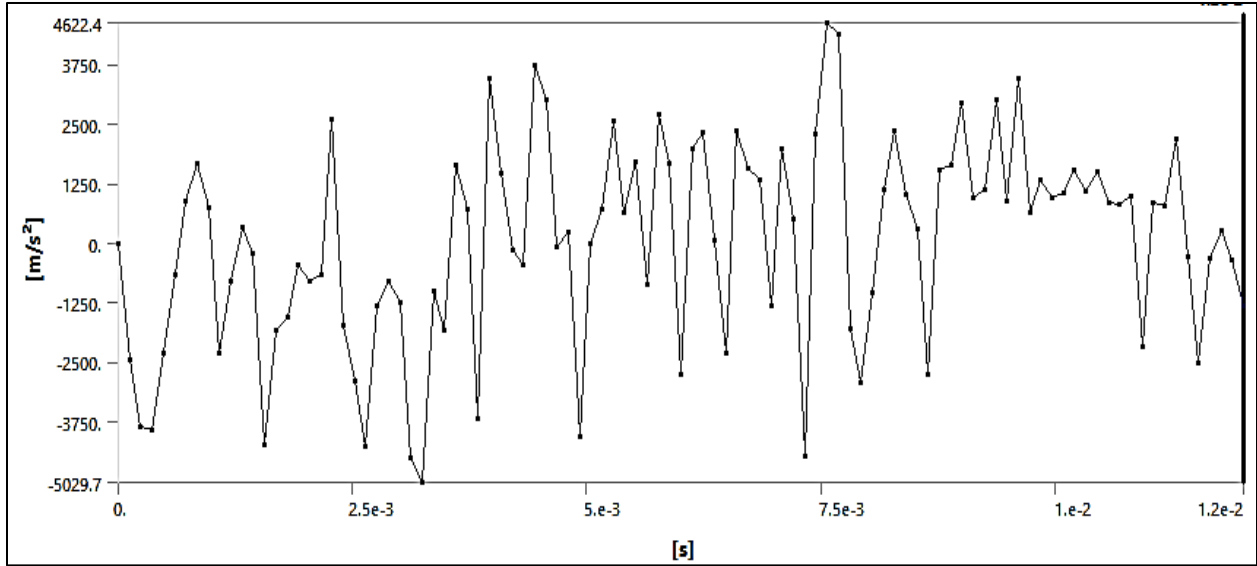


Figure 4.29 : Acceleration-time graph of hollow beam (Case 3)

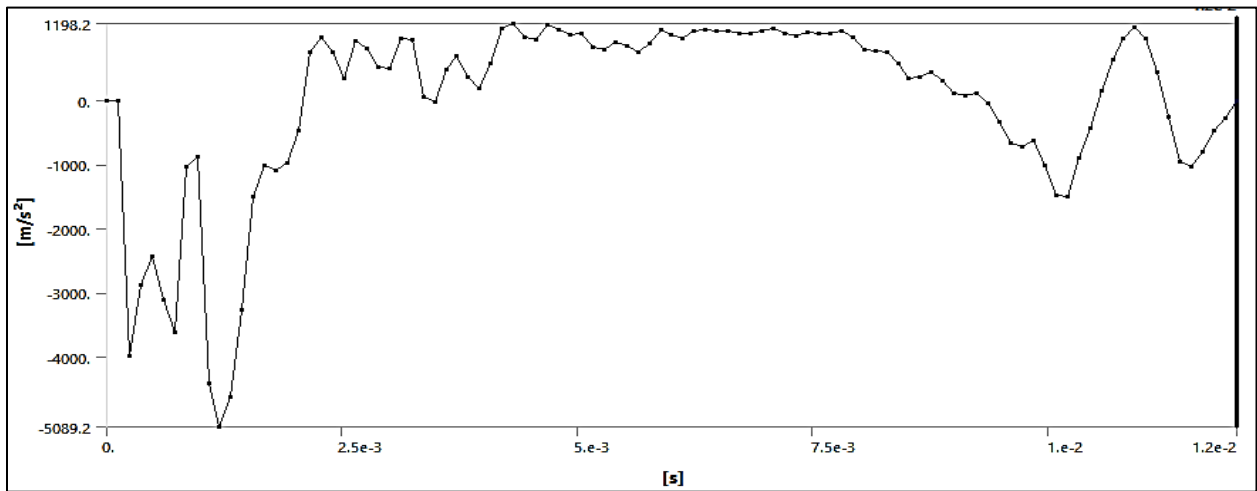


Figure 4.30 : Acceleration-time graph of foam sandwich beam - bonded (Case 4)

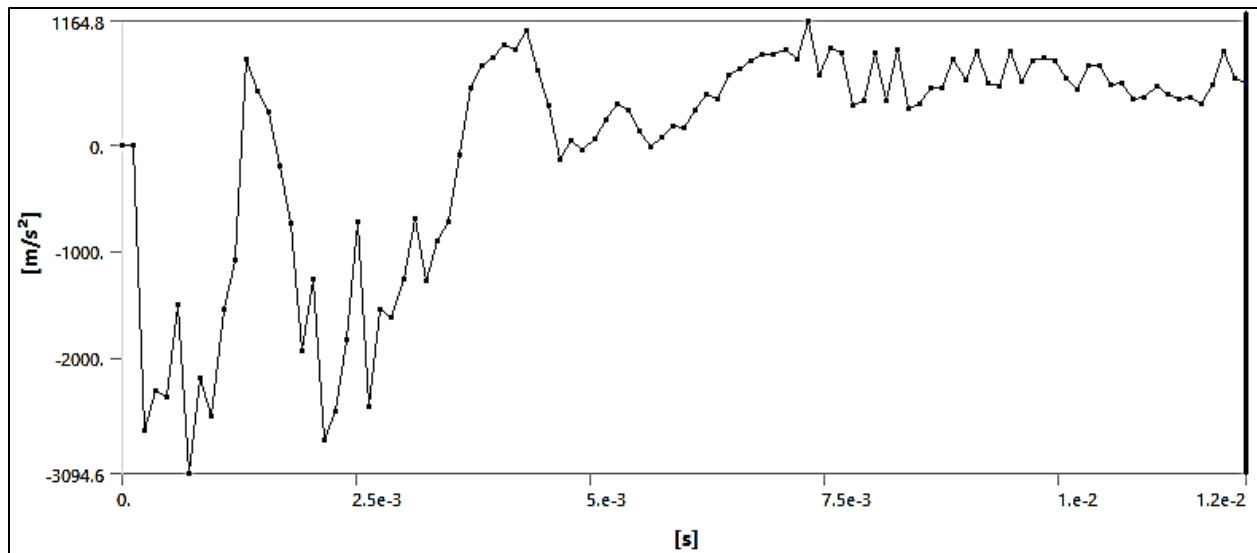


Figure 4.31 : Acceleration-time graph of foam sandwich beam - non-bonded (Case 5)

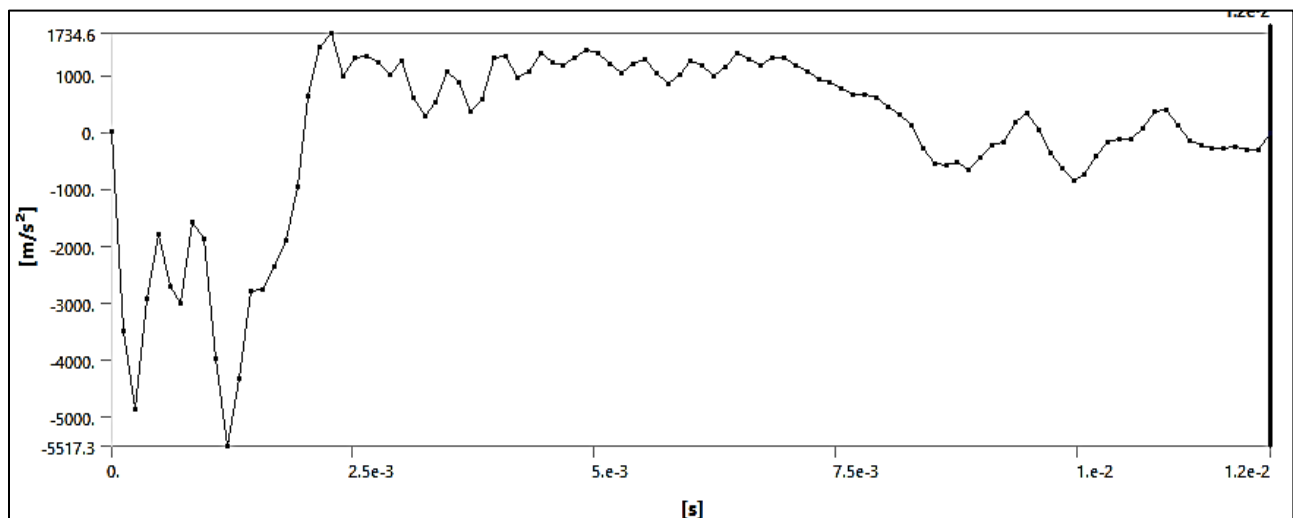


Figure 4.32 : Acceleration-time graph of foam sandwich beam- rigid and bonded (Case 6)

4.3 Two-Channel Hollow and Sandwich Beam (PU foam 93kg/m³)

In this section we will discuss the results of Case 7 and Case 8. Previously, a hollow simple beam was investigated, and the results are discussed previously and compared to its alternative foam-sandwich. The results show that foam-sandwich is a better alternative in terms of reaction force and acceleration damping. Therefore, it needs to be further investigated that whether the performance is geometry dependent or not. So, a two-channel beam is analyzed by keeping the

same external dimensions as that of hollow simple beam. The details of the beam is given in the table:

Nomenclature	Material	Density (kg/m ³)	Hollow	Sandwich
Skin Weight	SS Non-linear	7810	4.98 kg	4.45 kg
Wall surface	SS Non-linear	7810	1.08 kg	0.96
Foam 1 Weight	Flexible Polyurethane foam	93	Nil	0.33 kg
Foam 2 Weight	Flexible Polyurethane foam			0.33 kg
Skin thickness	-		2.24 mm	2.0 mm
Total Weight	-		6.06 kg	6.07 kg

Table 4-6 : Two-channel hollow and foam-sandwich beam

4.3.1 Deformation

The maximum deformation shown by ANSYS analysis in case of two-channel hollow beam is 68mm, while for foam-sandwich the maximum deformation is 54mm as shown in figure 4.33 and 4. 34.

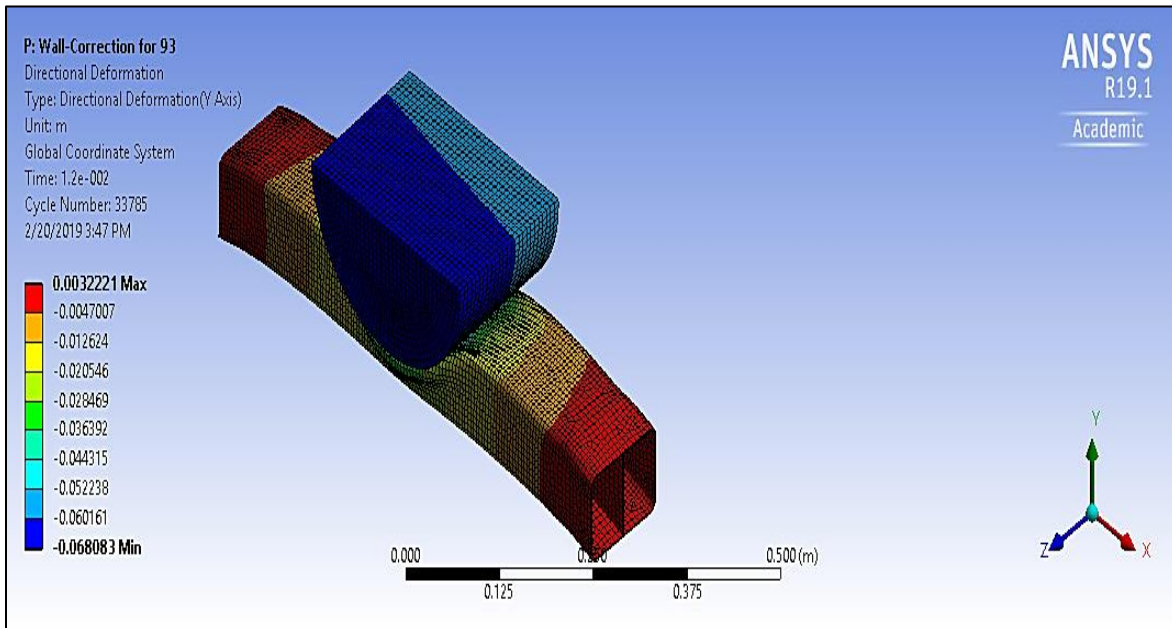


Figure 4.33 : Maximum deformation of two-channel hollow beam (Case 7)

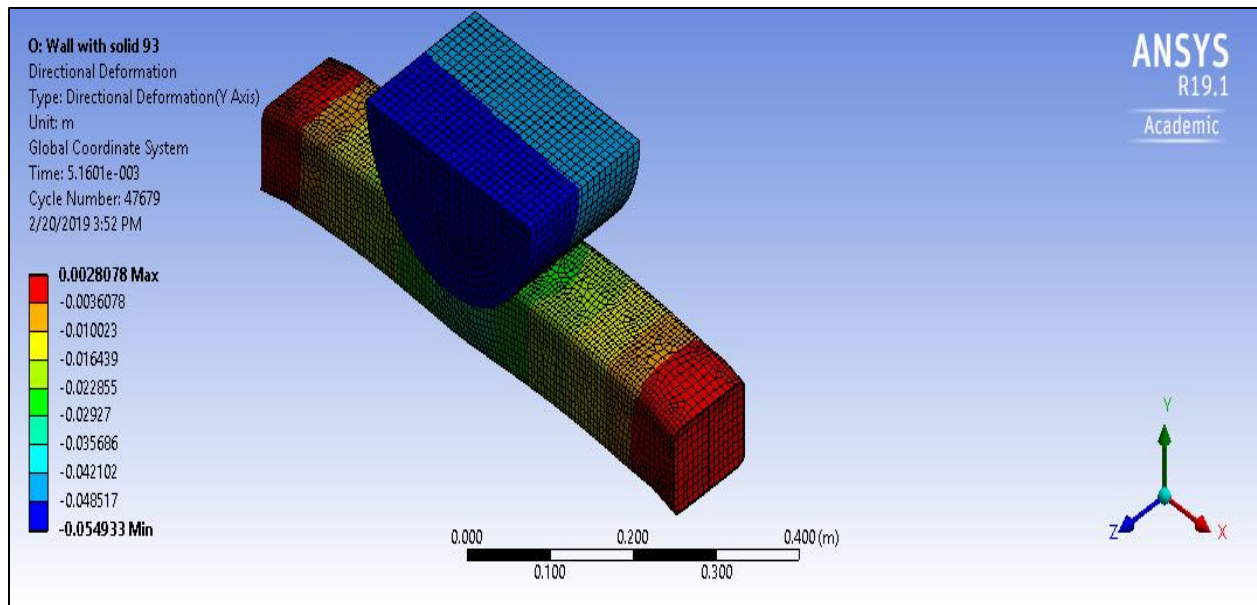


Figure 4.34 : Maximum deformation of two-channel foam sandwich beam (Case 8)

In this case, we can conclude again that the foam-sandwich is stiffer as compared to hollow beam when subject to impact. The energy summary also shows that the same configuration is better in absorbing the energy and reducing the kinetic energy of the external body quickly as compared to hollow beam. For example, if we see the graph of both configurations, we can see that at 5 milli-sec the external body still have Kinetic energy of 1000 J, while the other one has reduced it to almost 0. Moreover, the intersection point, which means that the internal energy of beam becomes equal to the total kinetic energy possessed by external body reaches earlier in foam-sandwich beam.

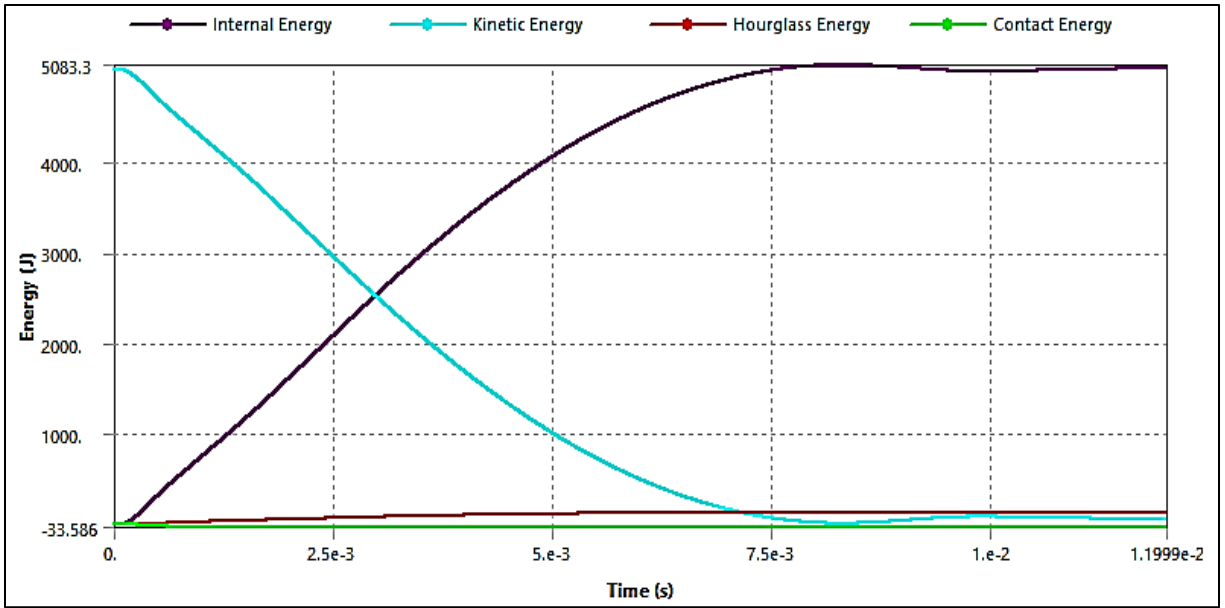


Figure 4.35 : Energy graph of two channel beam (Case 7)

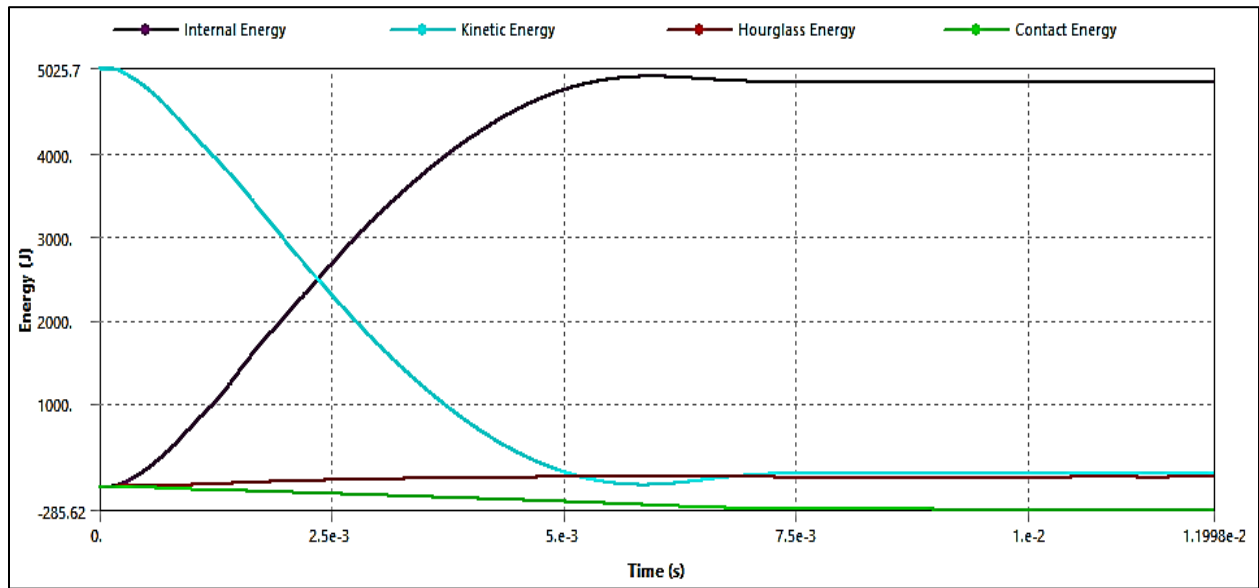


Figure 4.36 : Energy graph of two channel foam sandwich beam (Case 8)

4.3.2 Reaction Force-time curve

The reaction force in two-channel hollow beam shows the peak magnitude of 29000 N approximately. This is a quite big reaction force while in the foam-sandwich the peak magnitude is 25000 N. Similarly, the reaction forces are reduced to minimum amount quickly in the second

case and hence shows that the structure has good capability to absorb the external energy. If we compare with the previous cases, we can see that the difference between the peak reaction forces of simple hollow beam and its equivalent foam-sandwich beam was approx. 780 N for the 93kg/m³ polyurethane foam. In this case the difference is 4000N. This shows that if we use high density foam in the structure it will reduce the reaction forces considerably.

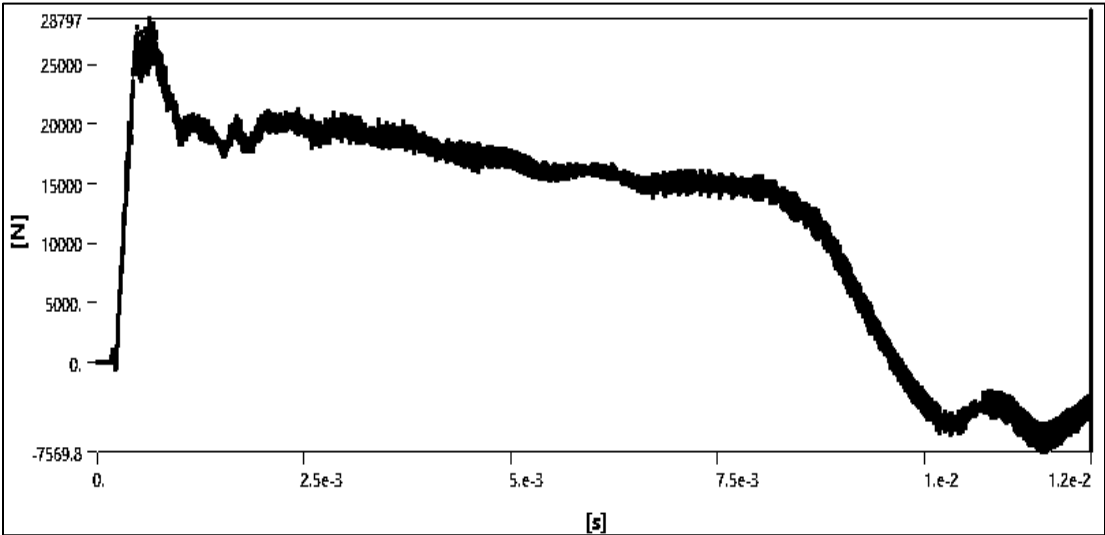


Figure 4.37 : Reaction force-time graph of two channel hollow beam (Case 7)

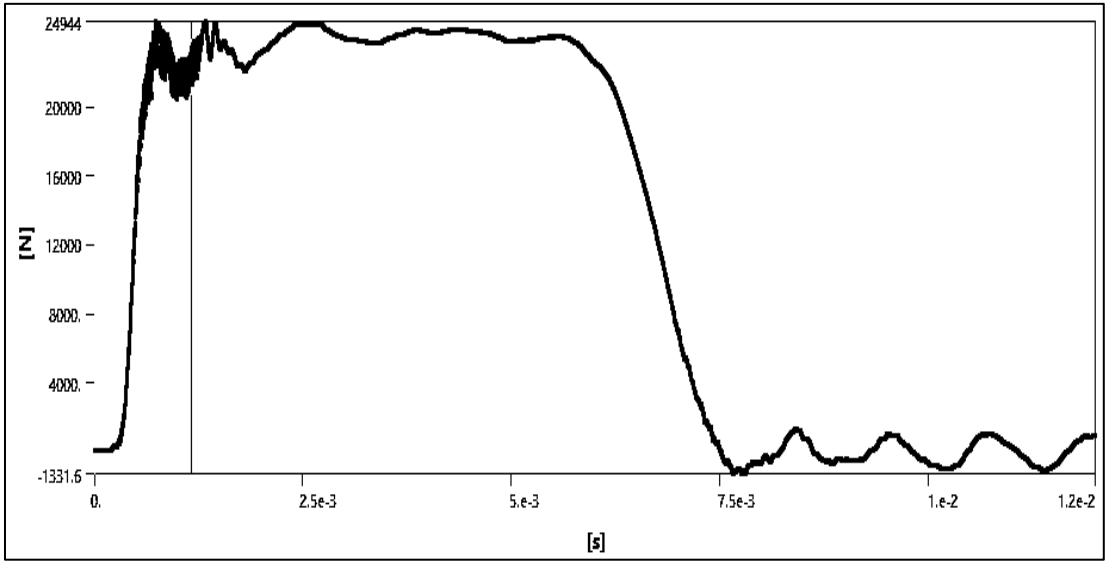


Figure 4.38 : Reaction force-time graph of two channel foam sandwich beam (Case 8)

4.3.3 Velocity (y-axis)

In hollow 2-channel beam, the velocity-time graph in the direction of collision is obtained which shows that velocity diminishes at a slow rate as compared to foam-sandwich. It is clear from the velocity-time graph of both the configurations. The stiffness of the line in the first figure is more than the second figure. If we compare the results with the previous simple hollow beam and foam-sandwich beams, we conclude that by using the heavier foam density the reduction in the velocity is quick and is almost directly proportional to the density of the foam.

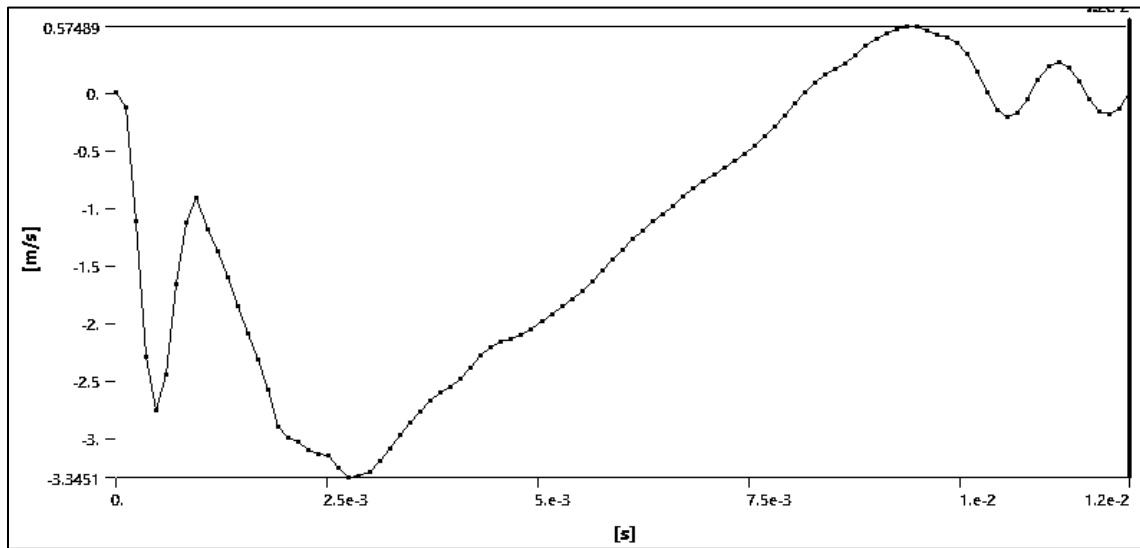


Figure 4.39 : Velocity-time graph of two channel hollow beam (Case 7)

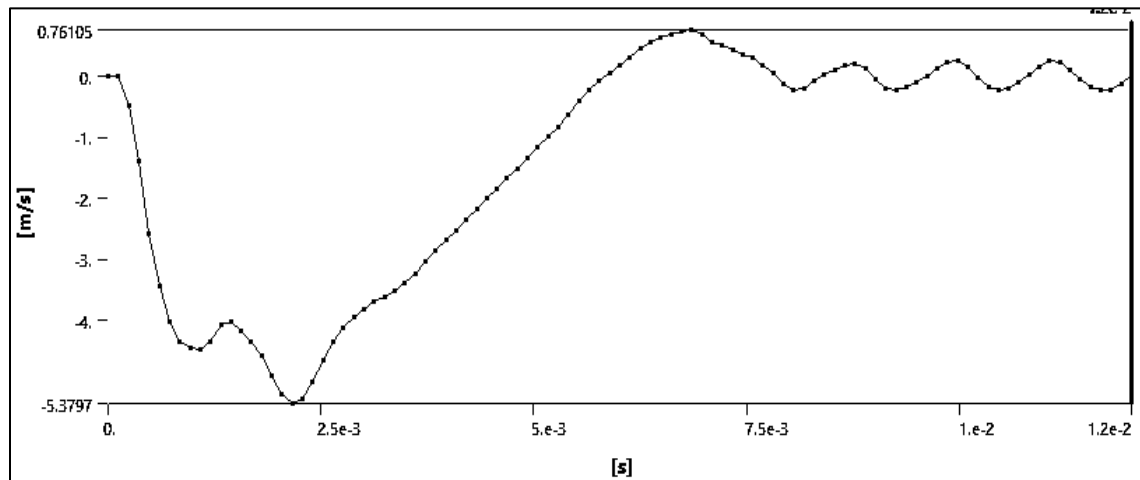


Figure 4.40 : Velocity-time graph of two channel foam sandwich beam (Case 8)

4.3.4 Acceleration (y-axis)

The acceleration of the structure is improved in the foam-sandwich structure and the dissipation is better. This shows that the structure stability can be improved by using foam as a core material specially in the application requiring impact. After 1 milli-second, the structure acceleration reduces considerably in the foam-sandwich structure while the hollow two channel structure is susceptible to violent vibrations and is evident from the figure. Moreover, the magnitude of peak acceleration is also reduced and there is a quite a large difference between this magnitude.

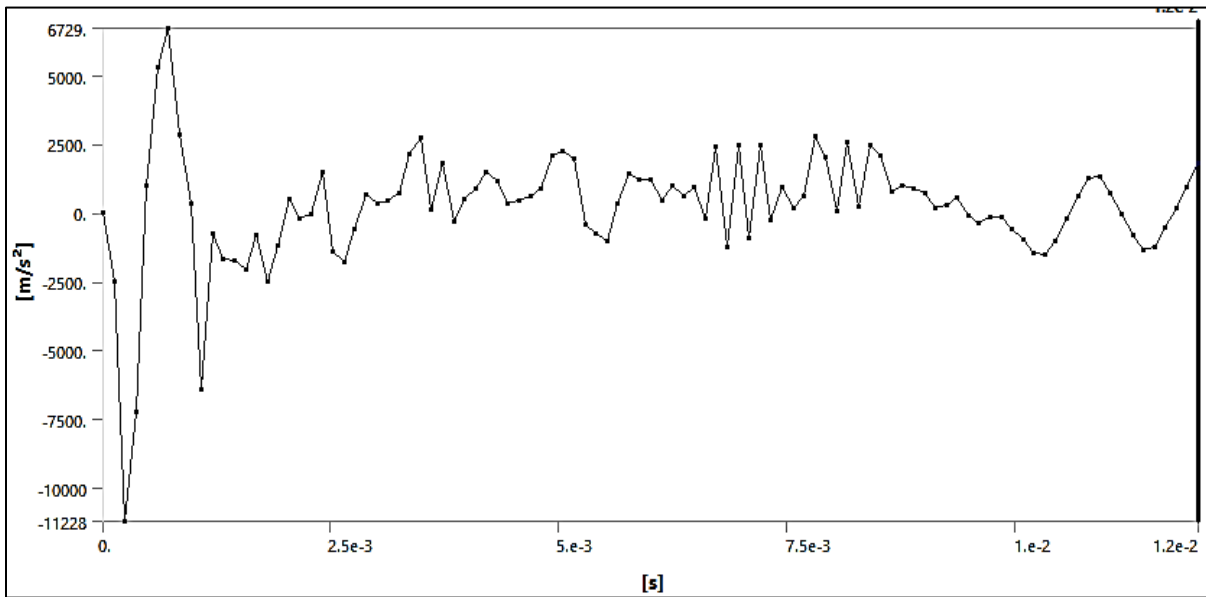


Figure 4.41 : Acceleration-time graph of two channel hollow beam (Case 7)

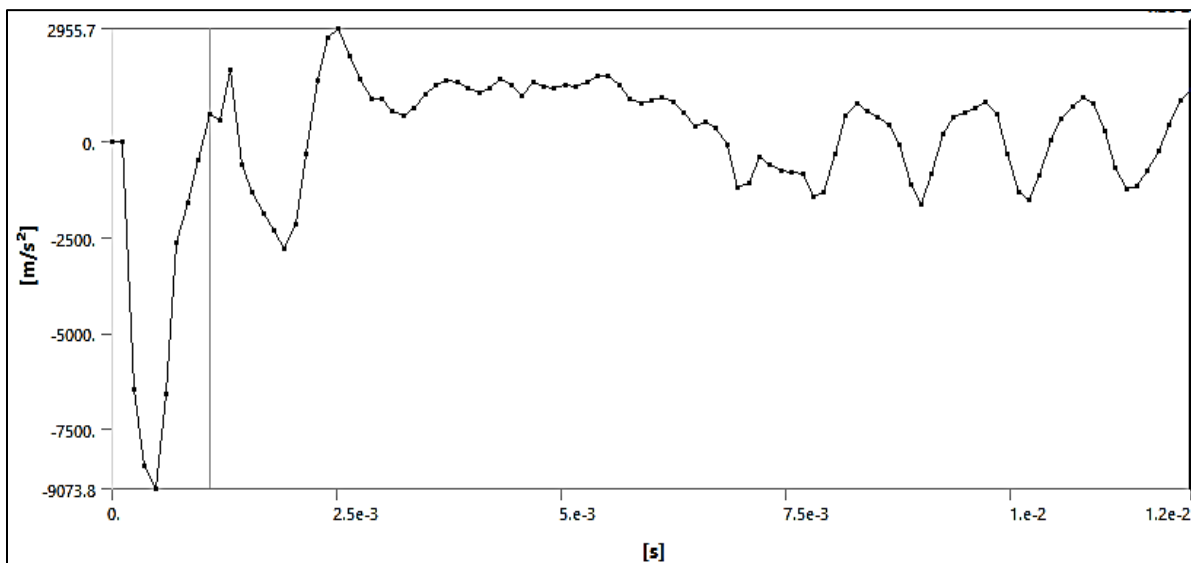


Figure 4.42 : Velocity-time graph of two channel foam sandwich beam (Case 8)

4.3.5 Acceleration (y-axis)

A two-channel hollow beam (case 7) kinetic energy-time graph is compared with the two-channel foam-sandwich beam (case 8). The peak magnitude of kinetic energy is low in former case while more in later case, but dissipation is better in the second case. This is also supported by the velocity-time graph discussed in the previous section.

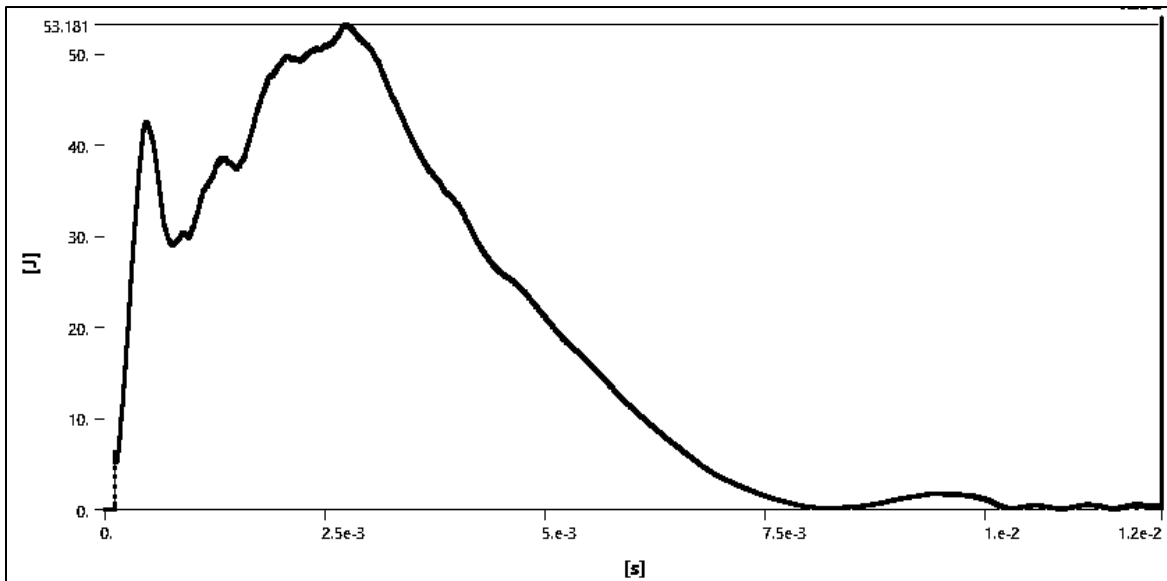


Figure 4.43 : Kinetic energy graph of two channel hollow beam (Case 7)

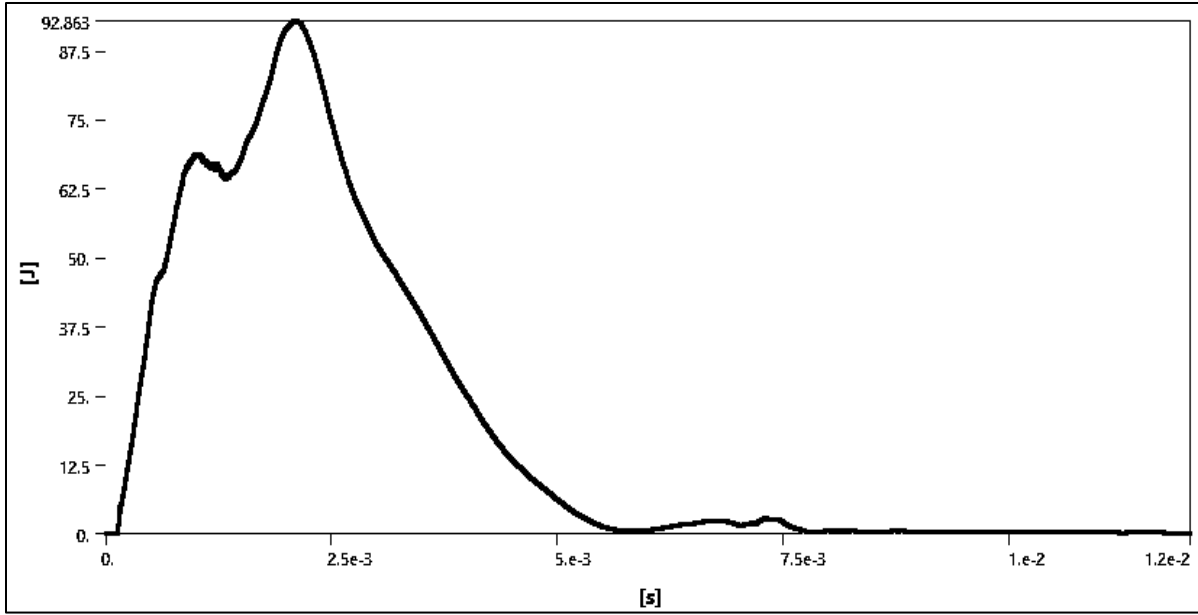


Figure 4.44 : Velocity-time graph of two channel foam sandwich beam (Case 8)

5. Conclusion

In this thesis, the effort is made to simulate and analyze different configuration of beams during impact. The impact time is chosen to be 12 milli-seconds and different output variables with respect to time are studied. The beams are simulated in such a way that the ends of the beams are fixed, and the impactor body is made to strike the beam with velocity of 54 km/h (15m/sec). The basic objective of this thesis is to study the behavior of the hollow beams and their equivalent weight foam sandwich beams. The Polyurethane foam is considered here as the core material in the foam sandwich beams. Two types of PU foam are considered in this analysis, i.e., flexible and rigid PU foam. Similarly, two types of densities of PU foam are considered to see the effect of density on the behavior of the foam sandwich beams. The densities are 40kg/m^3 and 93 kg/m^3 . In this analysis, two types of contact, i.e., bonded and non-bonded are considered between the foam and the skin of the beam to see effect of changing the contact type on the behavior of the body. In a nutshell, the comparison is made between the hollow beam and its equivalent weight foam sandwich beam and further the comparison is made between the foam sandwich beams of bonded and non-bonded contacts and as well as different densities of foam used in the analysis.

In the previous chapter, the results are discussed and explained in detail. To summarize the results and conclude, the table 5.1 shows the comparison of results of simple hollow beam and its equivalent foam sandwich beam. Further the contact type of foam and skin of the beam is changed to non-bonded and the coefficient of friction of 0.2 is taken arbitrary. It is clear from the table that the weights of the beam are equal, and the thickness of foam sandwich beam is less than the hollow one due to the presence of the foam. The results show that foam sandwich beam with bonded connection is stiffer among the all and the equivalent plastic strain experienced is less. Similarly, the reaction force experienced at the support in the foam sandwich beam with bonded contact is less than the corresponding hollow one, while the foam sandwich beam with non-bonded contact is the least among them. Thus, in terms of reaction forces and stiffness the foam sandwich beam is better while the non-bonded contact is better among them in terms of minimizing the reaction forces at the supports.

Simple (One-channel) Beam			
Polyurethane foam 40 kg/m³			
Type	Hollow (w/o foam)	Foam Bonded	Foam non-Bonded
Weight	4.74 kg	4.73	4.75
Thickness of skin	2.13 mm	2.0 mm	
End Time	12 ms (0.012 sec)		
Max. Deformation (mm)	97mm	72	107
Equivalent Plastic Strain (m/m)	0.237	0.198	0.25
Reaction Force (N)	13450	13428	12750

Table 5-1 : Comparison of Simple hollow beam and the foam sandwich beam (PU foam 40 kg/m³)

Similarly, the kinetic energy-dissipation-time graph and the acceleration-time graph of hollow and foam bonded shown in figure 4.6, 4.7, 4.10 and 4.11 shows that the peak acceleration is reduced considerably in the foam sandwich beam and the damping is observed to be more than the corresponding hollow beam.

The above conclusion is drawn by using the polyurethane foam of density 40kg/m³ and further there was need to investigate that how much the behavior changes by changing the polyurethane foam density. Therefore, a higher density of polyurethane foam, i.e., 93kg/m³ was selected and analyzed by keeping the simulation parameters same. Further, the rigid polyurethane foam of the same density was also analyzed. The following table shows the results:

Simple (One-channel) Beam				
Polyurethane foam 93 kg/m³				
Type	Hollow (w/o foam)	Foam Bonded	Foam Non-Bonded	Foam Bonded - Rigid
Weight	5.11	5.12	5.12	5.12
Thickness of skin	2.3mm	2.0mm	2.0mm	2.0 mm
End Time	12 ms (0.012 sec)			
Max. Deformation (mm)	88mm	69mm	98mm	54mm
Equivalent Plastic Strain (m/m)	0.22	0.18	0.24	0.16
Reaction Force (N)	15394	14617	12546 (u=0.1)	14384

Table 5-2 : Comparison of Simple hollow beam and the foam sandwich beam (PU foam 93 kg/m³)

From the table 5-2, it is again clear that in terms of reaction forces, the foam sandwich beam is better option as compared to corresponding hollow beam while the non-bonded is the best option among all. Here, it is important to mention that foam-bonded rigid polyurethane foam of same density is better than the foam bonded flexible polyurethane foam in all terms, and it is evident

from the table as well. The same conclusion can also be drawn for kinetic energy-time graph and acceleration-time graph shown in figures

In the last, the geometry is considered by changing the beam from single to two channel hollow and sandwich beam. The polyurethane foam of density 93 kg/m^3 is used and only bonded contact of foam sandwich beam is considered. The table shows the comparison between two-channel hollow and sandwich beam.

Two channel beam		
Polyurethane foam 93 kg/m^3		
Type	Hollow (w/o foam)	Foam Bonded
Weight	6.06	6.07
Thickness of skin	2.24 mm	2 mm
End Time	12 milli-second	12 milli-second
Max. Deformation (mm)	68	52
Equivalent Plastic Strain (m/m)	0.234	0.244
Reaction Force (N)	28800	25000

Table 5-3 : Comparison of two channel hollow beam and the foam sandwich beam

The same conclusion can be drawn from the above table that the foam bonded sandwich beam is better in terms of stiffness and minimum reaction forces. Moreover, the kinetic energy-time and acceleration-time graph shown in the figures 4.41, 4.42, 4.43 and 4.44 shows that the foam sandwich beam has better damping than its equivalent hollow beam.

The above all results show that the deformations in the foam sandwich beams are less as compared to the hollow beams, i.e., foam sandwich beams proved to be stiffer than the hollow beams of the same weight. The acceleration-time history also shows that the damping in the foam sandwich beam is better than the hollow beams and thus can be used in the applications where the damping is necessary. The kinetic energy-time graph of the beam body shows that the dissipation is quick in the foam sandwich beams which again is a positive aspect of such type of beams and can be preferred over hollow beams. The reaction force-time history comparison shows that the foam sandwich beams are better and transmit less impact force to the supports, which means less stress on the supports of the beams. This is needed much if we consider it as a case of front bumper beam of the vehicle. The less transmission of impact force to the supports means that crash box experiences less impact force which ultimately increases the passenger

safety during impact/collision. The results also show that the non-bonded foam gives better results as compared to bonded in terms of acceleration dissipation while the deformations are maximum in non-bonded foam. Also, the rigid polyurethane foam is better than the flexible polyurethane foams used in the beams. Further, a two-channel hollow beam and foam sandwich beams were compared, and the same results were found, i.e., foam sandwich proved to be better alternative in terms of dissipation, transmission of reaction-forces, and less level of accelerations of the body.

From the above discussion and keeping in view the results and graphs of chapter 4, it is concluded that the foam sandwich beams are better alternative to hollow beams during the impact. The reason is that the foams have a good ability to absorb the kinetic energy and attenuation of vibration due to its viscoelastic nature. Further, there is further needed to explore the behavior of the foam sandwich beams by using the density higher than 100kg/m^3 and increasing the dimensions and the contact area between the impactor and beam or by increasing or reducing the velocity of impact of the impactor body. Moreover, foams other than the Polyurethane foam also can be considered and shall be investigated for better vibration absorbing characteristics.

References

- [1] James H. M. and Guth E., "Theory of the elastic properties of rubber", Journal of Chemical Physics/ Volume 11/ Issue 10, 1943.
- [2] Mooney M., "A theory of large elastic deformation", Journal of Applied Physics, 11(9), pp. 582-592, 1940.
- [3] Rivlin R. S., "Large elastic deformations of isotropic materials. IV. Further developments of the general theory" Philosophical Transactions of the Royal Society of London, Series A, Mathematical and Physical Sciences, 241(835), pp. 379-397, 1948.
- [4] Rivlin R. S., and Saunders D. W., "Large elastic deformations of isotropic materials VII. Experiments on the deformation of rubber" Phi. Trans. Royal Soc. London Series A, 243(865), pp. 251-288, 1951.
- [5] Yang et al., A visco-hyperelastic approach to modelling the constitutive behavior of rubber, International Journal of Impact Engineering 24(6):545-560 · July 2000 .
- [6] Neo-Hookean solid -Wikipedia.
- [7] Majid Shahzada et al., Mechanical Characterization and FE Modelling of a Hyperelastic Material, Materials Research. 2015; 18(5): 918-924.
- [8] Hyperelastic material – Wikipedia.
- [9] R De Pascalis, Chapter 2 Strain energy functions - ESE - Salento University Publishing, 2010.
- [10] Mooney-Rivlin solid – Wikipedia.
- [11] Viscoelasticity – Wikipedia.
- [12] Presentation on "Introduction to Viscoelasticity" by Karina Chanley.
- [13] Presentation on "Non-linear analysis: Viscoelastic material analysis" by Jaclyn Grigsby – Autodesk.
- [14] W.N Findley et al., Creep and relaxation of Non-linear viscoelastic materials, Dover, 1989, pp 50.

[15] Dynamic mechanical analysis – Wikipedia.

[16] K.P. Staudhammer, L.E. Murr, M.A. Meyers. Fundamental issues and Applications of Shock-Wave and High-Strain-rate phenomena.

[17] <http://militzer.berkeley.edu/diss/node53.html>.

[18] Stanley P. Marsh. “**LASL SHOCK HUGONIOT DATA**”.

[19] Gibson, L. J., and M. F. Ashby. *Cellular Solids: Structure and Properties*. 2nd ed.

[20] Briody, C., Duignan, B. & Jerrams, S. (2011) Testing, modelling and validation of numerical model capable of predicting stress fields throughout polyurethane foam. Proceedings of the 7th European Conference on Constitutive models for Rubber (ECCMR). Dublin, Ireland, 20 – 23 September 2011.

[21] Ansys 19.1 Help Documentation.